Multi-agent system based active distribution networks

Please check the document version of this publication:

• A submitted manuscript is the version of the article upon submission and before peer-review. There can be important differences between the submitted version and the official published version of record. People interested in the research are advised to contact the author for the final version of the publication, or visit the DOI to the publisher's website.
• The final author version and the galley proof are versions of the publication after peer review.
• The final published version features the final layout of the paper including the volume, issue and page numbers.

Link to publication

Download date: 04. Oct. 2023

Multi-Agent System based Active Distribution Networks

PROEFSCHRIFT

ter verkrijging van de graad van doctor aan de
Technische Universiteit Eindhoven, op gezag van de
rector magnificus, prof.dr.ir. C.J. van Duijn, voor een
commissie aangewezen door het College voor
Promoties in het openbaar te verdedigen
op dinsdag 30 november 2010 om 16.00 uur

door

Nguyễn Hồng Phương

geboren te Hanoi, Viëtnam

Dit proefschrift is goedgekeurd door de promotor:

prof.ir. W.L. Kling

To my parents
To my wife Trang, and my son Shin

Promotor:

prof.ir. W.L. Kling, Technische Universiteit Eindhoven

Kerncommissie:

prof.dr.ir. P.P.J. van den Bosch, Technische Universiteit Eindhoven
prof.dr.ir. J.G. Slootweg, Technische Universiteit Eindhoven
prof.dr.ir. J. Driesen, Katholieke Universiteit Leuven
prof.dr.ir. J.A. La Poutré, Utrecht Universiteit

Andere leden:

univ.-prof.dr.-ing. J.M.A. Myrzik, Technische Universiteit Dortmund
dr. I.G. Kamphuis, Energieonderzoek Centrum Nederland
prof.dr.ir. A.C.P.M. Backx (voorzitter), Technische Universiteit Eindhoven

Multi-Agent System based Active Distribution Networks

This thesis gives a vision of the future power delivery system with its main requirements. An investigation of suitable concepts and technologies which enable the future smart grid, has been carried out. They should meet the requirements on sustainability, efficiency, flexibility and intelligence. The so called Active Distribution Network (ADN) is introduced as an important element of the smart grid concept. With an open architecture, the ADN is able to integrate various types of networks, i.e., micro grids or autonomous networks with different forms of operation, i.e., islanded or interconnected. By adding an additional local control layer, the so called cells of the ADN are able to reconfigure, manage local faults, support voltage regulation, or manage power flows.

Furthermore, the Multi-Agent System (MAS) concept is regarded as a potential technology to cope with the anticipated challenges of future grid operation. Analysis of the possibilities and benefits of implementing MAS shows that it is a suitable technology for the complex and highly dynamic operation of the ADN. By taking advantages of the MAS technology, the ADN is expected to fully enable distributed monitoring and control functions.

This MAS-based ADN focuses mainly on control strategies and communication issues for the distribution systems. The transition to the proposed concept does not require an intensive physical change compared to the existing infrastructure. The main point is that inside the MAS-based ADN, loads and generators interact with each other and the outside world. This infrastructure can be built up of several cells (local areas) that are able to operate autonomously by an additional agent-based control layer. In the MAS hierarchical control structure each agent handles three functional aspects: management, coordination, and execution. In the operational structure, the ADN addresses two main functions: Distributed State Estimation (DSE) to analyze the network topology, compute the state estimation, and detect bad data; and Local Control Scheduling (LCS) to establish the control set points for voltage coordination and power flow management.

Under the distributed context of the controls, an appropriate method for DSE is proposed. The method takes advantage of the MAS technology to com-

pute iteratively the local state variables through neighbor data measurements. Although using the classical Weighted Least Square (WLS) method as a core, the proposed algorithm reduces drastically the computation burden by dividing the state estimation into subtasks with only two interactive buses and an interconnection line in between. The accuracy and complexity of the proposed estimation are investigated through both off-line and on-line simulations. Distributed and parallel working of processors reduces significantly the computation time. The estimation method is also suitable for a meshed configuration of the ADN, which includes more than one interconnection between each pair of the cells. Depending on the availability of a communication infrastructure, it is able to work locally inside the cells or globally for the whole ADN.

As a part of the LCS, the voltage control function in MV networks is investigated in both steady-state and dynamic environments. The autonomous voltage control within each network area can be implemented via a combination of active and reactive power support of distributed generation (DG). The coordinated voltage control defines the optimal tap setting of the on-load tap changer (OLTC) of the HV/MV transformer while comparing the amounts of control actions in each area. Based on sensitivity factors, negotiations between agents are fully supported in the distributed environment of the MAS platform. Simulation results show that the proposed function helps to integrate more DG while mitigating voltage violations effectively. The optimal solution can be reached within a small number of calculation iterations. It opens the possibility to apply the proposed method as an on-line application.

In addition, a distributed approach for the power flow management function is developed. By converting the power network to a representative graph, the optimal power flow is regarded as the well-known minimum cost flow problem. Two fundamental solutions for the minimum cost flow, i.e., the Successive Shortest Path (SSP) algorithm and the Cost-Scaling Push-Relabel (CS-PR) algorithm, are introduced. The SSP algorithm is augmenting the power flow along the shortest path until reaching the capacity of at least one edge of the graph. After updating the flow, it finds another shortest path and augments the flow again. The CS-PR algorithm approaches the problem in a different way by scaling the cost and pushing as much flow as possible at each active node. Simulations of both meshed and radial test networks are made to compare their performances in various network conditions. Simulation results show that the two methods can allow both generator and power flow controller devices to operate optimally. In the radial test network, the CS-PR needs less computation effort than the SSP expressed in number of exchanged messages among the MAS platform. Their performances in the meshed network are, however, almost the same.

Last but not least, this novel concept of the MAS-based ADN is verified under a laboratory environment. The lab set-up separates some local network areas by using a three-inverter system. The MAS platform is created on different computers and is able to retrieve data from and to a hardware component, i.e., the three-inverter interfacing system. In the set-up, a function of power routing is established by connecting the three-inverter system with the MAS platform.

Three control functions of the inverters, AC voltage control, DC bus voltage control, and PQ control, are developed in a Simulink diagram. By assigning suitable operation modes for the inverters, the set-up successfully experimented on synchronizing and disconnecting a cell to and from the rest of the grid. On the MAS platform, a power routing algorithm is executed to optimally manage the power flow in the lab set-up. The results show that the proposed concept of the ADN with the power routing function works well and can be used to manage electrical networks with distributed generation and controllable loads, leading to more active networks and smart grids in general.

SAMENVATTING

Multi-Agent Systeem als basis voor Actieve Distributienetten

Dit proefschrift geeft een visie op het toekomstige elektriciteitsvoorzieningsysteem met haar belangrijkste eisen. Een onderzoek naar geschikte concepten en technologien die een toekomstige intelligente elektriciteitsnet mogelijk maken is uitgevoerd. Zij moeten voldoen aan de eisen met betrekking tot duurzaamheid, efficintie, flexibiliteit en intelligentie. Het zogenaamde Actieve Distributie Net (ADN) is gentroduceerd als belangrijk element van het intelligente netten concept. Met een open architectuur is het ADN in staat verschillende soorten netwerken, bijvoorbeeld microgrids of autonome netwerken met verschillende bedrijfsvoeringen, eilandbedrijf of gekoppeld, te integreren. Door het toevoegen van een extra lokale besturingslaag, zijn de zogenaamde cellen van het ADN in staat zich te reconfigureren, lokale storingen te managen, spanningsregelingen te ondersteunen of vermogensstromen te sturen.

Tevens wordt het Multi-Agent Systeem (MAS) concept beschouwd als een potentile technologie om te voldoen aan de te verwachten uitdagingen van het toekomstige netbeheer. Analyse van de mogelijkheden en voordelen van de toepassing van MAS toont aan dat het een geschikte technologie is voor de complexe en zeer dynamische werking van het ADN. Door de voordelen van de MAS technologie te benutten, is te verwachten dat het ADN een volledig gedistribueerde monitoring en besturing mogelijk zal maken.

Dit op MAS gebaseerde ADN richt zich voornamelijk op regelstrategien en communicatievraagstukken voor distributienetten. De overgang naar het voorgestelde concept vereist geen vergaande fysische verandering van de bestaande infrastructuur. Het belangrijkste punt is dat binnen het op MAS gebaseerde ADN, belastingen en generatoren een wisselwerking met zowel elkaar als met de buitenwereld hebben. Deze infrastructuur kan worden opgebouwd uit meerdere cellen (lokale gebieden) die in staat zijn autonoom te opereren door toevoeging van een extra op agenten gebaseerde besturingslaag.

In de hirarchie van de MAS regelstructuur behandelt elke agent drie functionele aspecten: het beheer, de cordinatie en de uitvoering. In de operationele structuur voert het ADN twee belangrijke functies uit: de gedistribueerde toe-

standschatting (DSE), om de netwerktopologie te analyseren, het maken van
een toestandschatting en het herkennen van onjuiste data; en de lokale aanstur-
ing (LCS), om de instelling van lokale regelingen voor de spanningshuishouding
en de vermogenssturing te bepalen. Binnen het kader van de gedistribueerde
regelingen is een geschikte methode voor de DSE voorgesteld. De methode
maakt gebruik van de MAS technologie om de lokale toestandsvariabelen it-
eratief te berekenen uit de metingen van de naastgelegen gebieden. Hoewel
gebaseerd op de klassieke kleinste kwadraten methode (WLS), reduceert het
voorgestelde algoritme drastisch de complexiteit van berekeningen door het
opdelen van het probleem van toestandschatting in subtaken met slechts twee
interactieve knooppunten en een tussenliggende verbinding. De nauwkeurigheid
en de complexiteit van de voorgestelde toestandschatting zijn onderzocht met
zowel offline en online simulaties. De gedistribueerde en parallelle werking van
de processors vermindert de rekentijd significant. De methode van toestand-
schatting is ook geschikt voor een ADN met een vermaasde structuur dat meer
dan n onderlinge verbinding tussen elk paar cellen bevat. Afhankelijk van de
beschikbaarheid van een communicatie-infrastructuur, is de methode in staat
lokaal te werken binnen de cellen, of globaal voor het gehele ADN.

Als onderdeel van de LCS, de functie van spanningshuishouding in mid-
denspanningsnetten (MV) is onderzocht in zowel stationaire omstandigheden
als in dynamische situaties. De autonome spanningshuishouding binnen elk
netdeel kan worden toegepast door middel van een combinatie van actieve en
reactieve vermogensondersteuning door gedistribueerde opwekking (DG). De
gecordineerde spanningsregeling bepaalt de optimale instelling van de online
trappenschakelaar (OLTC) van de HV / MV transformator en vergelijkt tevens
de aantallen regelacties in beide regio's. Gebaseerd op gevoeligheidsfactoren
worden de onderhandelingen tussen agenten volledig ondersteund in de gedis-
tribueerde context van het MAS platform. Simulatieresultaten tonen aan dat de
voorgestelde functie het mogelijk maakt meer DG te integreren door effectief de
spanningsafwijkingen te beheersen. De optimale oplossing kan worden bereikt
binnen een klein aantal iteraties. Dit opent de mogelijkheid om de voorgestelde
methode als een online applicatie te implementeren.

Daarnaast is een gedistribueerde aanpak voor de functie van vermogenss-
turing ontwikkeld. Door middel van het representeren van het elektriciteitsnet
als een graaf, kan de optimale vermogensverdeling beschouwd worden als het
bekende probleem van bepaling van de minimum kosten stroom. Twee fun-
damentele oplossingen voor het minimaliseren van de kosten stroom, zijnde het
opeenvolgende kortste pad (SSP) algoritme en het kosten schaling Push-Relabel
(CS-PR) algoritme, zijn gentroduceerd. Het SSP algoritme vergroot de vermo-
gensstroom langs het kortste pad tot het bereiken van de capaciteit van ten-
minste n pad in de graaf. Na het updaten van de vermogensstroom, vindt het
algoritme een ander kortste pad en verhoogt de vermogensstroom opnieuw. Het
CS-PR algoritme benadert het probleem op een andere manier door het schalen
van de kosten en het opleggen van zo veel mogelijk vermogen op elk actief knoop-
punt. Simulaties van zowel vermaasde als radiale testnetten zijn gemaakt om
de prestaties van de beide algoritmen onder diverse omstandigheden vergelijken.

De simulaties tonen aan dat de twee methodes het mogelijk maken dat zowel de regelingen van de generatoren en de apparaten voor vermogenssturing optimaal functioneren. In het radiale testnet blijkt, op basis van het aantal uitgewisselde berichten binnen het MAS platform, het CS-PR algoritme minder moeite met de berekening te hebben dan het SSP algoritme. De prestaties van beide methoden zijn in het vermaasde netwerk echter vrijwel gelijk.

Tot slot is dit nieuwe concept van het op MAS gebaseerde ADN geverifieerd in een laboratorium omgeving. De laboratorium opstelling scheidt een aantal lokale netten met behulp van een zogenaamd drie-inverter systeem. Het MAS platform is gecreerd op verschillende computers en is in staat om gegevens op te halen van en te versturen naar de hardware componenten, in dit geval het drie-inverter interface systeem. In de opstelling is de functie van vermogenssturing gerealiseerd door de koppeling van het drie-inverter systeem met het MAS platform. Drie regelfuncties van de inverters, zijnde de AC spanningsregeling, de regeling van DC spanning op het DC knooppunt en de PQ regeling, zijn ontwikkeld in Simulink. Door het toewijzen van geschikte bedrijfsvoeringsopties aan de inverters is de opstelling in staat een cel succesvol te koppelen aan en te scheiden van de rest van het net. In het MAS platform is een strategie voor de vermogenssturing uitgevoerd om de vermogensstroom binnen de opstelling optimaal te regelen. De resultaten tonen aan dat het voorgestelde concept van ADN, met inbegrip van de functionaliteit van vermogenssturing, goed werkt en kan worden toegepast om elektriciteitsnetten met gedistribueerde opwekking en stuurbare belastingen te beheren, wat leidt tot meer actieve en intelligente netten in het algemeen.

CONTENTS

LIST OF FIGURES

LIST OF TABLES

CHAPTER 1

INTRODUCTION

Electrical power systems are one of the largest and most important life support engineering systems. They spread everywhere in countries to supply electricity for hundreds of millions of consumers from hundreds of thousands of producers. Nowadays, a sustainable society not only demands a high reliability of electricity supply but also concerns with the environmental impacts from the power system. To achieve a reliable and sustainable electricity supply, there is an increasing need to use renewable energies like wind, or solar energy. The development of many intermittent and inverter-connected Renewable Energy Sources (RESs) will require the power system to have new ways of planning, operating, and managing the entire process [1]. In the other words, the power system is moving into a new era.

Recently, new concepts and technologies have been emerged. They aim to create a sustainable, efficient, flexible and intelligent electrical infrastructure which is able to cope with the integration of both large-scale and small-scale RESs as well as other Distributed Generations (DGs). This might lead to extremely complex interactions of centralization versus decentralization in control, and islanding versus interconnection in operation. Future networks will get a strong interdisciplinary characteristic with an increasing contribution of power electronics and Information and Communication Technologies (ICT).

This chapter gives a short description of the various changes in the power system. The complex context of the future network motivates the research and is defining the boundaries of the thesis scope on active distribution networks. The research questions and approach are then identified. An outline of the thesis is depicted at the end of the chapter.

1.1   The evolution of the power system

Electricity is traditionally transmitted from centralized generation, such as coal, hydro, or nuclear power plants to customers via the transmission and distribution networks. Due to a large-scale implementation of DG, the power delivery system is changing gradually from a "vertically" to a "horizontally" controlled and operated structure. Under the vertical-to-horizontal transition, the distribution network is anticipated as the most evolutionary part of the power delivery system with various challenging issues [2]. This section presents the most related concerns leading to the thesis objectives.

1.1.1   Impacts of distributed generation

DG is one of the most popular items in the electrical power system field of study in the last decade. It addresses introductions of Distributed Energy Resources (DERs), i.e., micro-turbines, Combined Heat and Power (CHP) installations, small hydro-power plants, wind turbines, photovoltaic systems, fuel cells, biomass technologies, into the distribution network. The DG units feed in both the Medium Voltage (MV) and Low Voltage (LV) network with a rated power typically in a range of 10-50MW [3]. Because RESs are mostly based on intermittent primary energy sources such as wind speed and solar radiation, renewable energy based DGs are difficult to be centrally dispatched and controlled. The rapid implementation of DGs, therefore, causes both technical challenges and opportunities for local optimization in the distribution network.

Negative impacts of DG are related to conflicts with the passive and less intelligent design of the existing distribution system. Serious technical problems and challenges appear when the penetration rate of DG increases.

- Voltage deviation/regulation is one of the biggest issues. Voltage rise occurs when the customer load is at the minimum level and power injection of DGs flows back to the public grid [4]. This limits DG penetration in extended radial distribution networks (rural areas).

- Rotating machine based DGs cause a significant increase of the network fault current levels. This is a critical hindrance to install more DGs in urban areas where the fault currents nearly approach the rating of the equipments.

- Large-scale implementation of DG affects the original protection designs of the existing distribution networks.

- With a significant amount of power injection, DG's contribution to stability issues including transient stability, long term dynamics, and voltage stability, needs to be considered.

- As typical locations of DG are close to customer connection points, power quality issues, mainly voltage deviations and harmonic distortions, at the

Point of Common Coupling (PCC) become a greater concern. Connection of DG's electronic AC/DC/AC interfaces makes the issue even more complex.

Along with the technical challenges to integrate DGs, they also create many opportunities to make the distribution network more intelligent and flexible.

- Power sources close to customer areas are expected to reduce power transfer losses and consequently avoid upgrading transmission and distribution infrastructure. However, the power losses levels are depending on the dispersion levels and to a certain extent also on the reactive power management [5]. RES's unpredictable generation characteristic might also cause increasing the power losses.

- Introduction of DGs can decrease the voltage drop that is significant in existing distribution networks. DGs can be used as standby sources by large customers to improve power supply quality and reliability.

- A cluster of DGs may provide island-mode operation for customers such as in the MicroGrid [6], [7].

The development of privately-owned DGs creates a change for end-users to participate in a transparent liberalization market [8]. These so called prosumer entities are expected to react on time-varying price signals. They challenge the network operators to materialize the added values of DGs in the future situation.

Figure 1.1, which is adapted from [9], [10], illustrates characteristics of some DERs in term of typical unit size, controllability, grid-connected way, and shared power capacities. Power generation from biomass has a more controllable characteristic and more contribution in the total power capacity than the others. Although having significant amount of power generation, solar PV is limited in controllability.

1.1.2 Changes of control structure and organization

The conventional control strategy to maintain system frequency and voltage is divided mainly on three layers, i.e., primary control, secondary control and tertiary control [11]. The primary control, normally based on droop control, reacts with frequency deviation from imbalance between generation and load. It aims to keep the system stable within seconds after disturbance occurring. The secondary control replaces the primary control over minutes to restore deviated frequency to its nominal value and to keep the exchange between control areas as programmed. The tertiary control ensures that the generators are dispatched in the optimal way to minimize the variable production costs taking the power balance and network constraints into account. Besides these three control layers, time control is mentioned to monitor and limit discrepancies observed between synchronous time and universal coordinated time in the synchronous area [12].

Voltage control has also the three essential layers but has its focus on local control objectives instead of a common goal of the system frequency. In the
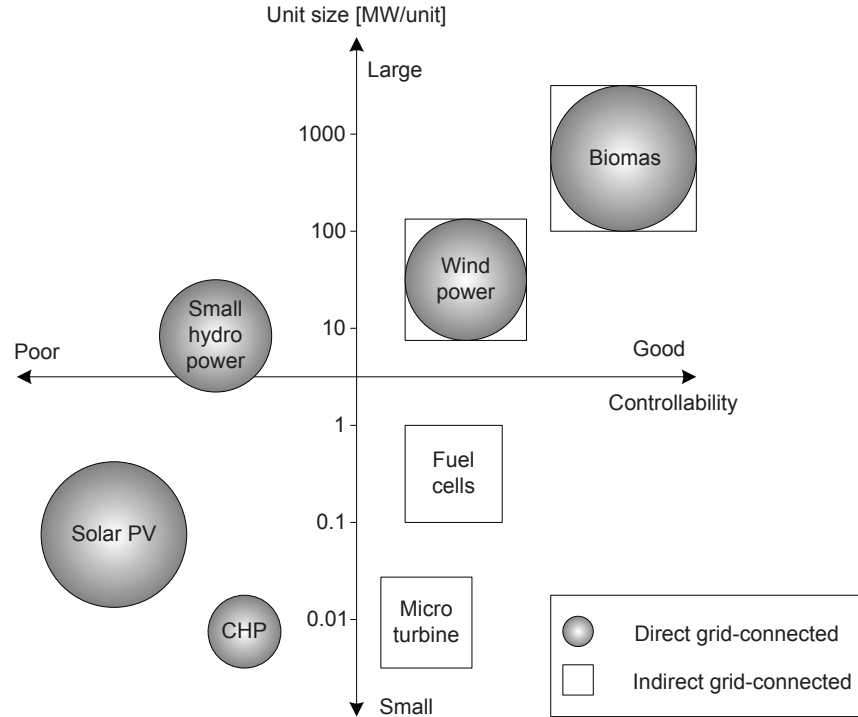
Figure 1.1: Unit size and controllability characteristics of some distributed energy resources.

transmission system with a high X/R ratio, the local bus voltages are influenced mainly by the reactive power flows. As the distribution system has normally a low X/R ratio, the voltage control is depended both on active and reactive power.

These control layers were initially integrated in the power system as vertically regulated monopoly acting in a certain region. Over many decades, the monopolistic control structure has operated in a reasonably reliable and stable level. The advantages of competition among energy suppliers and wide choice for electricity consumers have motivated the deregulation and restructuring of the power system into markets in most part of the world [13]. This has led to various segments of Independent System Operators (ISOs), Transmission companies (Transcos), Generation companies (Gencos), Distribution companies (Discos), Scheduling Coordinators (SCs), and Power Exchanges (PXs). Only entities related to the scope of the thesis are described in this section. The other entities of the electricity market are well defined in [13].

The Transmission Network Operator (TNO) is considered as the owner of the transmission network while the ISO is designated as the operator of the transmission system who is responsible for maintaining the balance between ge-

neration and consumption. Since electricity cannot be stored in large amounts, the power balance control through the coordination of participants' related activities is an essential aspect for a stable and secure operation of the system [10]. Depending on the organizational structures in different electricity markets, the so called ancillary services providing various control features, i.e., spinning reserve, economic dispatch, regulation, frequency control, Automatic Generation Control (AGC), reactive power and voltage control, and black-start capability, may be purchased [13]. It stimulates the development of ancillary services markets besides the electricity market [14]. In the Netherlands, TenneT is the unification of the TNO and the ISO [15] which is quite common in Europe and such an entity is called Transmission System Operator (TSO).

The Distribution System Operator (DSO) is responsible for the real-time monitoring and control of the distribution system. Based on transparent, non-discriminatory and market based procedures, the DSO may procure the energy to cover energy losses and might be responsible for emergency capacity in its local area. In addition, the DSO may be required to give priority to generating installations using renewable energy sources or waste or producing combined heat and power [16]. As a Distribution Network Operator (DNO) owns and operates a distribution network, DNOs and the DSO constitute together the distribution system [17].

The large-scale implementation of DG transforms the existing passive distribution networks with unidirectional electricity transmission into active bidirectional power flow systems [18]. With innovative ICT technologies, flexible planning approaches, advanced components and power control facilities, the DSO is expected in the future to manage local balancing to avoid the possible congestions, control voltage and power flows, provide ancillary services and islanding capabilities. Consequently, the DSO can increase its contribution in the integration of the TSO to manage the whole electric system. Cooperation of the TSO and the DSO will focus on "load-follows-supply" approach with more flexibility to react to changing demands, the importance and complexity of real-time balancing markets, the role of aggregators representing small and possibly medium-size consumers and producers, and more hierarchical control structure [19].

Figure 1.2 presents the structure of a modern power system under the new context. The Centralized Generators (CGs) and DGs are involved in the energy trading. The TSO-ISO is managing the transmission system and the DSO is managing the distribution system and they share the responsibilities on balancing power and providing ancillary services. In the distribution system, additional control functions such as local balancing, real-time power routing, and power matching might be arisen besides available functions of distribution management, smart metering, and Demand Side Management (DSM).

Power matching is a continuous system-wide activity which is centrally organized based on generators who follow on a coordinated way their programs. With a massive amount of intermitted power sources, the power matching is supported by decentralized actions triggered on price signals and markets. Real-time local balancing gives the possibility of local area networks to self support
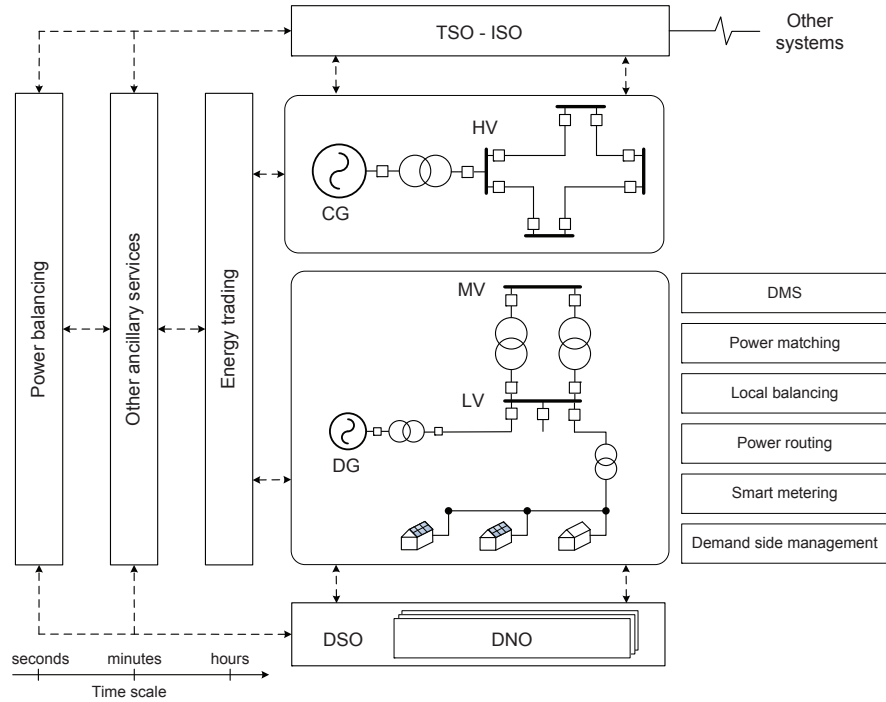
Figure 1.2: Organization of the modern power system.

their demand by DERs. Power routing aims to deal with transmission bottle-necks related to the actual load and generation schedules of the market parties. Note that this might require power electronic devices to physically control the power flow. Under the decentralized context, power routing is needed to solve the network constraints.

1.1.3 Increasing role of communication and distributed processing

Supervisory Control and Data Acquisition (SCADA), Energy Management System (EMS), and Distribution Management System (DMS) are used by ISO, TSO, TNO, DSO, and DNO to fulfill their missions of real-time monitoring and control functions. Especially in the distribution network, the introduction of RESs will be more efficient once the development of the EMS/DMS system for meeting grid requirements takes off, while maintaining high standards of quality and reliability of services as well as connectivity. The ICT infrastructure can be enhanced to manage the operation of millions of small-scale generation units by monitoring a range of variables and ensuring efficiency of generation.

Recognizing the various challenges in the near future, the power and energy community is starting to make a stronger connection between ICT and the

electrical power infrastructure. This will provide a more effective and "smart" operation for the future grid. Near real-time information allows utilities to manage the power network as an integrated system, actively sensing and responding to changes in power demand, supply, costs, and quality across various locations. However, large-scale integration of ICT in the distribution system might also introduce vulnerabilities which influence the reliability of the power network [20].

Nowadays, smart metering and sensor systems start appearing in the distribution network. This is expected to provide large amounts of information for management and control purposes in the future networks [21]. DSM can be implemented and supported by two-way smart meters and smart sensors on equipment communicating through ICT, managing the demand of consumers according to the agreements reached with the customers [22]. Advanced ICT infrastructure opens the possibility for real-time and scalable market mechanisms to reduce uncertainty of instantaneously changing prices and to arrange short-time reserves [23].

To deal with this more complex future situation of the power systems, distributed computational processing, monitoring, and controls, has emerged the need for a dynamic decision making and management of the grid. By dividing the entire network into a number of control areas, such distributed processing has main advantages and makes the hierarchical monitoring and control more reliable, flexible, and efficient than the centralized one [17]. The advancement of computer and communication systems supports the distributed processing through innovative techniques and theories of Multi-Agent System (MAS), distributed management and control, adaptive self-healing, object-oriented modeling, and common information and accounting models.

1.2 Research objectives and scope

1.2.1 Objective

As mentioned before, increasing amounts of DG units yields various technical issues on the distribution system which challenges network operators on finding better solutions for planning, operation, and management. Enabling technologies of power electronics, advanced communications, and distributed controls opens possibilities to overcome those challenges. The approach, however, needs to be carefully considered to fully satisfy different circumstances of the future power network.

As a main objective of the project is creating an efficient and flexible distribution system, it is essential to build up a new robust control framework. The proposed structure must be able to cope with current issues in the distribution network, i.e., real-time monitoring, voltage deviations, and congestion management. That requires developing new concepts and technologies to operate the future grids. The investigated network concepts must be feasible to upgrade from the current network infrastructure. They need also to be acceptable by

both power utility companies and customers. These aims to stimulate a transition from the current passive distribution network to an active and flexible infrastructure to fulfill the requirements of the future power delivery system.

1.2.2   Research questions

Derived from this main research objective, several research questions are addressed as follows:

- What are the main requirements of the future power distribution system?

- Which are the network concepts and technologies promising and feasible in the future?

- How to control, manage, and operate the future network?

- What will be the performance of that network?

1.2.3   Scope

The longer the time span from present to future is, the more uncertain the developments are. In most of previous research works future network development and distributed generation penetration are discussed in period of the next decade. Regarding mature development of known concepts and technologies this research focuses on network solutions viable for a longer period.

The main focus of this research is laid on the distribution networks. Special attention is given to network control, the role of power electronics, and application of ICT.

1.3   Research approach

The research approach consists of the following three steps:

- **Identifying promising concepts and technologies for the future power distribution system.** An investigation of suitable concepts and technologies which draw out attentions at the present has been carried out. They are discussed regarding sustainability, efficiency, flexibility and intelligence. The Active Distribution Network (ADN) is then introduced as the backbone of the future power distribution system and MAS is described as a potential technology to cope with the anticipated challenges of future grid operation.

- **Development of MAS-based Active Distribution Networks.** The various functions of the ADN, i.e., distributed state estimation, voltage regulation, and power flow management, are developed. These functions are based on the distributed agent environment to realize the advantages of MAS technology in managing the ADN. The research investigates the

main benefits of these functions in the distributed context by software simulations. The power control system is simulated in Matlab/Simulink while the MAS platform is created in a Java Agent Development Framework (JADE).

- **Verification of the laboratory experiments.** In the laboratory a practical set-up is built which includes various electrical components (hardware), a MAS platform (middleware), and a control interface (software). The innovative aspects of the MAS-based ADN concept are experimentally verified.

1.4 EOS long term research program - the EIT project

The research presented in this thesis is performed within the framework of the "Electrical Infrastructure of the Future" project (Elektrische Infrastructuur van de Toekomst - EIT project) which belongs to the program of energy research (Energie Onderzoek Subsidie - EOS program), sponsored by the Ministry of Economic Affairs of the Netherlands. The main objective of the EOS program is to extend the knowledge concerning energy efficiency and sustainable energy in the Netherlands and covers the route from the idea until market introduction.

The EOS project is initiated by the Electrical Energy Systems group of the Eindhoven University of Technology. In total 7 PhD students and 2 postdoctoral researchers, work closely together on different projects included EIT, FlexibEL, KTI, RegelDuurzaam, and TREIN.

The EIT project is realized in cooperation with KEMA and ECN. The main objective of the project is to study the electrical infrastructure of the future that must be sustainable, efficient, flexible and intelligent.

The now existing network is too passive, not intelligent enough, and not able to control the different situations and is therefore vulnerable. The following trends can be viewed:

- The way in which electrical energy is generated will be changed structurally: more local generation, a lot of stochastic output and need for storage.

- Increase of energy demands, necessity of energy management and system integration within the essential precondition of the primary process of the user, desire to save energy and demand response.

- Change of customer demands and needs of the society as it concerns quality and reliability, increasing sensitivity of apparatus and industrial processes for tolerances in the voltage.

- Individualization of the services to the customer, premium power for privileged applications and market oriented solutions to control bottlenecks in the system and combination of services.
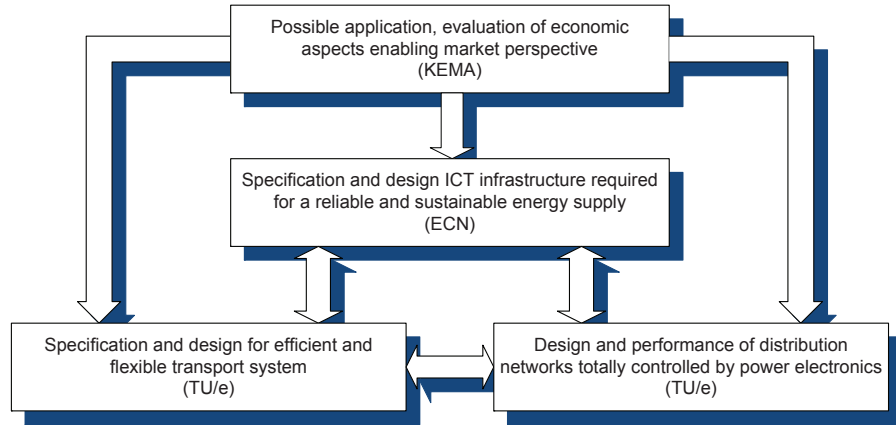
Figure 1.3: Organization of the EIT project.

The proposed project focuses on the technical infrastructure of the future and aims to answer the essential questions in this field. The research is fundamentally based and is handled in four exploration themes:

1. Functional specification and design of efficient and flexible transport systems.

2. Design and performance of a distribution network fully controlled by power electronics.

3. Specification and design of ICT infrastructure necessary for a reliable and sustainable energy supply.

4. Possible applications, evaluation on economical aspects and enabling of market perspectives.

The relationships between these topics are illustrated in Figure 1.3. The thesis work is on the first topic.

1.5   Outline of the thesis

This introductory chapter is followed by the following chapters:

- **Chapter 2: Active Distribution Networks.** An investigation of suitable concepts and technologies which creates a step forward the smart grid has been carried out. They should meet the requirements on sustainability, efficiency, flexibility and intelligence. The so called ADN is introduced as an important element of the future power delivery system. Furthermore, the MAS concept is regarded as a potential technology to cope with the anticipated challenges of future grid operation. This MAS-based

ADN focuses mainly on control strategies and communication topologies for the distribution systems. This infrastructure can be built up of several cells (local areas) that are able to operate autonomously by an additional agent-based control layer. It includes two main parts: Distributed State Estimation (DSE) to analyze the network topology, compute the state estimation, and detect bad data; and Local Control Scheduling (LCS) to establish the control set points for voltage coordination and power flow management.

- **Chapter 3: Distributed State Estimation.** Under the distributed context of the controls, an appropriate method for DSE is proposed. The method takes advantage of the MAS technology to compute iteratively the local state variables through local data measurements and exchanged information. The accuracy and complexity of the proposed estimation are investigated through both off-line and on-line simulations. Distributed and parallel working of digital processors improves significantly the computation time. This estimation is also suitable for a meshed configuration of the ADN, which includes more than one interconnection between areas. Depending on the availability of a communication infrastructure, it is able to work locally inside areas or globally for the whole ADN.

- **Chapter 4: Voltage regulation.** As a part of the LCS, the voltage control function is investigated in both steady-state and dynamic environments. The autonomous voltage control within each network area (cell) can be deployed by a combination of active and reactive power support of DGs. The coordinated voltage control defines the optimal tap setting of the On-Load Tap Changer (OLTC) while comparing amounts of control actions in each area. The proposed function helps to integrate more DG while mitigating voltage violation effectively. The optimal solution can be reached within a small number of calculation iterations.

- **Chapter 5: Power flow management.** This chapter proposes new methods to manage the active power in the distribution network, a function under the framework of the ADN concept. Applications of the graph theory are introduced to cope with the optimal power generation (DGs - cells dispatch) and inter-area power flows. The Successive Shortest Path algorithm and the Cost-Scaling Push-Relabel algorithm are proposed as solutions for these problems. The algorithms are implemented in a distributed way supported by the MAS technology.

- **Chapter 6: Laboratory-scale demonstration.** The novel concept of MAS-based ADN is verified under a laboratory environment. The lab setup separates some local network areas by using a three-inverters system. The MAS platform is created on different computers and is able to retrieve data from and to hardware components, i.e., the three-inverter system. The results show that the proposed concept works well and can be used to manage electrical networks with distributed generation and controllable loads, leading to active networks.

- **Chapter 7: Conclusions.** The thesis ends with general conclusions and recommendations for future research.

CHAPTER 2

ACTIVE DISTRIBUTION NETWORKS

As discussed in the previous chapter, several new power network concepts are developed to facilitate the integration of Distributed Energy Resources (DERs) and Renewable Energy Sources (RESs) within context of a sustainable development. Although differing in approach and implementation, they share the same objective of transferring the current passive distribution networks into active networks. This chapter summarizes the main network concepts based on current researches and application orientations. The concept of an Active Distribution Network (ADN) is then explained as a backbone for the future power delivery system.

In addition, innovative applications of the Information and Communication Technology (ICT) and power electronics are described. This chapter addresses the application of a Multi-Agent System (MAS) as the most suitable technology to fully enable the monitoring and control functions of the ADN. In an operational structure of a MAS-based ADN, the power router is introduced as a flexible interface between cells in the ADN combined with applications of power electronics and agents. Finally, the MAS technology is described more in detail to reveal its benefits and challenges in the distributed context of the future grid.

2.1 Introduction

The traditional power system has been designed as a vertically based structure with three separate parts of generation, power transmission and consumption for many decades ago. Recently, this infrastructure has received many pressures from socio-economic and technology development as well as environment requirements. It is anticipated that the major impacting factors for the electricity infrastructure are the digital society, liberalization power market, distributed generation, and the limited possibility of transmission and distribution extension [24].

Among them, the introduction of DER and RES in distribution networks is a dominant factor that causes a new evolution in the electrical infrastructure. Several scenarios in European Union (EU) countries forecast that the penetration level of DG is over 15% in 2010 and around 30% in 2020 [25], [26], [27]. Recently, the EU climate and energy package has been approved to reach 20% of renewable in total energy consumption in 2020 [28]. In United States (US), a Renewable Systems Interconnection (RSI) study has been launched to facilitate the more extensive adoption of renewable distributed electric generation since 2007 [29].

With such a large-scale implementation of DG, the distribution network has to be changed gradually moving from the downstream unidirectional power flow to a bidirectional power flow. This "vertically" based to an "horizontally" based transition will create a number of challenges in system planning, operation, and management.

Taking into account a large-scale deployment of DGs and an enhanced Power Quality (PQ) expectation in the future, a robust active distribution network is needed to replace the existing passive and less intelligent one. Designing the future grid should be based on the main requirements according future circumstances. The network needs to be *efficient* and *flexible* to cope with arising challenges in operation such as bidirectional power flow, voltage deviation, short-circuit current increase, stability and reliability issues. Network structures must be redesigned in an adjustable and scalable way for varying needs in the future. The system will be more *intelligent* in order to self-adjust and to be adaptable in autonomous operations. Hence, the supply and demand will be controlled optimally in either steady states or dynamic conditions. Moreover, concepts and technologies for the future network need to take social and environmental aspects into account for a *sustainable* development.

2.2   Future distribution system

Since the current distribution network has some limitations for providing appropriate functions for the challenging future, several new network concepts and technologies have been proposed recently. This section reviews some important concepts and technologies, and investigates their compatibility with the future network requirements.

2.2.1   Network concepts

MicroGrid

Electrical power systems were created originally as local isolated networks, with small-scale load and generation. Benefit from economy of scale and reliability enhancement stimulated a huge development of the bulk power systems which have large-scale generation often far from load. Recently, the concept of a MicroGrid has been considered as a modern version of the original power systems to exploit local DERs.

The MicroGrid concept would be a possible solution to increase penetration of DER in LV distribution systems [6], [7]. By integrating DER together with storage devices and controllable loads, a MicroGrid can possibly operate both in islanded mode and interconnected to the main grid [7]. The MicroGrid concept focuses mainly on internal objectives and their solutions. Its behaviors in island mode possibly caused by losing connection with the MV network is of major concern. Potential technical benefits expected from the MicroGrid are energy loss reduction, mitigation of voltage deviations, relief of peak loading in the network, and enhancement of supply reliability. Following up the idea of aggregating MicroGrids, the implementation of multi MicroGrids is investigated to fully exploit the benefits of the concept in technical, economic, and environmental terms [30].

Autonomous Network

In the MV networks with more complexity and larger size, the concept of Autonomous Network is introduced as a way of network management [31], [4], [14]. Although providing self-controlled functions like in the MicroGrid, the Autonomous Network concerns more about optimizing network performance during normal operation. Particular functions, i.e., controlled power exchange, maintaining voltage profile, as well as stability issues, are addressed.

An Autonomous Demand Area Power System (ADAPS) is proposed to obtain effective use of energy from DG for both customers and suppliers [32]. Two main devices are introduced in this system including a Loop Power Controller (LPC) and a Supply and Demand (S&D) matcher. The LPC device is used to flexibly control power flows (fault current possible), and to avoid power congestion and voltage problems. The S&D interface is based on an advanced communication network to deal with balance between supply and demand sides.

FRIENDS

In Japan, the Flexible, Reliable and Intelligent Electrical eNergy Delivery System (FRIENDS) has been known as a potential approach to resolve not only current issues caused by introduction of DG but also potential problems under the deregulated environment [33]. The most innovative part of this concept is the Quality Control Center (QCC) acting as an interface between the distribution system and the customers. QCCs operate switches in the network, several kinds of DG and storages, and coordinate with each other by the communication network. FRIENDS, therefore can offer various levels of quality of supply for its customers. Flexible reconfiguration in emergency operation deployed by fast static-type switches is another advantage of the concept. Besides, it is possible to perform autonomous control actions such as voltage regulation or reactive power control.

Active Network

In [34], Van Overbeeke has proposed a vision of Active Networks (ANs) as facilitators for DG. The solution is based on three main aspects including interconnection among networks, local control areas (cells), and ancillary services as specified attributes of a connection. While the first is to provide more than one power flow path, manage congestion by re-routing power and isolate faulted areas effectively, the third feature supports system stability and is charged to individual customers. However the most revolutionary change is proposed in the second feature, the local control areas or "cells". Hence, one more control level will be installed for each cell component to manage and control the system inside and across the cell boundaries. It can be deployed with different typical actuators such as voltage and reactive power controllers, Flexible AC Transmission Systems (FACTS) devices, remotely controllable loads and generators.

Advanced Distribution Automation (ADA) and Active Network Management (ANM) are particular terms of the Active Network which addresses systems including control and communication network. While ADA is developed in US as a solution to improve system reliability, ANM is a headline title in United Kingdom (UK) with its main focus on facilitating of distributed and renewable generation [35]. Current developments of ANM are on solving major technical issues of voltage control, power flows, and fault level. Decentralized Autonomous Network Management is a typical example enabling ANM concepts [36]. The proposed control approach ensures that the power flows in all the circuits are staying within their capacity limits based on the MAS technology. More possible functionalities for ANM can be included such as demand side management, network reconfiguration, and network restoration.

Smart Grid

As an emerging concept of intelligent technology utilizations, the Smart Grid has currently drawn more and more attentions and tends to become a mainstream for the future power delivery system. Many large research centers are engaged with the Smart Grid development, for example, European Technology Platform (SmartGrids) [37], US Department of Energy (GridWise) [38], Electric Power Research Institute (IntelliGrid) [39]. However, there is no global definition of the Smart Grid yet.

According to the US Department of Energy, the Smart Grid is defined in [40] as follows:

Definition 2.2.1 *An automated, widely distributed energy delivery network, the Smart Grid will be characterized by a two-way flow of electricity and information and will be capable of monitoring everything from power plants to customer preferences to individual appliances. It incorporates into the grid the benefits of distributed computing and communications to deliver real-time information and enable a near instantaneous balance of supply and demand at the device level.* ∎
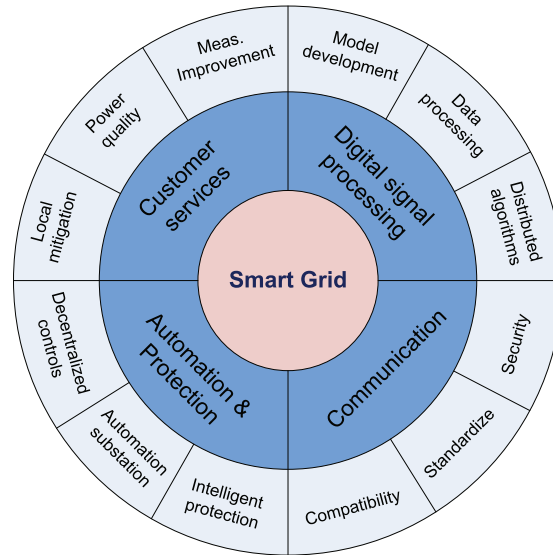
Figure 2.1: Possible technical aspects for R&D on Smart Grid.

The European Technology Platform SmartGrids describes smart grids by following definition [41]:

Definition 2.2.2 *Electricity networks that can intelligently integrate the behavior and actions of all users connected to it - generators, consumers and those that do both in order to efficiently deliver sustainable, economic and secure electricity supplies.* ∎

As can be seen from these definitions, the Smart Grid concept is more or less an overall picture framework of the future network that utilizes the new concepts as described before. Core technologies implemented in the Smart Grid include distributed intelligent devices, communication network, advanced simulation software, and power electronic applications. Figure 2.1 summarizes the technical aspects of a Smart Grid which are getting increased R&D attention in the near future. The Smart Grid works with both central and distributed generation. Based on a Virtual Power Plant [42] or Virtual Utility [43] concept, clusters of DGs can be aggregated to operate as a large central power plant. Therefore, bidirectional power flow is a main characteristic of the gird.

In the US, the number of Smart Grid projects at the end of 2009 exceeded 130 projects [44] with $4 billion in US federal funds. In 2010, the top 10 countries by Smart Grid stimulus investments in millions are China ($7,323); US ($7,092); Japan ($849); South Korea ($824); Spain ($807); Germany ($397); Australia ($360); UK ($290); France ($265); and Brazil ($204) [45]. It is anticipated that investment on Smart Grid technologies can reach globally $200 billion during the period from 2008 to 2015 [46].

2.2.2   Enabling technologies

In order to enable above concepts in the future, suitable network technologies need to be introduced. In this section, state of the art of such technologies is investigated briefly.

Power electronics

The application of electronic devices known from transmission level into the distribution systems is a current direction. DC coupling in the MV networks, based on the back-to-back High Voltage Direct Current (HVDC) concept with IGBT technology is a typical example [47]. Advantages of this application include interconnecting sub-networks without short-circuit current increase, controlling reactive power and voltages separately, and supplying power to an isolated network with possibility a different voltage level, frequency and phase angle.

The FACTS technology plays an essential role in modern power systems. Its utilization in distribution system is expected to enhance the capability of the network. Some electronic devices involved in this aspect are the Distributed Static Compensator (DSTATCOM), Dynamic Voltage Restorer (DVR), and Solid-State Transfer Switch (SSTS). In the same sense as installing FACTS close to load side, DGFACTS systems lead to integrated solutions of such devices to optimally improve the stability and quality of supply of different network parts [48]. In another direction of application, researches on interfaces between DG and the utility network are important to mitigate possible drawbacks of RES [49].

The Custom Power concept is based on the use of power electronic controllers installed at the customer side to supply value-added, reliable, high quality power [50]. This concept is focused on the local system within a certain customer area. But it is possible to be incorporated with other devices to get an overall impact. The world's first distributed premium power quality installation has been installed in Delaware, Ohio with the integration of state-of-the-art power quality devices such as DVR, and ASVC [51].

The Power Electronics Building Block (PEBB) is a major initiative of the US Navy's Office of Naval Research [52]. By including a defined functionality, standardized hardware, and control interfaces, the PEBB can be used to build power systems in much the same way as personal computers.

Information communication technology

The function of ICT in the electricity infrastructure is expected to be more prominent in the future. It is considered as a key technology to enable any new network concept mentioned in the previous section. Advanced ICT-based control framework focuses on providing dedicated ancillary services, e.g., reserve capacity, voltage support and network constraint alleviation. It allows intelligent solutions by giving consumers and producers clear, real-time financial incentives to adapt their consumption/production according to the actual needs of the power system.

ICT applications in distribution system control and management are examined in the EU-CRISP project [53]. Is has shown ICT capabilities in protection, reconfiguration, and Internet-based control. In [54], an integration of various communication networks, i.e., radio, fiber optics, power line carrier and telecommunication cables, is considered as requirement and solution for a secure power system. ICT-based applications are also seen as crucial in the transition toward Smart Grids. To accelerate the introduction of ICT into Smart Grids, the SEESGEN-ICT project aims to investigate requirements, barriers and possible solutions [55].

Multi-agent system

MAS has been mentioned recently as a potential technology for many fields of power system applications. Belonging to the area of artificial intelligence, MAS can offer a certain degree of intelligent behavior in autonomous systems [56]. Applications of MAS in power systems include disturbance diagnosis, restoration, protection, power flow and voltage control [36], [57]. Several research projects have begun to investigate MAS as an approach to manage distributed generation, virtual power plants and Micro Grids as it provides a flexible control of distributed systems [58], [59], [60], [61]. Furthermore the MAS approach has attracted attention in the area of protective systems, power systems operation, trading, and control centers support [62], [63].

The PowerMatcher concept is a application of the MAS technology for power trading through an electronic market [53]. Via a bottom-up electronic market mechanism, the PowerMatcher concept is applied successfully in two field tests of the CRISP project and in a μCHP based Virtual Power Plant (VPP) in the Netherlands [64].

2.2.3 Compatibility for the future networks

The future grid needs to be designed in an efficient, flexible, intelligent and sustainable way to adapt with future conditions and expectations. According to above descriptions of the new network concepts, the sustainability is dominant because all concepts concern about the DER and RES integration. MicroGrid is introduced as a bottom-up approach which is focused on island operation during various network disturbances. As a step further, FRIENDS and Autonomous Networks are able to manage the power exchange flexibly by electronic devices (FRIENDS) [33] or price-based mechanisms (Autonomous Network) [14]. Active Network is distinguished from others while it concerns both autonomous operation and optimal coordination. With an open architecture, the AN can integrate different network concepts as parts (cells) of it. In [65], a review on aggregation approaches are initially mentioned. ICT applications enable many possibilities for intelligent control algorithms to achieve not only local optimization but also global objectives in AN.

The Smart Grid has a contrary viewpoint to MicroGrid with a top-down vision for the future grid. It expects to integrate all latest technologies, which
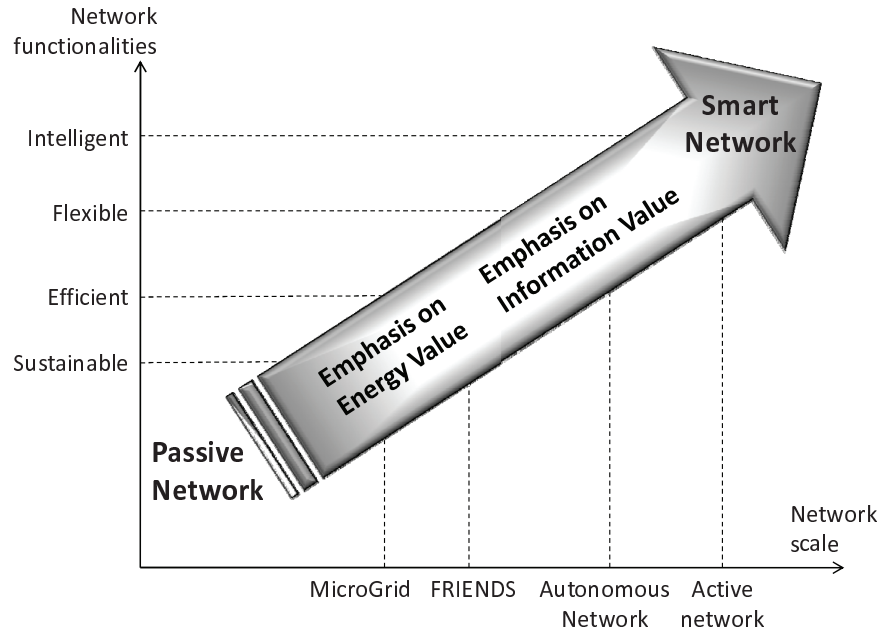
Figure 2.2: Evolution toward Smart Grid.

implies great efforts of engineers, large investment, and governments' incentive policies. In other words, the Smart Grid is an umbrella term which covers different new concepts and technologies in both the transmission and distribution grid [66]. Figure 2.2 is modified from [37] to illustrate the new network concepts on the road map to the Smart Grid.

AN and Smart Grid have structures fully meeting the requirements of the future grids. Under the scope of the research, we consider the Active Network as a backbone for the future grid. But also the other concepts will show up as certain parts of the future network. Hence, the grid based on ANs needs to be able to integrate with other network types formed by Autonomous Network, FRIENDS, or MicroGrid. Figure 2.3 shows a possible layout of the future network with an integrated structure.

The integrated layout makes the future grid more complex with differences between sub-networks, in decentralization and centralization, or between island and interconnection. These challenges for system planning, control, and management are not simple to be handled by the existing technologies. In order to cope with these problems, there is a need to apply power electronics, high bandwidth digital communication, and distributed control, such as FREEDM System [67]. In the new context, MAS technology is considered as a suitable platform to fully enable potential applications. In fact, MAS has been utilized already in promising concepts such as MicroGrid and FRIEND [56], [68].
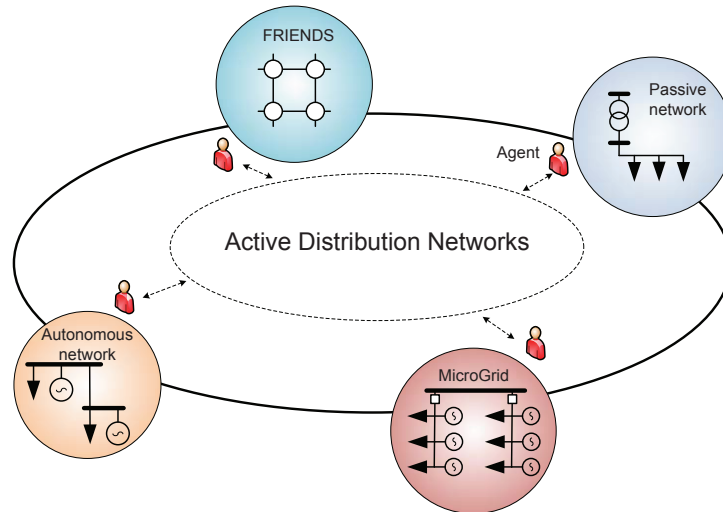
Figure 2.3: Integration of the future networks.

These successful applications have shown their capability to be implemented in a large-scale area of the system. With support of ICT, MAS is expected to enable efficiency, flexibility and intelligence of the future network.

2.3 Active distribution networks

2.3.1 Related definitions

Conventional distribution networks are in itself stable and passive with unidirectional electricity transmission. The term of ADN is introduced recently since the distribution network becomes active with DER and RES units influencing power flows [18]. This concept needs to incorporate flexible and intelligent control based on distributed intelligent systems. Innovative information technologies will be key factors to enable the concept.

A common major feature of ADN is its capability of handling bi-directional power and information flows based on the latest automation, information and communication technologies, as well as on corresponding metering services [69]. Due to the driving aspects of resources, politico-economic context, power infrastructure, and energy policy, particular research areas on ADN in the EU and US are slightly different [70].

As the EU is more focused on creating a highly distributed environment, with the large penetration of DG, there is a need to have a flexible, reliable and accessible distribution grid. A related definition of ADN is identified by CIGRE C6.11 Working Group (WG), as follows [71]:

Definition 2.3.1 *Active distribution networks (ADNs) are distribution net-*

works that have systems in place to control a combination of distributed energy resources (generators, loads and storage). Distribution system operators (DSOs) have the possibility of managing the electricity flows using a flexible network topology. DERs take some degree of responsibility for system support, which will depend on a suitable regulatory environment and connection agreement. ■

In the US and Canada, the term of ADA is more popular to address the future distribution system [72], [73]. In [74], ADA is defined as a highly automated system with a more flexible electrical system operated via open-architecture communications networks. Its major concerns are about communication and control infrastructure, automation of controllable equipment and functions, application of appropriate advanced technologies, integration of DER, modeling and real-time simulation. Security and reliability are identified as crucial factors in the ADA under the step toward the Smart Grids. IEEE Smart Distribution WG is making an effort to bring the ADA concept a step further to Smart Distribution System (SDS) [75], [76].

2.3.2   MAS-based ADN

This thesis elaborates and expands on the novel idea of interconnected ANs proposed by Van Overbeeke [34]. Basically, the AN is built up from several cells, i.e., local sub-networks. Within each cell, an additional control layer is established. Hence, they can operate autonomously as MicroGrid or Autonomous Network. Interconnections among the cells are essential to provide exchange between areas of power supply and demand. Obviously, the transition to AN requires a more meshed configuration of the distribution network. Most investment is needed for control strategies and communication topologies of the power system. In the AN, each cell can provide possible services as follows:

- Self-managing: the cell can reconfigure itself and has black start functionality after a disturbance.

- Local fault management: the cell can locate faults and isolate a cascading phenomenon within its boundaries.

- Voltage control: the cell can monitor and control its local bus voltages to ensure a suitable voltage range for its area.

- Power flow management: the cell can manage power inside and across cell's boundaries.

MAS-based ADN is a more specific application of the AN with the support of MAS technology. As mentioned earlier in Section 2.2.2, MAS can be used for managing autonomous control actions and coordination. Within a cell of MAS-based ADN, controllable components, i.e., controllable generators and loads, inverters, or OLTC transformers will be represented by agents (software) that can operate autonomously with local targets or cooperate with other agents to
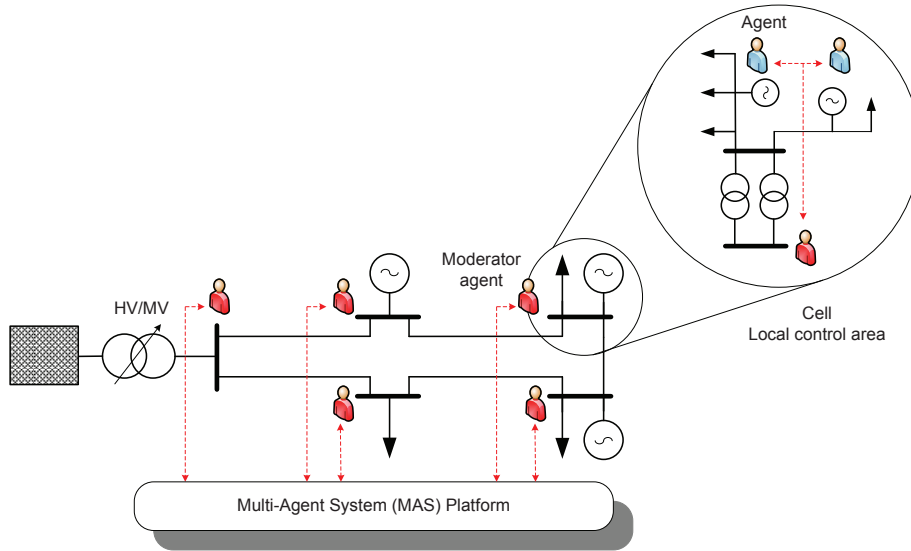
Figure 2.4: MAS-based Active Distribution Network.

achieve area tasks. A superior agent is installed for each cell as a moderator to manage autonomous actions as well as to communicate with other cells.

Figure 2.4 shows a possible configuration of a MAS-based ADN. In this MV meshed network, each substation is considered as a cell and managed by a moderator agent. The zoomed-in part of the substation shows an example of a LV radial network with some DG units. These controllable components are represented by local agents. Communication between local agents and their moderators is deployed by a MAS platform.

Operational structure of MAS-based ADN

When an additional control layer is installed for each cell component, the control architecture of the moderator of the cell has the same functions as a DMS [77]. With the support of the MAS application, the moderator not only concentrates on the autonomous area but also communicates with its neighbors. The two main parts of the control structure of the moderator are DSE and LCS, shown in Figure 2.5. The DSE analyzes the network topology, computes the state estimation, and detects bad data. Depending on the information received from the DSE, the LCS establishes the control set points for the different actuators such as voltage regulation or active and reactive power control of FACTS, local generators and controllable loads.

To enable this autonomous control architecture, MAS technology is an appropriate approach. A hierarchical control structure for MAS-based ADN adapted from [56] is presented in Figure 2.6. In this structure, each agent is considered as an autonomous actor handling three issues: management, coordination,
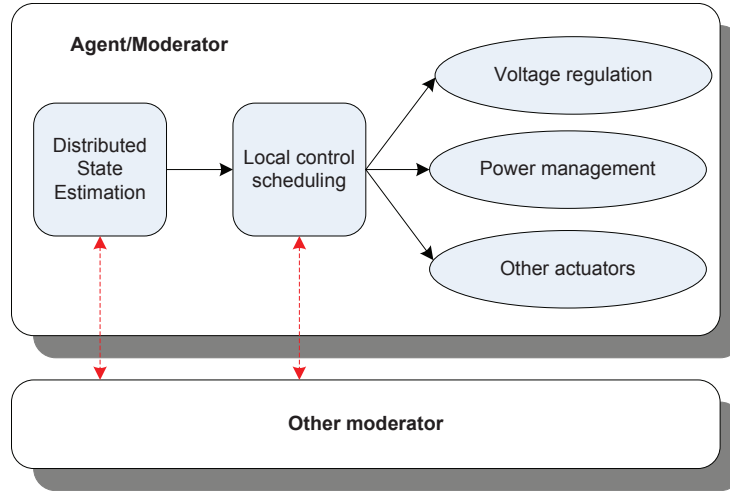
Figure 2.5: Control architecture of the moderator.

and execution. Management is the top layer which performs the objective func-
tion for different control targets, i.e., voltage control, P-Q control, or state
estimation. Depending on the particular situations, the coordination layer de-
fines new control set points as a solution for the given objective functions. The
execution layer activates the control actions regarding the relevant parameters.

According to the proposed structure, the moderator of each cell needs to have
a certain observation level, i.e., critical measurements, to initiate autonomous
control actions. Exchanging information among the cells complements the local
area networks on missing measurements which leads to more accurate state
estimation.

Smart Power Routers - Flexible interfaces

Recently, the concept of an Intelligent Power Router (IPR) is proposed as a new
function in power delivery systems [78]. By connecting to generators, power
lines, or customers, an IPR device not only can observe the current network
condition but can also cooperate with others to find alternative power flow
paths if needed. Mostly, the IPR objective function is only on minimizing load
shedding while satisfying the operating constraints. This simple algorithm has
its limits to reach the optimal operation of a complex system. The application
of Flexible AC Distribution Systems (FACDS) devices for control purposes in
distribution networks enables this concept to get better performance. Though
the application of power electronics needs a high investment cost, it will support
the network operators to maximize the use of the existing network with more
intelligent control functions.

In this thesis, the concept of a smart power router is established as a combi-
nation of an agent (software) and a power flow controller (hardware), as shown

Voltage regulation   Power management   State estimation

Coordination control level

Management	Management	Management
Coordination	Coordination	Coordination
Execution	Execution	Execution

TCP/IP

Autonomous control level

Management	Management	Management
Coordination	Coordination	Coordination
Execution	Execution	Execution

Actuator	Actuator	Actuator

Figure 2.6: ADN operational structure based on MAS.

in Figure 2.7. Each moderator representing a cell can obtain local area information such as the power flow on incoming (outgoing) feeders, power generation and reserves, power load demands, and costs of production and load priority. Besides managing autonomous control actions, this moderator agent can send messages to communicate with the same level agents. The Power Flow Controller (PFC) is an application of AC/DC/AC converters and can act as an intelligent node [79] which controls the power flow for its feeders based on the set points given by the moderator.

With such control functions, the smart power router is expected to create a flexible environment for the future grid. Cells, MicroGrid, Autonomous Network, or others can be integrated in the ADN by the Voltage Source Inverter (VSI) based PFC of this interface. Installing power routers in critical network points (as routers on the Internet) can help to control the power flow actively in order to avoid congestion problems.

2.4   MAS technology

MAS technology is an emerging modern technology which is based on agent-oriented programming (AOP) which is a relatively new concept to translate the conventional artificial intelligence into mainstream of distributed systems [80]. In the last few years, the MAS technology has been developed for a range of applications in power systems [57], [81]. Since the power system is getting more
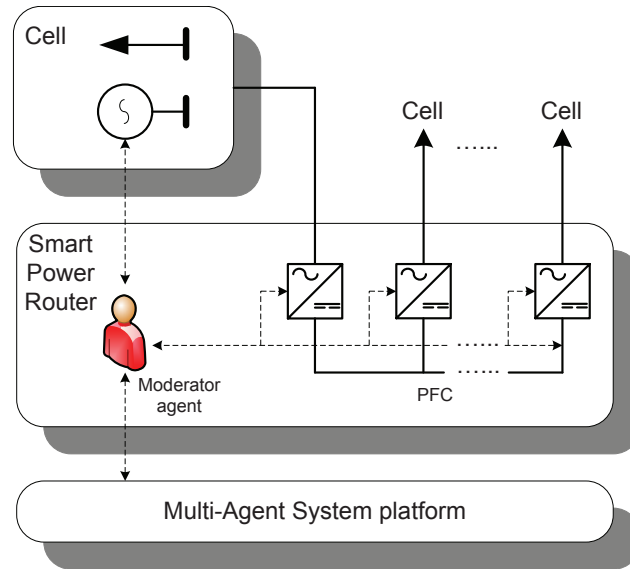
Figure 2.7: Power router configuration.

complex with uncertainties of DER and RES leading to highly dynamic operations and open control architectures, agent-based approach is an appropriate technology to enhance system operation [82]. This section investigates some important aspects of MAS and its adaption in the context of ADN.

2.4.1   Agent definition

Among many definitions of *agency* in the field of MAS, a popular one used in power engineering [83] is adapted with a new definition in [84] as follows:

Definition 2.4.1 *An agent is a software or hardware entity situated in some environment and is able to react to change in its environment (reactivity), be driven by a set of tendencies (pro-activeness), and be able to interact with other agents (social ability). A multi-agent system is a system comprising two or more agents.* ∎

The definition, however does not clearly distinguish the agents from a number of existing software and hardware systems and system engineering approaches [57]. Actually, some systems reveal a part of the agent's features. As an example, an Intelligent Electronic Device (IED) performs various control and protection functions according to changes in their environment, i.e., voltage drop, current increase. It shows a certain degree of *reactivity*, *pro-activeness*, and *social ability*. To make a distinction, Russell and Norvig consider an agent as a tool for analyzing the system instead of an absolute characterization that divides the world into agents and non agents [85]. The next sections explain more about advanced features of the MAS technology.

2.4.2   Agent benefits and challenges

In [57], the authors have summarized some main benefits of the use of MAS technology in power engineering applications as follows:

- *Flexibility*, which is the ability to respond correctly to changing situations. MAS is able to take agents out of operation easily and adds a new one while the others are running.

- *Extensibility*, which is the ability to add new functionality to a system without the need to re-implement the existing functionality.

- *Distribution*, which is the possibility to be placed in different environments and still have the same goals and abilities.

- *Open architecture*, which is the ability to understand different programming languages and to communicate in a flexible way between any agents.

- *Fault tolerance*, which is possibility to seek alternative agents to provide the required services when the appointed agent fails.

On the other hand, there are a number of technical issues to be considered in order to implement MAS technology effectively. They are described briefly as follows:

- *Platforms and toolkits*, which are important to develop agents that are flexible and extensible with an open architecture. There are a number of platforms and toolkits for using MAS technology. Among them, JADE seems to be the most appropriate with ADN application functions.

- *Analysis and design methodologies*, which assist in gaining understanding of a particular system and in designing it. Different methodologies are developed for particular interests. In power engineering applications, the design approach is normally object-oriented which solves some specific problems [81]. A potential drawback of this method might come from interaction with other agents which have different objectives.

- *Communication*, which includes issues of communication languages, data standards and ontologies. The Knowledge Query and Manipulation Language (KQML) is one of the first Agent Communication Language (ACL) to be used by different researchers across different fields. Recently, the Foundation for Intelligent Physical Agents (FIPA)-ACL which complies with JADE has become more popular in power engineering. Although using the same language such as KQML or FIPA-ACL, agents still in some applications misunderstand with others due to lacking of "vocabularies", e.g., substation or circuit breaker definitions. This is the ontology problem when the terms and concepts of the agents are not homogeneous. Furthermore, agents' ontology needs to comply with existing power engineering standards, i.e., IEC 61850 [86], Common Information Model

(CIM), etc., [87]. An Agent-based Unified Modeling Language (AUML) is being developed to support system designers coping with those troubles [88].

- *Security*, which is a trade-off of the agent open architecture. Accidental and malicious attacks might affect not only local power networks but can also spread out rapidly to the whole network. There must be measures to determine the level of trust between agents and the security of messaging.

2.4.3 Agent modeling

As the agent's environment represents some physical components taking actions from and giving perception to the agent, it can be distinguished into two main categories, i.e., *discrete* vs. *continuous*. A system with a finite set of states is considered as discrete and vice versa. For simplification, this research investigates only discrete environments as follows:

$$E = \{e_1, e_2, \cdots, e_n\}$$

In the ADN, the agent's environment consists of physical controllable components of the local area network in which the agent can monitor through sensors or access to data from other sources. The agent autonomous reaction is viewed as a primary control layer which reacts immediately on a change of the system. With *pro-activeness* and *social ability*, these agents are able to flexibly exchange information with others in improve the performance of the local area network.

In general, the decision function of an agent a is separated into *perception*, *deliberation*, and *action* subtasks. The *perception* function computes a percept $p_a \in P_a$ from the system's state E. For example, the *perception* function can identify how much load in a local area network is demanded based on voltage and current measurements. *Deliberation* is the core part of the agent's behavior which defines how the agent uses p_a to compute new internal state $s_a \in S_a$. In the ADN, the *deliberation* function deploys a main algorithm for negotiating an additional amount of power from neighbors to meet the load demand. Finally, the *action* function makes a decision based on s_a and produces the action of a. Figure 2.8 illustrates the agent's behavior modeling and its environment.

2.4.4 MAS control structures

The previous section presented a so called single agent control structure which had access to all actuators and sensors of the network and thus was directly controlling the physical network. With two or more agents, the control structure has more complexity which needs to be categorized into particular interests of the single layer and a hierarchical structure [58]. If all agents consider only their own part of the network and are able to access only sensors and actuators in that particular part of the network, then the MAS structure is referred to as a single-layer structure. When some agents have authority over other agents then the MAS structure is a multi-layer control structure.
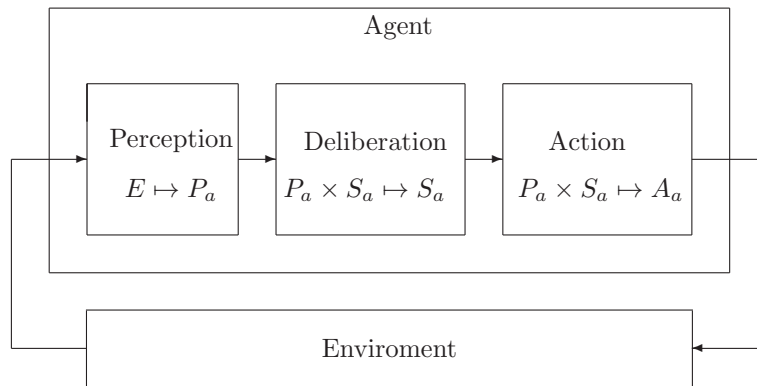
Figure 2.8: Agent modeling.

Single layer structure

Each agent in a single layer structure is restricted to gather information and produce action for a part of the network, as illustrated in Figure 2.9. The agents operate locally as far as possible on local data but still ensure an optimal global target. They are able to decide whether to fulfill a request or to define the priority of a task *autonomously*. As the agents have *social ability* they are able to communicate with each other, information is shared among the agents. It improves the error *tolerance* while a neighboring agent can use this information to take over a part of the responsibility of the action of the failing agent. In addition, the single layer structure allows for *extension* simply by deploying a new agent with the same goals and abilities.

Hierarchical structure

In a hierarchical structure, some superior agents have authority over other agents in the way of monitoring and controlling, as illustrated in Figure 2.10. Therefore, the agents on different levels in the hierarchy have different functions, goals, and abilities. The agents on a higher layer typically take more responsibility and procure slower actions than the agents in lower layers. These superior agents act as coordinators of inferior agents to provide set points, give constraints, or get information. They can also communicate with their same level neighbors as in the single layer structure. In addition, it is *scalable* when they are considered as inferiors of the agents in higher layer.

2.4.5   MAS coordination

Coordination is one of the most attractive features of MAS which enables autonomous system architecture [56]. Regarding the global objective, there are two basic principles of coordination, i.e., cooperation and negotiation.
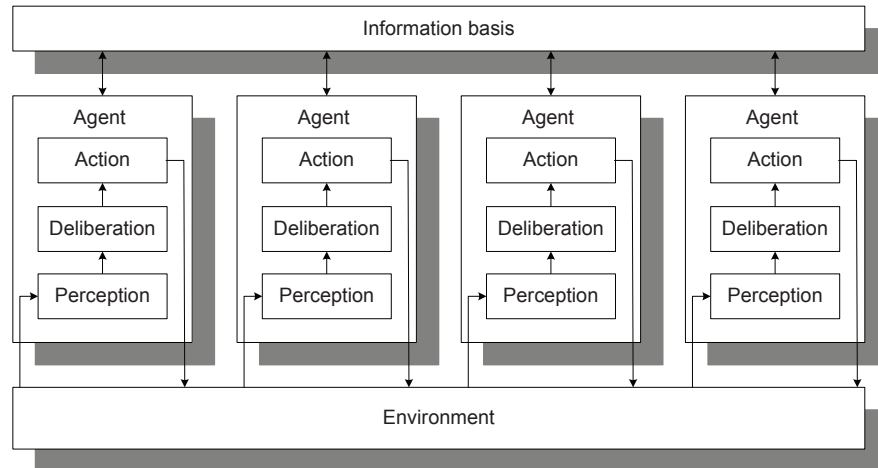
Figure 2.9: Single layer control structure of MAS.

Cooperation

In cases of having similar goals or common problems, cooperation among the agents on the basis of distributed problem solving can be used to achieve the global goal. The economic operation of the ADN belongs to this kind of behavior where MAS makes an effort to get optimal benefits globally. The Contract Net Protocol (CNP) is effective mechanism which provides behaviors of announces, bid, and award cycles for this purpose [89].

Negotiation

In contrast to the cooperation scheme, agents with conflicting goals create a competition where negotiation needs to be applied to maximize the pay-offs of the agents. Technical issues in the ADN are mostly related to this negotiation scheme because local objective functions often conflict with the common goal. For example, an agent starts a negotiation with others when its local load demand increases because it has not enough power reserve to reach the local goal. The negotiation takes generation costs of other neighbors, penalty costs due to power transmission losses, and network constraints into account to optimize between the common and the local objectives.

2.4.6   MAS platform

As mentioned in section 2.4.2, issues of communication language, ontology, toolkits, data standards and interoperability need to be considered when implementing the MAS technology. Nowadays, various agents' platforms have been developed such as Cougar [90], Cybele [91], .NET and Java Agent Development
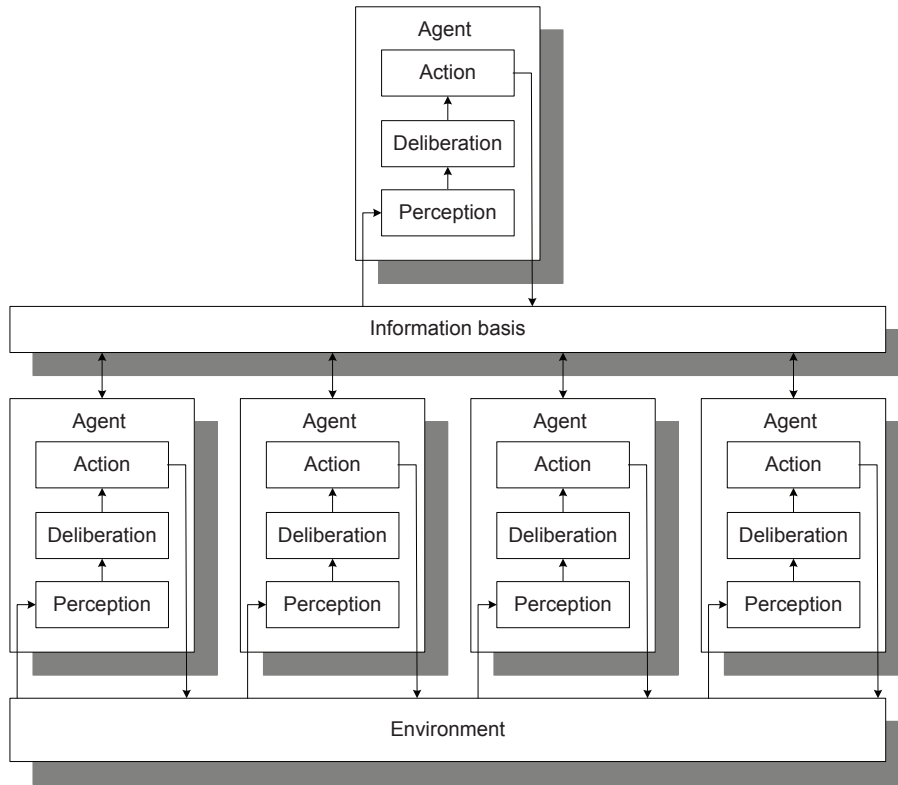
Figure 2.10: Hierarchical control structure of MAS.

Framework (JADE) [92]. JADE is one of the most widespread agent-oriented middlewares. This platform supports a clear design and implementation, has obvious documentation, provides easy deployment of agents on limited devices, operates as completely distributed middleware and has a flexible structure for easy extension with add-on modules [93]. In this research, JADE is selected as the most suitable platform for developing agent-based monitoring and control functions of the ADN.

JADE has a run-time environment for hosting and executing agent functions, a library of classes for programmers to develop their agents and a suite of graphical tools for administrating and monitoring the activity of running agents. A container is a running instance of a JADE run-time environment as it can contain several agents. A set of active containers is called a platform. The main container is a single special container which must always be active in a platform and all other containers register with it as soon as they start. If another main container is started somewhere in the network it constitutes a different platform and to which new normal containers can possibly register. Figure 2.11 gives an impression about the JADE agent platform.
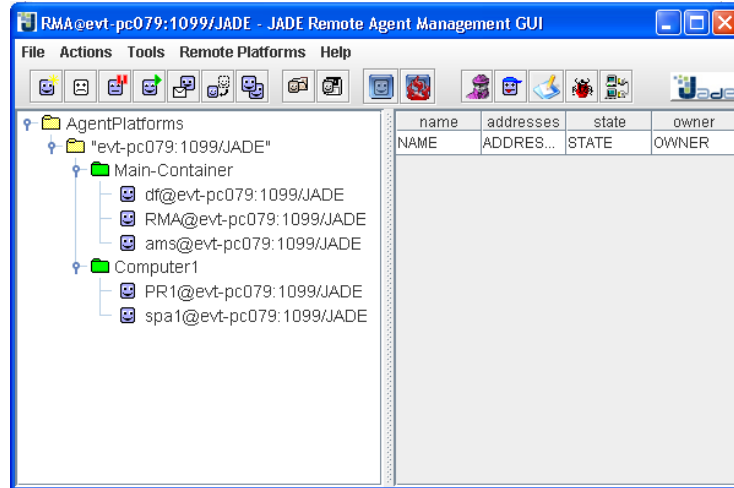
Figure 2.11: An impression of the JADE agent platform.

2.5   Summary

This chapter discusses a particular vision of the future power system was given with its main requirements. An investigation of suitable concepts and technologies which creates a step forward to the smart grid concept has been carried out. They are discussed regarding requirements of sustainability, efficiency, flexibility and intelligence. The ADN is then used as the backbone of the future power delivery system. Besides, MAS is described as a potential technology to cope with the anticipated challenges of future grid operation.

The MAS-based ADN focuses mainly on control strategies and communication topologies for the distribution systems. The transition to the proposed concept does not require an intensive physical change to the existing infrastructure. The main point is that inside the MAS-based ADN, loads and generators interact with each other and the outside world. This infrastructure can be built up of several cells (local areas) that are able to operate autonomously by an additional control layer. Based on a combination of the MAS technology and power electronic devices, these cells can coordinate with each other via flexible interfaces, so called power routers.

The MAS technology is, then explained in more detail. Benefits and challenges of implementing MAS are discussed. It was shown that it is a suitable technology for a complex and highly dynamic operation and open architecture as the ADN. Detailed agent modeling divides agent behaviors into different subtasks, i.e., perception, deliberation, and action. According to particular interests, the introduction of multi agents creates complex control structures which can be categorized to single layer and multi-layer structures. Presenting coordination in MAS addresses additional advantages which makes MAS different from other control systems.

By taking advantages of the MAS technology in a combination with applications of power electronics and distributed controls, the ADN covers mostly functions of other network concepts, i.e., MicroGrid or Autonomous Network. To have a comprehensive view about this concept, following chapters will investigate the monitoring and control aspects of the ADN.

CHAPTER 3

DISTRIBUTED STATE ESTIMATION

Due to the limited amount of collected measurement data and the rather passive way of operating the system, monitoring capabilities of the current distribution network are still under developed. In the previous chapter, the concept of an Active Distribution Network (ADN) based on decentralized operation of local area networks has been introduced. In its control structure, the Distributed State Estimation (DSE) is a crucial component to provide information for control functions in the Local Control Scheduling (LCS).

In this chapter, current state estimation techniques applied in both the transmission and distribution systems will be reviewed. The classical Weighted Least Square (WLS) method is briefly explained. Then will be presented a proposal for a completely decentralized state estimation method suitable for the ADN. The method takes advantage of the Multi-Agent System (MAS) technology to compute iteratively the local state variables through neighbor data measurements. Other aspects of topology analysis, observability, and bad data detection and identification are also considered. The accuracy and complexity of the proposed estimation are investigated through both off-line and on-line simulation. The IEEE 14-bus and 34-bus networks are studied in the off-line simulation while a 5-bus test network is used for the on-line case.

3.1 Introduction

State Estimation (SE) plays a vital role to facilitate real-time monitoring and control functions in the transition of the distribution network from passive to active operation. SE was firstly introduced by Schweppe and Wildes with a classical weighted least square (WLS) method [94]. In an effort to reduce computation burden, several hierarchical state estimation methods are proposed and summarized in [95]. Under the emerging tasks for the network operators on all voltage levels, especially DSE has gained more interests [17].

According to the way of defining network areas, different algorithms of DSE have been particularly proposed. In [96], Ebrahimian and Baldick introduced a robust DSE algorithm based on linearized augmented Lagrangians for overlapping bus boundaries. This method showed practical and realistic performances. In [97], a straightforward and effective algorithm for overlapping tie-line boundaries was presented by Conejo et al. The method applies iteration steps to estimate local state variables as long as the boundary state variables do not change significantly. A global state estimation for both the transmission and distribution systems proposed in [98] by Sun and Zhang is also based on the iteration technique. A concept of an ultra fast decentralized state estimation for the whole electric power system was presented in [99] by Zaborsky et al. Given at each bus a microprocessor, the bus state variables can be calculated by processing local bus information and its neighbour information. With the support of an adequate communication system, this method can increase significantly the computation speed.

In a different approach, the extended Kalman filtering (EKF) theory has been applied for network parameter estimation [100], static state estimation [101], and dynamic (continuous) state estimation [102]. However, EKF needs to collect recursively time-historic data, update covariance vectors and treat heavy computation matrices. Those steps limit the application of EKF in a real large-scale power system.

A DSE based on the concept of a MAS, i.e., an application of information and communication technologies, was presented in [103] by Nordman and Lehtonen. By exchanging messages among bus agents, the method has shown significant advantages in state estimation, bad data detection and identification steps. However, the research has just illustrated the feasibility of the concept with current sensors.

Along with the development of new network concepts, i.e., MicroGrid [6], [7], Smart Grid [41], [40], there is an increasing need to have an adaptive state estimation method to enhance distributed monitoring and control functions. In [104], the SuperCalibrator concept is introduced which is based on a statistical estimation process that fits GPS-synchronized measurements and all other available data into a three-phase, breaker oriented, instrumentation inclusive model suitable for decentralized state estimation using substation data of the grid.

This chapter elaborates the concept of a Completely Decentralized State Estimation (CDSE) method according to reference [99] and integrates the novel aspect of a MAS based solution in [103]. The main emphasis of the proposed method is related to utilizing the advantages of MAS application and iteration techniques to improve the performance of the state estimation suitable for use in the ADN concept. More precisely, we assume having one agent at each network bus (or cell in the ADN) to deploy the DSE algorithm. A local step of state estimation yields local state variables of neighbor buses which will be sent to the neighbors under the MAS platform. Since the agent receives new estimated variables, it compares with its own data based on the maximum likelihood estimation. Off-line simulations are created under Matlab scripts to investigate the accuracy of the proposed method compared to the classical WLS

static state estimation. To fully reveal advantages of the MAS technology, an on-line simulation, in which the proposed method works continuously during the simulation time, is deployed under Simulink and the JADE platform.

Main contributions of the chapter are related to:

- The use of local measurements instead of the complex global data.

- The use of an asynchronous algorithm in which each agent process the algorithm locally, and does not have to wait others. The algorithm allows some agents having faster and executing more iterations than others.

- The use of MAS technology which allows the state estimation implementing in the on-line applications.

3.2 Background of state estimation

3.2.1 Weighted Least Square state estimation

This section gives a brief description about the classical WLS estimation. A detailed explanation of the method is presented in [94], [105].

Basic idea of SE is to determine the most likely state of the system based on the quantities that are measured. Maximum Likelihood Estimation (MLE) is a statical method widely used. The MLE function is given as joint probability density function as follows:

$$f_m(z) = f(z_1)f(z_2)\cdots f(z_m) \tag{3.1}$$

where:

$$z_i: \text{ith measurement,}$$
$$z^T: [z_1, z_2, \ldots, z_m].$$

Each measurement is considered as a Gaussian probability density function $N(\mu_i, \sigma_i^2)$ defined by following equation:

$$f(z_i) = \frac{1}{\sqrt{2\pi}\sigma_i} e^{-\frac{1}{2}\{\frac{z_i-\mu_i}{\sigma_i}\}^2} \tag{3.2}$$

where μ_i is mean or expected value of z_i; σ_i is standard deviation of z_i.

For simplicity, the above objective function is replaced by its logarithm that is the so called Log Likelihood Function (LLF):

$$L = \log f_m(z) = -\frac{1}{2}\sum_{i=1}^{m}\left(\frac{z_i-\mu_i}{\sigma_i}\right)^2 - \frac{m}{2}\log 2\pi - \sum_{i=1}^{m}\log \sigma_i \tag{3.3}$$

The objective of the MLE is to maximize this function by varying the mean value μ_i and standard deviation σ_i of the density function which leads to the

following problem:

$$\text{maximize:} \quad \log f_m(z)$$

$$\text{or,}$$

$$\text{minimize:} \quad J(x) = \sum_{i=1}^{m} \left(\frac{z_i - \mu_i}{\sigma_i} \right)^2 \tag{3.4}$$

$$\text{subject to:}$$

$$z_i = h_i(x) + r_i; i = 1, \dots, m \tag{3.5}$$

where x is the system state vector; $h_i(x)$ is the non-linear function relating the measurement z_i to the state vector; r_i is the residual for the measurement z_i.

The equation 3.4 can be rewritten in a general form of the WLS as follows:

$$\text{minimize:} \quad J(x) = \sum_{i=1}^{m} \frac{z_i - h_i(x)^2}{R_{ii}}$$

$$= [z - h(x)]^T \mathbf{R}^{-1} [z - h(x)] \tag{3.6}$$

where $\mathbf{R}$ is the variance vector of the measurement errors:

$$\mathbf{R} = diag\{\sigma_1^2, \sigma_2^2, \dots, \sigma_m^2\}.$$

The application of a Gauss-Newton method for finding the non-linear optimal conditions leads to an iterative solution as shown here:

$$\Delta x^{k+1} = [\mathbf{G}]^{-1} \mathbf{H}^T(x^k) \mathbf{R}^{-1} [z - h(x^k)] \tag{3.7}$$

$$\text{where:}$$

$$\mathbf{H}(x^k) = \frac{\partial h(x^k)}{\partial x^k} \text{ is the Jacobean matrix,} \tag{3.8}$$

$$\mathbf{G} = \mathbf{H}^T(x^k) \mathbf{R}^{-1} \mathbf{H}(x^k) \text{ is the Gain matrix.} \tag{3.9}$$

3.2.2   Distributed state estimation

The computation of the gain matrix for a large-scale power system is extremely heavy, which limits the application of the WLS method only to transmission systems. Hence, several improvements were proposed to reduce the computation burden, for instance, a decoupled formulation or DC estimation. For the same purpose, the centralized state estimation problem formulated by equation 3.6 can be replaced by a decentralized state estimation problem as follows [97]:

$$\text{minimize:} \quad \sum_{a=1}^{n} J(x_a) + \sum_{a=1}^{n} \sum_{b \in B(a)} J(x_a, x_b) \tag{3.10}$$

where x_a is the state variable vector of the network area and x_b is the state variable vector of the boundary.
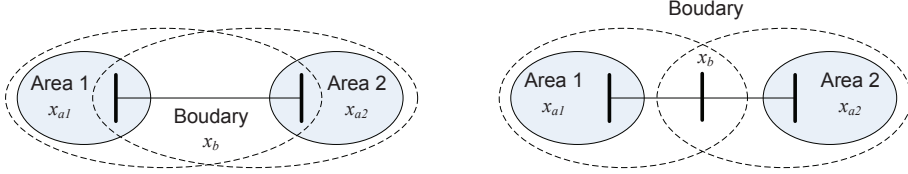
Figure 3.1: Possible ways of defining sub-networks for the DSE solutions.

By dividing the centralized state estimation problem into smaller decentralized objective functions, the local state estimation can be implemented with scaled down size of the computation matrices. According to the way of defining sub-networks (including tie-lines or not), there are particular solutions regarding the information exchange and objective of the coordination layer. Figure 3.1 illustrates possible definitions of the boundaries of the sub-networks (cells) for the DSE solutions.

3.3   MAS-based state estimation

This section describes a different DSE method, CDSE, which reduces drastically the size of the matrices and computational effort. The idea of CDSE was firstly proposed by Zaborszky et al. [99]. The method is based on the assumption of having a dedicated microprocessor at each local bus. Hence, the bus local state variables can be estimated by neighbor bus information. Depending on the accuracy requirements, the method offers three grades of estimation. While the 1st grade uses over-simplified algebraic equations to estimate ultra fast the state variables, the 3rd grade considers all correlations of the variables on a central computer to get the most accurate values. The 2nd grade estimation, which lies in between, can be obtained relative fast with a considerable accuracy. In addition, it can be implemented straightforward in a distributed way. Because of the compatibility with the concept of the ADN, the 2nd grade estimation is used as a basic formulation for the proposed CDSE.

When the ADN is based on a MAS control structure, SE plays a vital role to enable the actuators in the control system of the ADN. Depending on the control stages, i.e., cell control level, or ADN control level, the SE of the sub-network (cell) processes its own real-time and pseudo-measurement information and coordinates with neighbors to get the whole network state variables.

A state estimation scheme among cells is shown in Figure 3.2. The SE agent of each cell performs three functions. Firstly it collects measurements of the local network area, for example $[V_i, P_{ij}, Q_{ij}]$. In case of lacking of measurements, pseudo-measurements are added.

These data are used in the coordination phase to estimate state variables for the neighbor cells, for instance, $[V_j^i, \theta_{ij}]$. With the knowledge about the line impedance from i to j, the state variables $[V_j^i, \theta_{ij}]$ can be computed straightforward by a classic WLS method through equation 3.6 and 3.7. The variances of
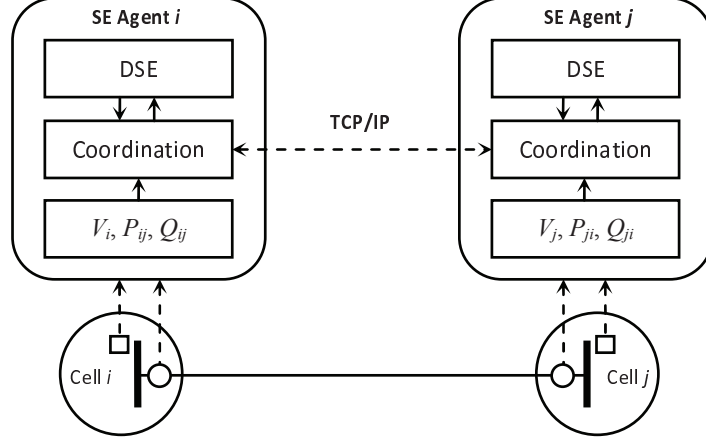
Figure 3.2: Agent-based distributed state estimation.

these local state variables, $[\sigma_j^i, \tau_{ij}]$, can be obtained by the diagonal elements of $[G^{-1}]$ [106]. Note that the size of the gain matrix in this case is just $[3x3]$. For further computation, these state values with their variances are then considered as "pseudo-measurement" values with a Normal distribution:

$$N(V_j^i, \sigma_j^{i\,2}) \; ; \text{ and } N(\theta_{ij}, \tau_{ij}^2).$$

As the coordination function allows exchanging the information between the cells, each cell will have a list of "pseudo-measurement" data as follows:

$$[V_i^{meas}, V_i^1, \ldots, V_i^{m_i}, \theta_{i1}, \ldots, \theta_{im_i}]$$

with their variances:

$$[\sigma_i^{meas}, \sigma_i^1, \ldots, \sigma_i^{m_i}, \tau_{i1}, \ldots, \tau_{im_i}]$$

where m_i is a number of the neighbor cell connected to cell i; V_i^{meas} and σ_i^{meas} are real-time measurements (or pseudo-measurements) of the voltage magnitude at the reference bus of cell i.

These data arrays are sent to the management layer which deploys the DSE function. Regarding the voltage magnitude data, the state estimation of equation 3.6 is then rewritten as:

$$\text{minimize: } J(\overline{V_i}) = \frac{\left(V_i^{meas} - \overline{V_i}\right)^2}{\mathbf{R}_{V_i}^{meas}} + \sum_{j=1}^{m_i} \frac{\left(V_i^j - \overline{V_i}\right)^2}{\mathbf{R}_{V_i}^j} \qquad (3.11)$$

where:

$$\mathbf{R}_{V_i}^{meas} = \sigma_i^{meas\,2} \; ; \text{ and } \mathbf{R}_{V_i}^j = \sigma_i^{j\,2}.$$

It leads to the maximum likelihood estimation as follows:

$$\overline{V_i} = \frac{\frac{V_i^{meas}}{\mathbf{R}_{V_i}^{meas}} + \sum\limits_{j=1}^{m} \frac{V_i^j}{\mathbf{R}_{V_i}^j}}{\frac{1}{\mathbf{R}_{V_i}^{meas}} + \sum\limits_{j=1}^{m} \frac{1}{\mathbf{R}_{V_i}^j}} \tag{3.12}$$

Similarly, the maximum likelihood estimation for the bus voltage angles is formed by the following equation:

$$\overline{\theta_{ij}} = \frac{\frac{\theta_{ij}}{\mathbf{R}_{\theta_{ij}}} + \frac{\theta_{ji}}{\mathbf{R}_{\theta_{ji}}}}{\frac{1}{\mathbf{R}_{\theta_{ij}}} + \frac{1}{\mathbf{R}_{\theta_{ji}}}} \tag{3.13}$$

where:

$$\mathbf{R}_{\theta_{ij}} = \tau_{ij}^2.$$

These new local state variables are compared with the prior values, i.e., $[V_i^0, \theta_{i1}^0, \ldots, \theta_{im}^0]$. If there are no big changes, the algorithm stops. Otherwise, it updates the new local state variables as the prior state variables and sends backward information to the coordination layer to repeat the iterative loop until the local state variables converge. This proposed CDSE can be considered as an overlapping bus boundary type of DSE.

In Algorithm 3.1, the pseudo-code of estimation agent A_i is shown with two operation modes. The first mode is to update the local measurements from the power network and to exchange these data to the agent's neighbors by sending *Information* messages. In the second mode, the agents receive the *Information* messages and adapt these with their local data. When the agents update the information completely, they estimate their new state variables by equation 3.12 and 3.13. The second mode deploys the algorithm of DSE until it converges.

As can be seen from the proposed DSE procedure, the coordination task is performed before the local state estimation is done while most other DSE methods act in a contrary direction.

3.3.1 Topology analysis

On ADN level, the proposed DSE considers each cell as a bus. An overall topology analysis is then performed by examining of the interconnection line measurements. The operation status is defined with the criteria described in [17].

Agent A_i checks if the local current measurement indicates a topology change $\langle I_{ij} = 0 \rangle$, then it sends a *query-if* message to the neighbor agent A_j. After receiving the message, A_j checks its local current measurement and defines the status of branch $i-j$. This status is then sent to A_i by a *confirm* message. The message sequences for each interaction are illustrated on the sequence diagram in Figure 3.3.

Algorithm 3.1 Pseudo-Code for A_i actions in the CDSE method

$Receivede(Mode) \leftarrow Message(objective)$
if $Mode = 1$ **then**
    $Initialize()$
    $A_i \leftarrow Measurements(V_i, \theta_{ij}, P_{ij}, Q_{ij})$
    $A_i \leftarrow Update(V_i, \theta_{ij}, P_{ij}, Q_{ij})$
    $Information(V_i, \theta_{ij}, P_{ij}, Q_{ij}) \rightarrow neighbor_i$
end if
if $Mode = 2$ **then**
    $(V_i^j, \sigma_i^{j^2}); (\theta_{ij}, \tau_{ij}^2) \leftarrow Information(V_j, \theta_{ji}, P_{ji}, Q_{ji})$
    if (complete update) **then**
        $(\overline{V_i}, \overline{\theta_{ij}}) \leftarrow (V_i^j, \sigma_i^{j^2}, \theta_{ij}, \tau_{ij}^2); \forall j \in m_i$
        if $(\overline{V_i}, \overline{\theta_{ij}}) = (V_i^0, \theta_{ij}^0); \forall j \in m_i$ **then**
            Stop
        else
            $(V_i^0, \theta_{ij}^0) = (\overline{V_i}, \overline{\theta_{ij}})$
            $Information(V_i^0, \theta_{ij}^0, P_{ij}, Q_{ij}) \rightarrow neighbor_i$
        end if
    end if
end if
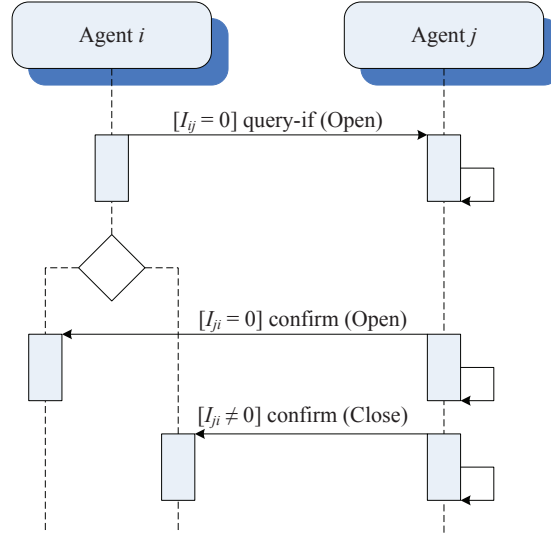
Figure 3.3: Sequence diagram for topology analysis between areas.

3.3.2   Observability analysis

In the DSE methods, the observability is normally determined by investigating a minimum spanning tree [17]. The power flow measurements are used to form the

spanning tree. In case of lacking power flow measurements, the power injection measurements are used.

The proposed method can determine the observable branches by exchanging the local measurements between two nodes. Then, the power system is converted into a directed graph $\mathcal{G}(V, E)$, in which $V = \{v_1, \ldots, v_n\}$ presents the set of vertices (buses in the power system) and $E \in V \times V$ presents edges e_{ij} if the branch $i - j$ is observable. The edge length (edge cost) c_{ij} is associated with a number of measurements on bus i, bus j, and branch $i - j$ and the function of the branch. A shortest path algorithm of the graph theory is used to find the minimum spanning tree of $\mathcal{G}(V, E)$ [107].

3.3.3 Bad data detection and identification

In the proposed method, the maximum likelihood estimation is implemented to estimate the local state variables. Consequently, a bad data detection and identification can be applied straight forward by each bus agent.

A popular technique, the Chi-squares χ^2-test, is simply made by forming the square of the computed state variables as follows:

$$y_i = \frac{\left(\overline{V_i} - V_i^{meas}\right)^2}{\mathbf{R}_{V_i}^{meas}} + \sum_{j=1}^{m_i} \left(\frac{\left(\overline{P_{ij}} - P_{ij}^{meas}\right)^2}{\mathbf{R}_{P_{ij}}} + \frac{\left(\overline{Q_{ij}} - Q_{ij}^{meas}\right)^2}{\mathbf{R}_{Q_{ij}}} \right) \quad (3.14)$$

where:

$g_{ij} + jb_{ij}$ is the admittance of the series branch connecting buses i and j,

$g_{si} + jb_{si}$ is the admittance of the shunt branch connecting bus i,

$\overline{P_{ij}} = \overline{V_i}^2 \left(g_{si} + g_{ij}\right) - \overline{V_i V_j} \left(g_{ij} \cos \overline{\theta_{ij}} + b_{ij} \sin \overline{\theta_{ij}}\right),$

$\overline{Q_{ij}} = -\overline{V_i}^2 \left(b_{si} + b_{ij}\right) - \overline{V_i V_j} \left(g_{ij} \sin \overline{\theta_{ij}} - b_{ij} \cos \overline{\theta_{ij}}\right).$

When one of χ^2 distribution values is over the threshold of bad data detection, the local state estimation is suspected.

The bad data identification is then started based on the largest normalized residual test. The normalized residuals of all "pseudo measurement" data are calculated by following equations:

$$r_{V_i}^N = \frac{\left| V_i^{meas} - \overline{V}_i \right|}{\sqrt{\mathbf{R}_{V_i}}} \quad (3.15)$$

and,

$$r_{\theta_{ij}}^N = \max \left(\frac{\left| P_{ij}^{meas} - \overline{P_{ij}} \right|}{\sqrt{\mathbf{R}_{P_{ij}}}} ; \frac{\left| Q_{ij}^{meas} - \overline{Q_{ij}} \right|}{\sqrt{\mathbf{R}_{Q_{ij}}}} \right) \quad (3.16)$$

The "pseudo measurement" with the highest value for the normalized residual will be regarded as bad data and removed. The χ^2 test is investigated again and repeated until no more bad data is detected. This procedure is depicted in Figure 3.4.
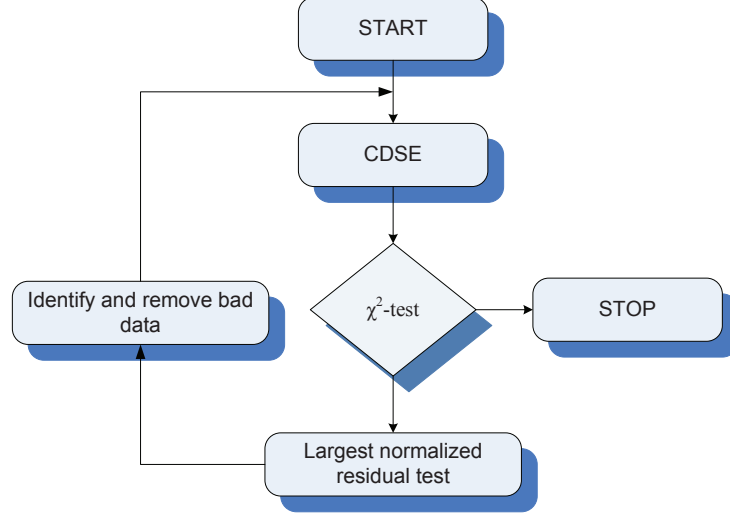
Figure 3.4: Flow chart of bad data detection and identification.

3.3.4   Algorithm properties

This proposed CDSE method can be considered as a specific case of the overlapping bus boundary type of DSE [96], [108], in which the state estimation aims to force state variables in overlapping areas to assume the same values. A general convergence theorem of these asynchronous iterative algorithms is well described in [109]. In [17], a specific convergence analysis of parallel and distributed state estimation is introduced. That convergence analysis is adapted to a general form of the distributed state estimation proposed in this paper which is formulated as follows:

$$x_i(k+1) = Sx_i(k) + SR_i(x_i(k))\mathbf{R}_i\mathbf{X}_i^T(t); \forall i = 1, \ldots, n \qquad (3.17)$$

where:

$\mathbf{R}_i$: is the row i in the covariance matrix $\mathbf{R}$ in the iteration $k+1$,

$R_i(x_i(k))$: is average variance value of $\mathbf{R}_i$ in the iteration k,

$\mathbf{X}_i^T(t) = [x_i(\tau_i^1(t)), \ldots, x_i(\tau_i^{m_i}(t))]$,

$$S = \left(\frac{\frac{1}{R_i^{meas}}}{\frac{1}{R_I^{meas} + \sum_{j=1}^{m_i} \frac{1}{R_i^j}}} \right).$$

Note that $x_i(\tau_i^1(t))$ is estimated value of x_i by agent at bus j and transmitted to bus i at the time $\tau_j^i(t)$. As an asynchronous iterative algorithm, the CDSE method allows value of $\tau_j^i(t)$ varying in the range of $[0, t]$. It is the synchronous distributed state estimation if for any bus i and j, there is exists $\tau_j^i(t) = t$ [17].
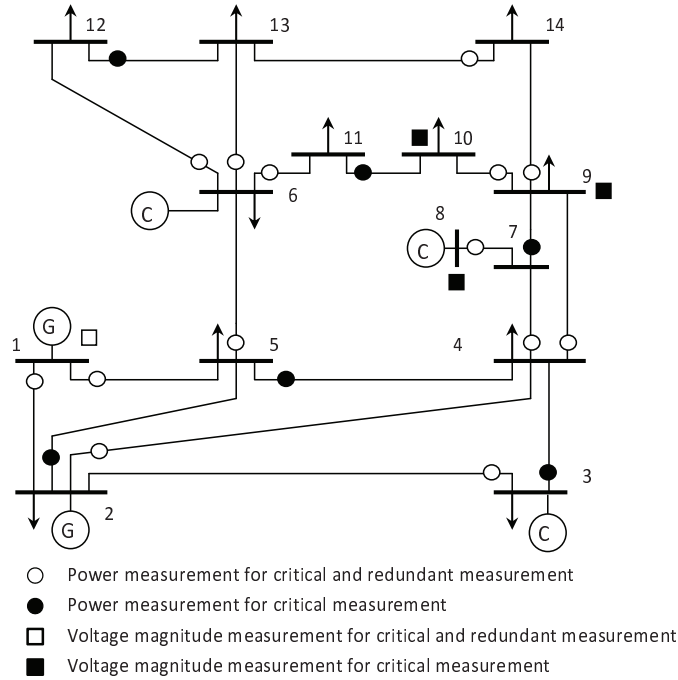
Figure 3.5: Single-line diagram of the IEEE 14-bus test network.

Equation [3.17] is based on condition of the variance matrix $\mathbf{R}$ for pseudo-measurements which is obtained by the diagonal elements of $\mathbf{G}^{-1}$. Its diagonal dominant characteristic guarantees the convergence of the CDSE algorithm [17], [110].

3.4   Case studies

To investigate practical applications of the proposed CDSE method, both off-line and on-line simulations are performed. In the off-line simulation, the proposed algorithm is implemented under Matlab scripts. The simulation aims to compare the accuracy of the new method with the classical WLS estimator. The on-line simulation is implemented to see the detailed interaction between MAS and the power system. During the simulation time, measurement data will be collected and exchanged on the MAS platform. Representative agent of each bus in the test network will perform the proposed algorithm completely in a decentralized way. It is deployed under a framework of Matlab/Simulink and JADE [92].
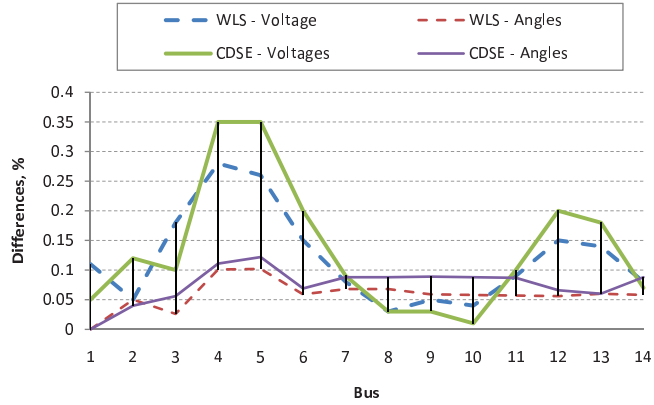
(a) Differences of estimations from true values and convergence.
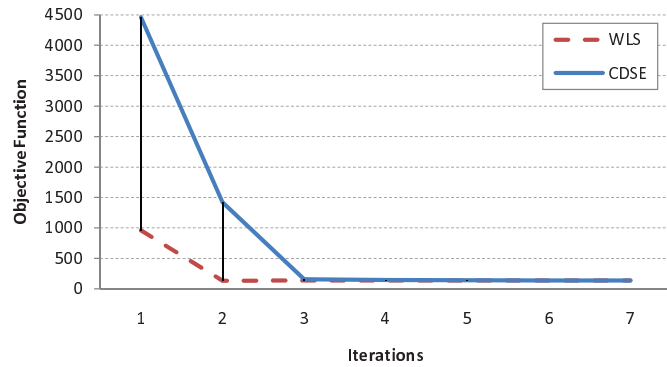
(b) Convergence of the objective function.

Figure 3.6: Case of redundant measurements.

3.4.1 Off-line simulation

The off-line model investigates both meshed and radial network configurations. The IEEE 14-bus (meshed configuration) [111] and 34-bus (radial configuration) [112] networks are used for the investigation of several case studies.

Meshed configuration

The IEEE 14-bus network, as shown in Figure 3.5, is used for the investigation of several case studies. The effectiveness and computation speed of the proposed algorithm are compared with the conventional WLS method.

The proposed method is investigated with redundant measurements, i.e., 4 voltage magnitude measurements (at bus 1, 8, 9, and 10) and power flow measurements on all lines (20 lines). Results of the proposed method are compared

with the conventional WLS method and the true values, which are the results of a power flow computation. The percentile differences of the estimation from the true values are depicted in Figure 3.6(a). As can be seen from the figure, the CDSE can come reasonably close to the true values with an estimation error smaller than 0.4%. It is comparable with the performance of the conventional WLS method.

Figure 3.6(b) presents the change of the minimized objective function $J(x)$ in equation 3.11 along with the iterations. In this case, the CDSE takes 7 steps to get convergence which means that the tolerance is less than $10^{-6} p.u.$ Please note that the proposed algorithm operates in a distributed and parallel way. Observable iterations belong to the slowest agent while others might achieve convergence much faster. But after all, the threshold value of the objective function is reached just after 3 iterations.

A case of critical measurements is tested with one voltage bus measurement (at bus 1) and power measurements on 14 lines. Figure 3.7(a) shows the differences of CDSE and WLS estimation from the true values. While the WLS method keeps almost the same estimation error, CDSE is impacted slightly because of missing voltage magnitude measurements. However, the maximum estimation error is still smaller than 0.6%.

Figure 3.7(b) shows the convergence process of CDSE and WLS methods in case of the critical measurements. Due to missing of essential voltage magnitude measurements, CDSE yields quite large values for the objective function in the first iterations. It can be understood by the distributed characteristic of the method. Correct estimated voltage magnitudes need some iteration steps to spread out to the whole network. The method reaches convergence within 4 iterations when the impact of exchanging information is broad enough.

With the redundant measurements as mentioned in the first case as starting point, the influence of bad data with 15% difference from measured data is included in 5 measurements as shown in Table 3.1. After finishing the procedure of DSE, each bus agent starts detecting and identifying bad data. The Chi-squares χ^2-test finds 8 suspected buses. The normalized residuals of all measurements belonging to these suspected buses are computed and compared to find out the maximum value, which is the bad measurement. In this case, V_9 is firstly identified. Consequent steps are summarized in Table 3.2.

Table 3.1: Bad data included in measurements of the IEEE 14-bus test network

Measurements	Without bad data	With bad data	Bad data elimination
V_9	1.051	1.09	1.0504
P_{4-9}	0.1610	0.1852	0.1611
Q_{9-10}	0.0282	0.0310	0.0240
P_{9-14}	0.0953	0.1096	0.0948
Q_{9-14}	0.0271	0.0312	0.0260

Figure 3.8 shows the impact of bad data on the state estimation and the effectiveness of the bad data detection and identification. Before eliminating
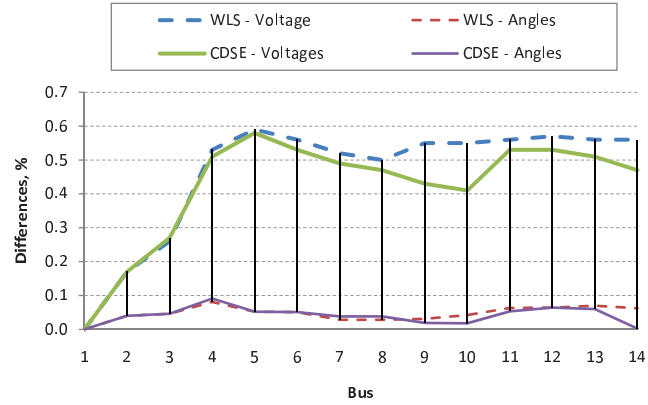
(a) Differences of estimations from true values and convergence.
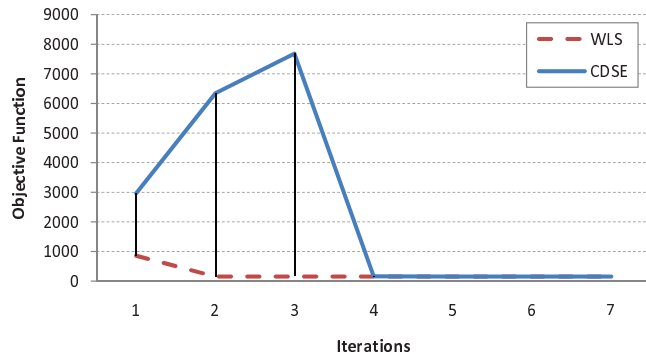
(b) Convergence of the objective function.

Figure 3.7: Case of critical measurements of the IEEE 14-bus test network.

Table 3.2: Bad data detection and identification procedure of the IEEE 14-bus test network

Iteration	Eliminated measurements	r_{max}^N
1	V_9	16.61
2	P_{4-9}	2.99
3	Q_{9-10}	2.62
4	P_{9-14}	2.26
5	Q_{9-14}	1.39

the error measurements, the differences in estimation are more than 2% at some buses. The procedure of bad data detection and identification improves significantly the accuracy of the estimation which is below 0.5% finally.
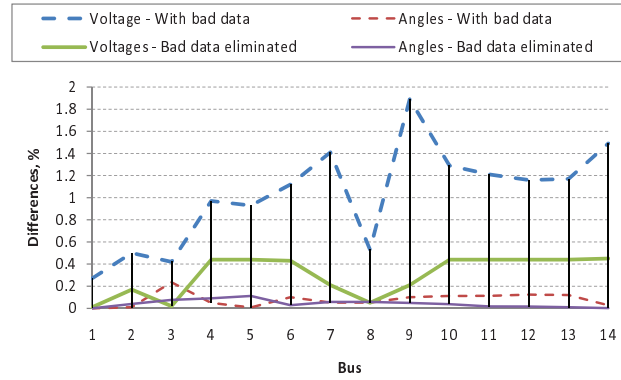
Figure 3.8: Differences of estimations from true values before and after bad data eliminated of the IEEE 14-bus test network.

Radial configuration

Due to the fact that the distribution networks are lacking measurement data, only the case of critical measurements is considered in the IEEE 34-bus radial test network. It is assumed to have 3 voltage magnitude measurements (at bus 1, 9, and 24) and the power flow measurement on all 32 lines. Figure 3.9 shows the single-line diagram of the IEEE 34-bus test network.
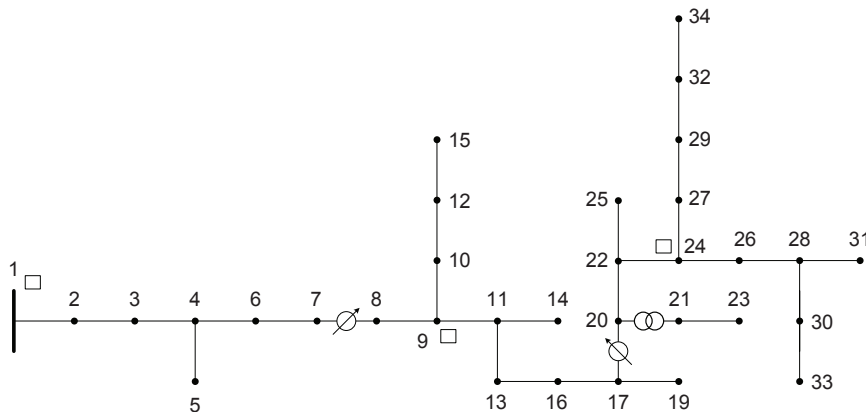
Figure 3.9: Single-line diagram of the IEEE 34-bus test network.

Figure 3.10(a) shows that the proposed CDSE method can give estimated values with the percent differences below 0.05%. Although having relative accurate estimated voltage angles, the CDSE is slightly vulnerable with estimated voltage magnitudes because of lacking overlap information among agents of the

buses. This leads to 16 iterations to acquire the convergence, as can be seen in Figure 3.10(b).
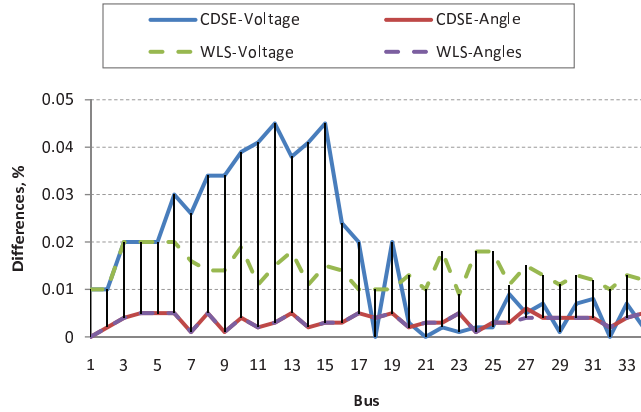
(a) Differences of estimations from true values and convergence.
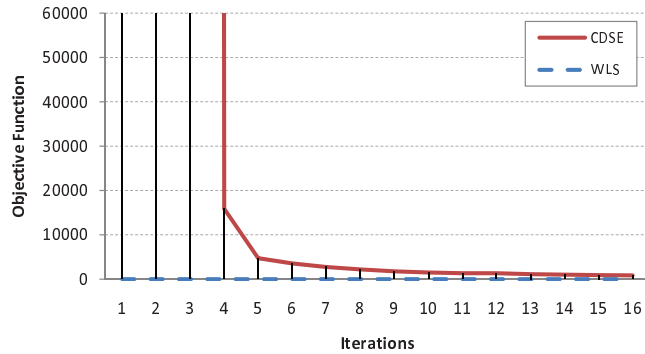
(b) Convergence of the objective function.

Figure 3.10: Case of redundant measurements of the IEEE 34-bus test network.

3.4.2   On-line simulation

An on-line simulation is performed with a 5-bus test network, as shown in Figure 3.11, under a Matlab/Simulink and JADE platform. Data of the 5-bus test network are provided in Table 3.3 and 3.4. In the Matlab/Simulink simulation, each bus of the 5-bus network consists of an embedded function block. The embedded function block is a part of the agent which is connected with the MAS platform (JADE). The local measurements of each bus are transferred through this block to be processed at the MAS platform.

Table 3.3: 5-bus test network - Bus data

Bus	Voltage set point	Generation		Loads	
	p.u.	MW	MVAr	MW	MVAr
1	1.05	-	-	5	2
2	1.02	10	-	10	4.5
3	1.02	10	-	10	4.5
4	-	-	-	5	2.5
5	-	-	-	5	2

Table 3.4: 5-bus test network - Line data

	R	X	B
	p.u.	p.u.	p.u.
All lines	0.625	0.445	8.3e-4
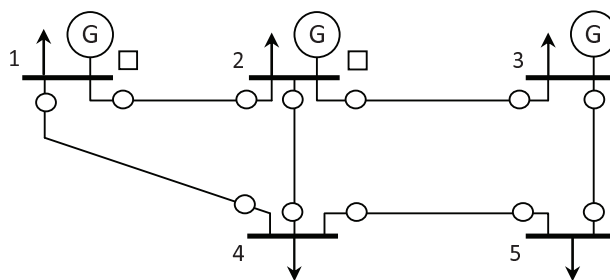
Figure 3.11: Single-line diagram of the 5-bus test network.

Normal operation with measurement noise

Under normal operation, the bus voltages and real power flows are at relatively steady-state values. Those values, however, are distorted by noise from bad data sources, i.e., measurements devices, or communication channels. They cause so called variances and bad data for estimation. In this simulation, the measured data of the bus voltages and power flows are polluted with distributed random fluctuations, 0.004 and $0.008p.u.$ respectively. In addition, 15% deviations from the standard values are injected in V_2 and P_{23} as a bad data effect. These data are shown in Figure 3.12.

Through the embedded function, 100 samples of each measured data are collected to generate the mean and standard deviation of the normal distribution. Pseudo-measurements are used to replace missing measurements by pre-defined values with large variance. These data are then transferred to the MAS platform to deploy the algorithm of DSE. The communication period, i.e., from the first time of sending information to the MAS platform to the second one, is about $40ms$.

Figure 3.13 shows the results of the simulation after $200ms$. In the first
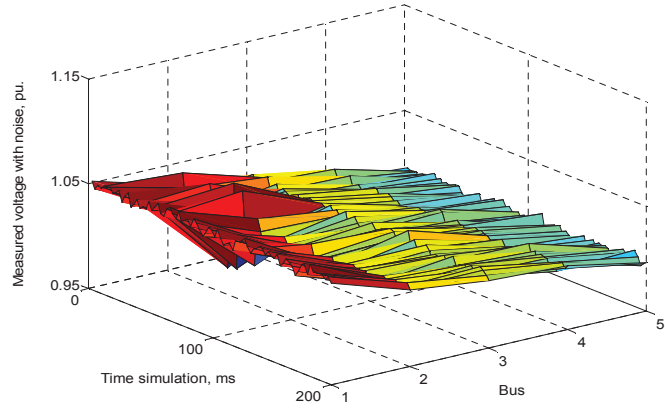
(a) Voltage bus measurements.
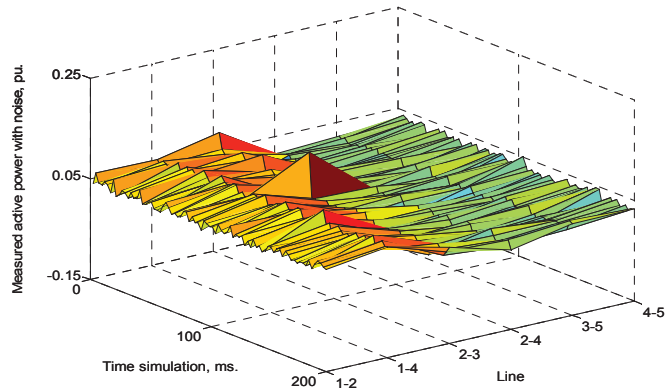
(b) Active power measurements.

Figure 3.12: Measurement data with noise in case of normal operation.

period, $0 - 80ms$, the embedded functions gather measured data and generate information for the MAS platform. The values shown in this period are the differences between the true values and pre-estimated values. These pre-estimated values might be the nominal values or can be taken from a previous stage of estimation. In the period from $80 - 120ms$, estimated data are obtained. Note that these values are estimated taking into account bad data. After $120ms$, new estimation values are yielded when the bad data are detected and removed. At the end of the simulation, the voltage differences and the active power differences from the real values are less than 0.1%.

Network topology change

At $t = 10ms$, the switches at two ends of the line 2-4 open. Consequently, there is no power flow through line 2-4, as shown in Figure 3.14. In the two first
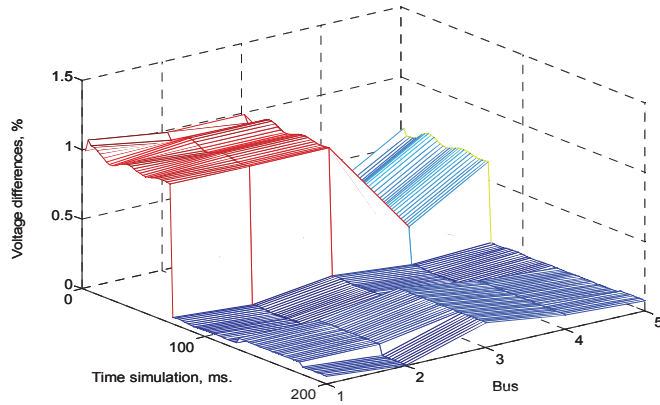
(a) Voltage bus estimation.
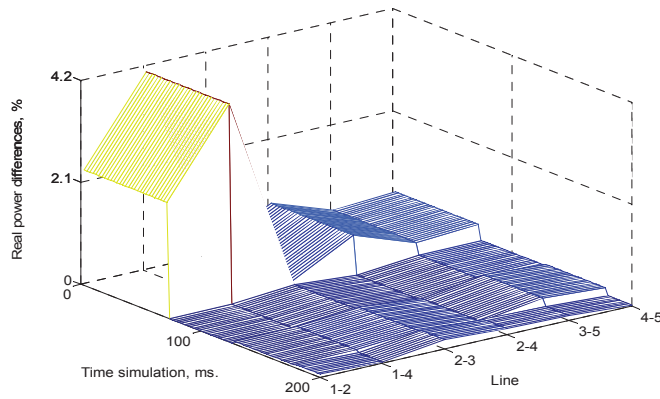
(b) Active power estimation.

Figure 3.13: Differences of estimations from true values in case of normal operation.

communication periods, the measurements of the network in the normal state are still processed. As a result, the differences of voltage magnitude and real power flow are significant in these periods, as shown in Figure 3.15.

Naturally, the largest tolerance comes from the estimation values of V_4 (1.2%) and P_{24} (2.5%). At the same time, the SE agents have detected the network topology change by checking current measurements. New measurements are used to yield the updated state variables which reach closely to the true values in the next communication periods. At the end of the simulation, all of the differences are guarantee less than 0.1%.
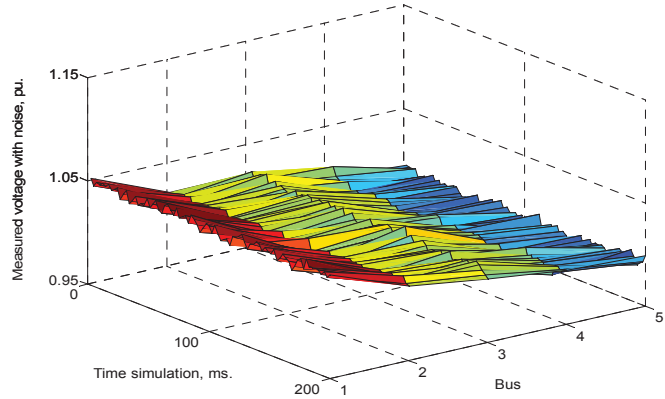
(a) Voltage bus measurements.
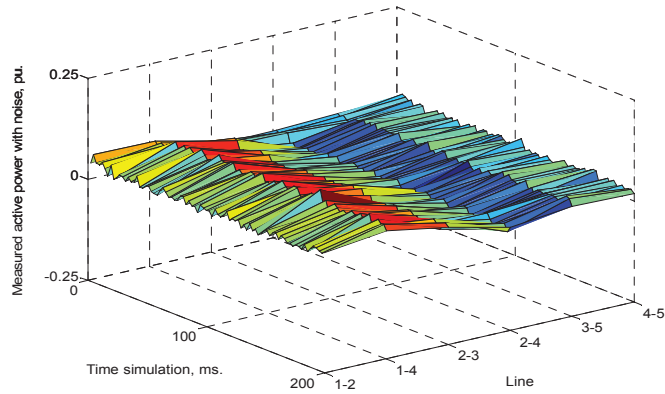
(b) Active power measurements.

Figure 3.14: Measurement data with noise in case of network topology change.

Increase load demand

In this case, the bad data influence is not taken into account. At $t = 60ms$, the load demand of bus 5 increases 20%. It causes voltage oscillation and power flow changes. As can be seen from Figure 3.17, the percentage values of the voltage differences swing respectively according to the voltage oscillation from in the period from $60 - 120ms$. As CDSE performs in each $40ms$ period, measurement data is collected at $t = 80ms$, and CDSE estimates a new state of the network at $t = 120ms$. At the end of the simulation ($t = 250ms$), the voltage differences and the active power differences are less than 0.6%.
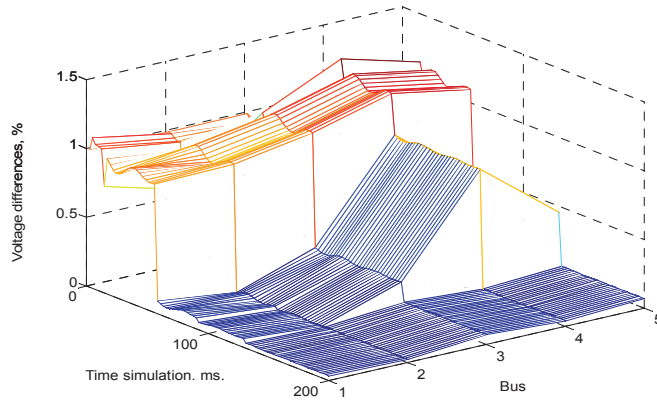
(a) Voltage bus estimation.
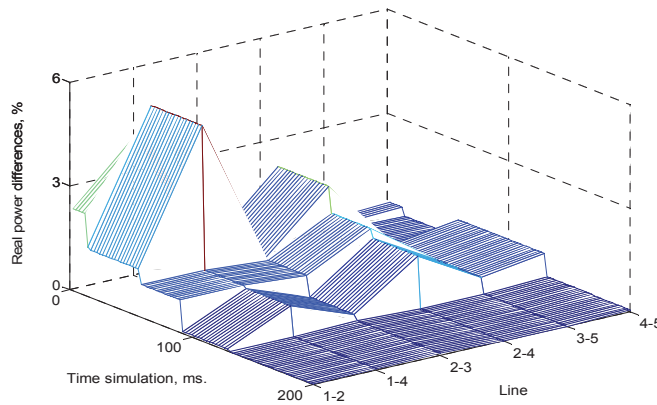
(b) Active power estimation.

Figure 3.15: Differences of estimations from true values in case of network topology change.

3.5 Summary

This chapter proposes a completely decentralized state estimation method for an Active Distribution Network (ADN). Basically, the proposed method also uses the WLS technique to estimate local voltage and angle differences. However, the scale of computation matrix with only two interactive buses and an interconnection line in between is much smaller than the central SE and the other DSE methods. In addition, each typical bus of the power system are connected normally with maximum four other buses. Therefore, the processor of each bus can get convergence within few loops. Distributed and parallel working of processor improves significantly the computation time.

It can be seen from the off-line simulation that the proposed method can obtain accurate solutions which are comparable with the conventional WLS
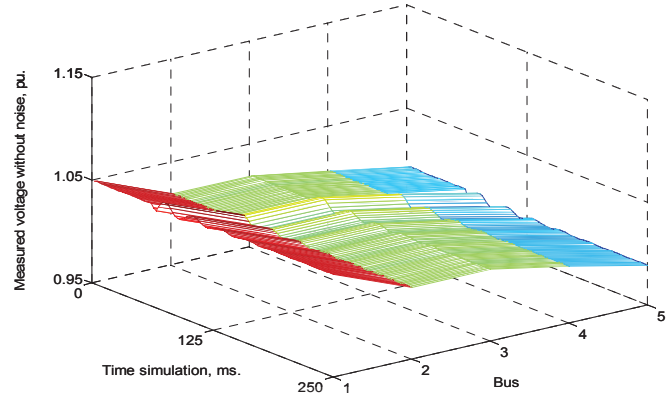
(a) Voltage bus measurements.
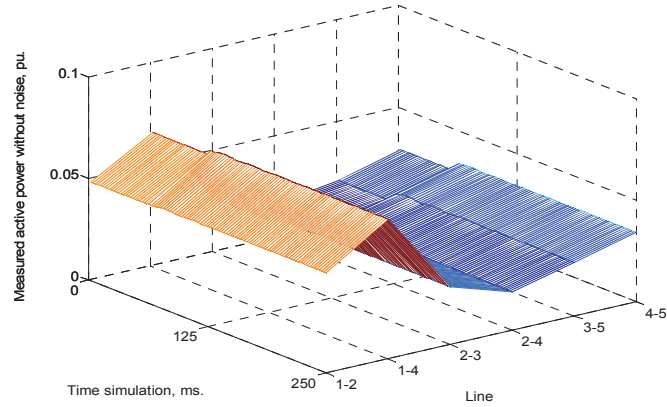
(b) Active power measurements.

Figure 3.16: Measurement data with noise in case of increase load consumption.

method. The bad data detection and identification are also applied effectively. The off-line simulations show that the proposed estimation can work with both meshed and radial test networks. However, it is more suitable with the meshed configuration of the ADN design, which includes more than one interconnection between each pair of the cells.

The complexity of the proposed method is investigated through the on-line simulation. With the support of MAS, the CDSE can be straightforward implemented in a distributed way. It can give accurate estimation not only on the steady state but also adapt to the network changes. The on-line simulation introduces capability of the method in working with continuous, on-line (real-time) environment.

Depending on availability of communication infrastructure, the CDSE is able to work locally inside the cells or globally for the whole ADN. In addition, the development of smart metering provides more opportunities for this agent-based
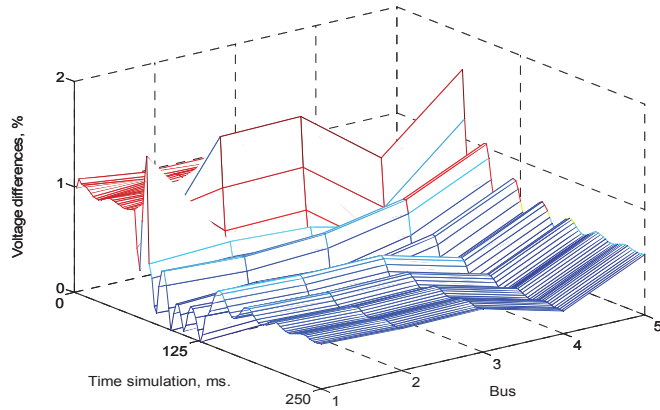
(a) Voltage bus estimation.
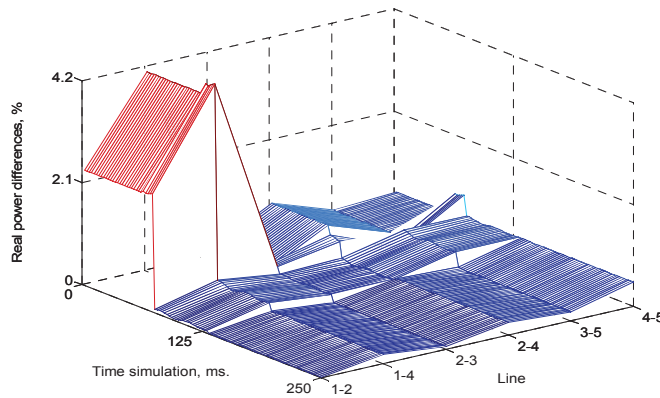
(b) Active power estimation.

Figure 3.17: Differences of estimations from true values in case of increase load consumption.

state estimation technique. By using the MAS technology, the state variables of the ADN can be estimated with overlay information among agents. Taking advantages from distributed and parallel operation, this proposed method can effectively support distributed control function of the ADN concepts.

CHAPTER 4

VOLTAGE REGULATION

As mentioned in Chapter 1, voltage deviation/regulation is one of the biggest issues which hampers the large-scale implementation of Distributed Generation (DG) in the distribution network. This chapter starts with an overview about the common methods dealing with the voltage variation problem and their limitations. Then, under the framework of an Active Distribution Network (ADN), the function of voltage regulation is further elaborated. The proposed solution combines active and reactive power support of DGs to autonomously control voltage within each cell of the ADN. In addition, a coordinated voltage control which defines the optimal tap setting of the On-Load Tap Changer (OLTC) while comparing the control actions in each cell, is presented.

A steady-state simulation for a typical Dutch Medium Voltage (MV) network is performed to investigate the feasibility of the proposed method under different voltage change scenarios. In addition, a dynamic simulation included a Multi-Agent System (MAS) platform in Simulink has been developed to validate the negotiating algorithm among agents. The simulation test results show that the agent-based voltage control can help the ADN to integrate more DGs and mitigate voltage violations effectively. The optimal solution can be reached within a small number of calculation iterations.

4.1   Introduction

Voltage deviation at the customers' point of connection is one of the most important aspects of the supply voltage/voltage quality. In EN50160 standard [113], the voltage magnitude variation on both Low Voltage (LV) and Medium Voltage (MV) networks is limited within $\pm 10\%$ of the nominal voltage during 95% of the time of a week.

In the Netherlands, the grid code extends these voltage standards for the LV and MV network as follows [114]:

- **Low voltage network:** The nominal voltage is $230V$. The voltage deviation is $\pm10\%$ for 95% of the week, mean 10-minutes rms values, while all 10-minutes rms values of a week have to be within -15% and $+10\%$ of the nominal voltage.

- **Medium voltage network:** The nominal voltage is a contracted value that the grid operator and the customer are agreed upon. The voltage deviation is $\pm10\%$ for 95% of the week, mean 10-minutes rms values, while all 10-minutes rms values of a week have to be within -15% and $+10\%$ of the nominal voltage.

These standards limit DG penetration in the distribution network as will be illustrated later. Main solutions for controlling voltage deviations in a distribution network are summarized as follows [115], [116]:

- Voltage control by the OLTC of the HV/MV transformer.

- Reactive power control with DGs and compensators.

- DG active power control.

Many works have been carried out to evaluate suitable solutions that facilitate connecting more DGs. Some works focus on intelligent control of the HV/MV transformer [4], [117]. Alternative approaches concern local voltage control at the DG's connecting point [116], [118]. In [119], Bignucolo et al. propose a coordination between the OLTC actions and the reactive power production of the DG units which enhances the capacity of the distribution network to absorb more DERs.

In [120], centralized and local voltage control methods are compared in detail. Centralized voltage control is based on an overall energy management scheme that first estimates the power system state by collecting several data, and then dispatches the DGs according to the Optimal Power Flow (OPF). Local voltage control is deployed by combining automatic voltage regulation on the transformers and power factor control of the DGs.

Figure 4.1 illustrates voltage variations in a typical example of a MV network to show limitations of the current control techniques. This network is designed in a ring configuration and operated as a radial network with two feeders separated by a Normally Open Point (NOP). Large amounts of DG power injection on the feeder 1 causes over voltage at the end of the feeder. The OLTC can adjust its set point to bring the voltage profile of feeder 1 back in the normal voltage range. However, this decrease in the voltage profile of the feeder 2 is dominated by load consumption. Therefore, the bus voltage at the end of the feeder might violate the minimum limit of the normal voltage range. To reveal faster the voltage deviation issue, it is supposed here and coming simulation in this chapter that the normal voltage range is within $\pm5\%$ of the nominal voltage.

Absorbing reactive power is normally considered as a solution to deal with this voltage rise problem. However, due to the high R/X ratio in cable networks, the voltage variations in such distribution networks are mainly influenced by
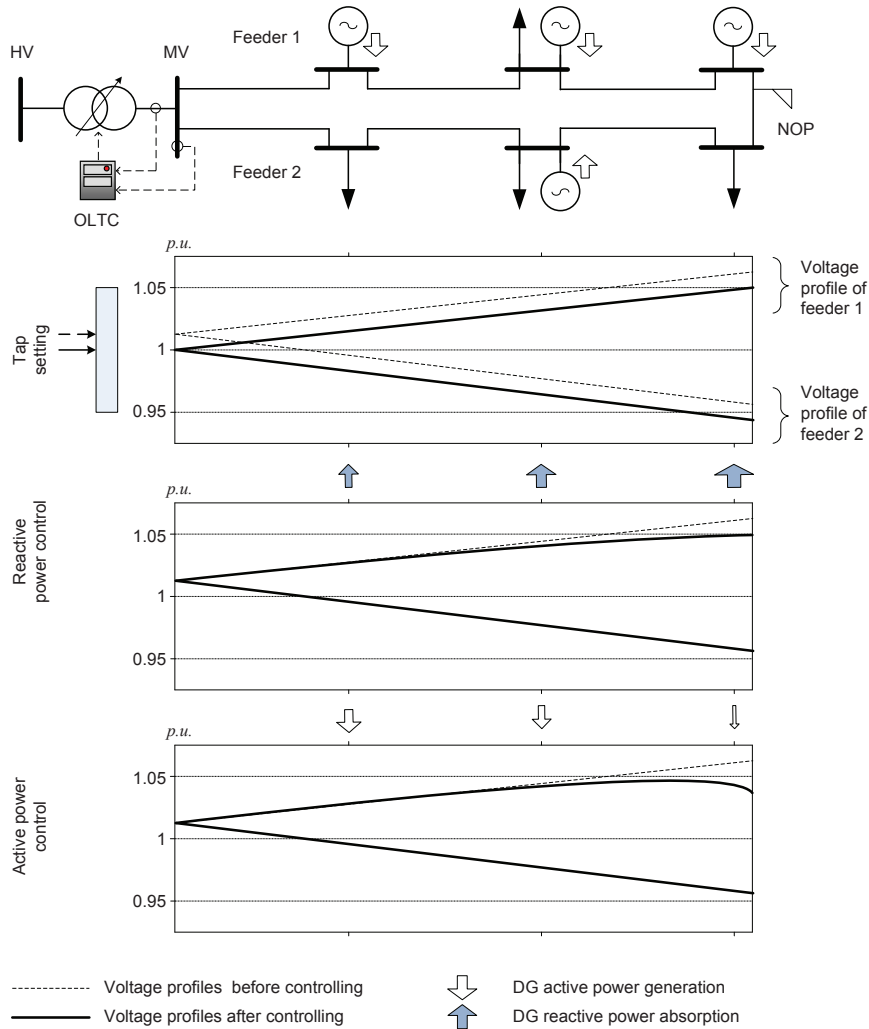
Figure 4.1: Voltage profile variations in the MV network with DGs.

the active power and the resistance of the cables [114]. Consequently, this technique requires generating large amounts of reactive power which might be out of generators' limits.

Curtailment of DG's active power generation is the least preferable method. But the bus voltage can be controlled effectively by adjusting the active power injection, so the method is interesting in case of controllable DGs.

This chapter introduces the concepts related to the mechanisms for voltage regulation applicable to the agent-based ADN design. An autonomous voltage control which regulates voltages by adjusting active and reactive power generation of DG units is applied for local area networks, i.e., feeders in the MV

network. A coordinated solution is then proposed for the whole ADN to get the most effective control solution.

4.2 Autonomous voltage regulation

This section describes a solution to control voltage autonomously in local area networks. Two feeders in the above example can be considered as cells in the ADN for which the method can be applied. A MAS platform is configured to handle the function of voltage regulation which is illustrated in Figure 4.2.
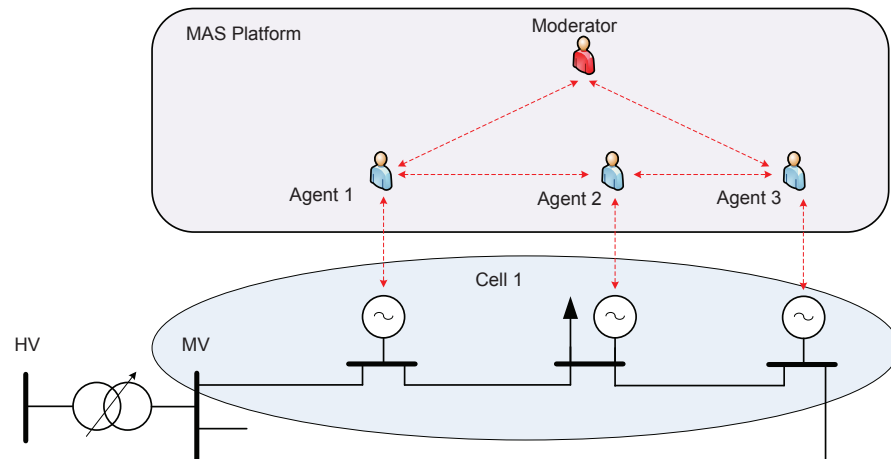
Figure 4.2: A configuration of Multi-Agent System to regulate voltage autonomously in a cell of the ADN.

4.2.1 Problem definition

Implementing voltage control functions on DG units has not been considered by the Distributed System Operators (DSOs) in the past due to technical limitations and because of the small amount of DG in the distribution network [114]. Nowadays converter-connected DGs can offer more opportunities for controlling voltage in the distribution network [121]. The combination of active and reactive power dispatch schemes can give better solutions to deal with different kinds of voltage changes. Based on this point of view, an approach to coordinate voltage regulation by appropriate dispatch of DG's active and reactive power is

presented. The main idea is to reach the optimal control as follows:

$$\text{minimize: } f_{cell} = \sum_{j=1}^{m_i} \omega_P \Delta P_{gj} + \omega_Q \Delta Q_{gj} \tag{4.1a}$$

subject to:

$$\sum_{j=1}^{m_i} \alpha_{jk} \Delta P_{gj} + \beta_{jk} \Delta Q_{gj} = \Delta V_k \tag{4.1b}$$

$$P_{gj}^{min} \le P_{gj}^0 + \Delta P_{gj} \le P_{gj}^{max} \tag{4.1c}$$

$$Q_{gj}^{min} \le Q_{gj}^0 + \Delta Q_{gj} \le Q_{gj}^{max} \tag{4.1d}$$

$$\forall j = 1, \dots, m_i \tag{4.1e}$$

where:

m_i	number of DGs in the cell i,
ω_P, ω_Q	weighting factors for adjusting 1 unit of P and Q,
$P_{gj}, P_{gj}^{min}, P_{gj}^{max}$	active power generation of DG j and its limits,
$Q_{gj}, Q_{gj}^{min}, Q_{gj}^{max}$	reactive power generation of DG j and its limits,
P_{gj}^0, Q_{gj}^0	current active and reactive power generation of DG j.

The weighting factors, i.e., ω_P and ω_Q, are used as a comparative relationship between active and reactive power changes needed to regulate voltage. They are introduced as proportions of cost for adjusting 1MW and 1MVAr.

Active and reactive power sensitivity factors, i.e., α_{jk} and β_{jk}, are defined as the voltage sensitivity of bus k with changing respectively active and reactive power of generator j.

4.2.2 Power sensitivity factors

The sensitivity of bus voltages due to the changes of active and reactive power generation can be represented by linear equations as follows:

$$\begin{bmatrix} \Delta P \\ \Delta Q \end{bmatrix} = \begin{bmatrix} J_{P\theta} & J_{PV} \\ J_{Q\theta} & J_{QV} \end{bmatrix} \begin{bmatrix} \Delta \theta \\ \Delta V \end{bmatrix} \tag{4.2}$$

where $J_{P\theta}$, J_{PV}, $J_{Q\theta}$, and J_{QV} are elements of the Jacobean matrix corresponding to derivations of the active and reactive powers from the bus voltage angles and magnitudes.

Due to the fact that MV networks may include mainly cables and lines with a relative high R/X ratio, equation 4.2 is impossible to be decoupled with the assumptions that ΔP is more sensitive to the $\Delta \theta$, and ΔQ is more sensitive to the ΔV.

However, the effect of active and reactive power generation change to bus voltages can be considered separately from equation 4.2 by following equations:

$$\Delta P = [J_{PV} - J_{P\theta}J_{Q\theta}^{-1}J_{QV}]\Delta V = [A]\Delta V \tag{4.3}$$

and,

$$\Delta Q = [J_{QV} - J_{Q\theta}J_{P\theta}^{-1}J_{PV}]\Delta V = [B]\Delta V \tag{4.4}$$

These equations stand for the capability of DGs in the network to contribute to voltage regulation by varying active and reactive power generation.

The relationship between the bus voltage and reactive power generation has been elaborated in [118]. With the assumption that the active power loads and active power output of the DGs will not change, equation matrix 4.4 can be rewritten as follows:

$$\begin{bmatrix} 0 \\ \Delta Q_g \end{bmatrix} = \begin{bmatrix} C_{11} & C_{12} \\ C_{21} & C_{22} \end{bmatrix} \begin{bmatrix} \Delta V_l \\ \Delta V_g \end{bmatrix} \tag{4.5}$$

Hence,

$$\begin{bmatrix} \Delta V_l \\ \Delta V_g \end{bmatrix} = \begin{bmatrix} [C_{21} - C_{22}C_{12}^{-1}C_{11}]^{-1} \\ [C_{22} - C_{21}C_{11}^{-1}C_{12}]^{-1} \end{bmatrix} \times \Delta Q_g \tag{4.6}$$

$$= [D]\Delta Q_g \tag{4.7}$$

From equation 4.7, the reactive power sensitivity factor β_{jk} for a voltage change at bus k is determined as follows:

$$\beta_{jk} = D_{kj} \tag{4.8}$$

which represents the voltage sensitivity of bus k with respect to a reactive power output change of generator j. The bus voltages can then be controlled by a reactive power dispatch based on ranking of the sensitivity factors β_{jk}.

Similarly, the relationship between the bus voltages and active power generation change can be established. This control could be incorporated for instance when the reactive power reaches its limit. While $\Delta Q = 0$, the active power change will be obtained from equation 4.3 as follows:

$$\begin{bmatrix} 0 \\ \Delta P_g \end{bmatrix} = \begin{bmatrix} E_{11} & E_{12} \\ E_{21} & E_{22} \end{bmatrix} \begin{bmatrix} \Delta V_l \\ \Delta V_g \end{bmatrix} \tag{4.9}$$

Hence,

$$\begin{bmatrix} \Delta V_l \\ \Delta V_g \end{bmatrix} = \begin{bmatrix} [E_{21} - E_{22}E_{12}^{-1}E_{11}]^{-1} \\ [E_{22} - E_{21}C_{11}^{-1}E_{12}]^{-1} \end{bmatrix} \times \Delta P_g \tag{4.10}$$

$$= [F]\Delta P_g \tag{4.11}$$

From above equation, an active power sensitivity factor α_{jk} for a voltage change at bus k is determined as:

$$\alpha_{jk} = F_{kj} \tag{4.12}$$

Consequently, an active power dispatch by using the sensitivity factors α_{jk} can also control the bus voltages.

The sensitivity factors show actually the relationship between the bus voltage change and an active (reactive) power injection. These values are based on power flow equations and the Jacobean matrix. The DSE function described in the previous chapter plays a key role in providing knowledge on the system state variables which is needed to yield these values.

4.2.3   Distributed implementation

The MAS-based ADN allocates the above sensitivity factors at respective agents of the buses to initiate autonomous control actions by moderator agents of the cells. The main element of the proposed algorithm is a negotiation between participants to get the most effective control actions. In a MAS application, a CNP is used as a popular mechanism for negotiation [89]. The FIPA contract network elaborates the CNP with addition of rejection and confirmation communication [122]. In this research work, we adapt the autonomous voltage control algorithm according to the CNP.

When a voltage violation occurs at a bus, the corresponding agent of that bus detects the problem and sends an $Information$ message to its moderator. The moderator sends a Call for Proposal (CFP) message to every DG agent within its cell. The content of the message includes the desired voltage change ΔV_k at control bus k. After receiving the CFP message, each DG agent A_j updates the value of its sensitivity factors α_{jk} and β_{jk} which can be calculated from equation 4.8 and 4.12. Although each DG can change both real and reactive power output, only one scheme is applied at the same time due to the assumption of considering P_g and Q_g separately. Therefore, a comparison of (ω_Q/β_{jk}) and (ω_P/α_{jk}) is needed to point out the most effective control action. Then A_j responds with a $Proposal$ message including its possible capacity to control the voltage at bus k or a $Refuse$ message. The moderator decides on the dispatch order of the proposals of the DGs based on ranking of the weighting factors compared to the sensitivity factors. Agents in the list of selection will receive an $Accept\_Proposal$ message from the moderator. The implementation of the autonomous voltage control as actions of the agents and the moderator are summarized as pseudo-codes in Algorithm 4.1 and 4.2. Each agent has a $Mode$ variable which can be changed according to received messages from its neighbors.

This process is repeated until the ΔV_i is less than ϵ (0.001) or all DGs real and reactive power outputs both reach their limit. Voltage control coordination with the OLTC and other cells can be implemented as a next step to achieve better results.

4.3   Voltage control coordination

Generally, the regulation of the OLTC is the most effective way to control voltage in the distribution network. However, with a large number of DGs, it is a difficult

---

Algorithm 4.1 Pseudo-Code for each agent A_j in the cell i

$Received(Mode) \leftarrow Message(objective)$
if $Mode = 1$ **then**
  $\Delta V_j \leftarrow Measurements(V_j, I_{jk}; \forall k \in neighbor_j)$
  if $\Delta V_j \neq 0$ **then**
    $Information(\Delta V_j) \rightarrow M_i$
  end if
end if
if $Mode = 2$ **then**
  $CFP(V_k) \leftarrow M_i$
  if (enough reserve capacity) **then**
    $[\Delta P_{gj}, \Delta Q_{gj}] \leftarrow Minimize[\omega_P/\alpha_{jk}; \omega_Q/\beta_{jk}]$
    $Proposal(\Delta P_{gj}, \Delta Q_{gj}) \rightarrow M_i$
  else
    $Refuse() \rightarrow M_i$
  end if
end if
if $Mode = 3$ **then**
  $Accept\_Proposal(V_k, \Delta P_{gj}, \Delta Q_{gj}) \leftarrow M_i$
  $(\Delta P_{gj}, \Delta Q_{gj}) \rightarrow DG_j$
end if

Algorithm 4.2 Pseudo-Code for moderator agent M_i of the cell i

---

$Received(Mode) \leftarrow Message(objective)$
if $Mode = 1$ **then**
  $Information(\Delta V_k) \leftarrow A_k$
  $CFP(V_k) \rightarrow A_j; \forall j = 1, \ldots, m_i$
end if
if $Mode = 2$ **then**
  $Proposal(\Delta P_j, \Delta Q_j) \leftarrow A_j$
  if (receive all responses) **then**
    $List \leftarrow Ranking[\omega_P/\alpha_{jk}; \omega_Q/\beta_{jk}]; \forall j = 1, \ldots, m_i$
    $Accept\_Proposal(V_k, \Delta P_{gj}, \Delta Q_{gj}) \rightarrow A_j; \forall j \in List$
  end if
end if

---

task to reach the optimal set points of the OLTC, especially when the HV/MV transformer is connected with certain generation feeder and other more load feeders.

Based on the MAS platform, control actions among cells can be coordinated in the ADN to solve the problem of voltage control. Figure 4.3 illustrates an example of communication established by moderator agents in different cells. A superior agent is used to observe the control actions in different cells and adjust the tap changer of the common transformer. The implementation steps for the
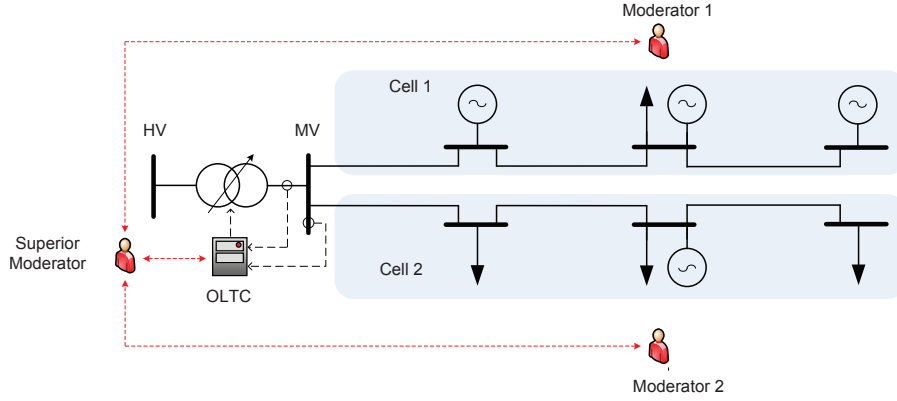
Figure 4.3: A configuration of Multi-Agent System to coordinate voltage regulation among cells in the ADN.

voltage control coordination are described in detail in the following sections.

4.3.1 Problem definition

In case of the voltage control coordination, the application of the OLTC is included in the objective function. The voltage control coordination in this section relates only to the cells (feeders) and the transformer connected to the same busbar of a primary HV/MV substation. With the scalable structure of the agent-based design, the proposed method can be expanded to apply for larger network. However, the voltage deviation is a local issue for which measures taken before the transformer connected to the violated location is not so effective.

Taken the OLTC into account, the problem of optimal voltage regulation of section 4.2 can be rewritten as follows:

$$\text{minimize: } f_\Sigma = \sum_{i=1}^{n} \left[\sum_{j=1}^{m_i} [\omega_P \Delta P_{gj} + \omega_Q \Delta Q_{gj}] \right] + \omega_T \Delta T \tag{4.13a}$$

subject to:

$$\sum_{i=1}^{n} \left[\sum_{j=1}^{m_i} [\alpha_{jk} \Delta P_{gj} + \beta_{jk} \Delta Q_{gj}] \right] + \gamma_T \Delta T = \Delta V_k \tag{4.13b}$$

$$T^{min} \leq T^0 + \Delta T \leq T^{max} \tag{4.13c}$$

$$P_{gj}^{min} \leq P_{gj}^0 + \Delta P_{gj} \leq P_{gj}^{max} \tag{4.13d}$$

$$Q_{gj}^{min} \leq Q_{gj}^0 + \Delta Q_{gj} \leq Q_{gj}^{max} \tag{4.13e}$$

$$\forall j = 1, \ldots, m_i. \tag{4.13f}$$

where n is number of cells connected to the same bus-bar as the transformer;

T^0, T^{min}, T^{max} are tap settings of the OLTC of the transformer and its limitations; ω_T is the weighting factor for the control actions of the OLTC; γ_T is the sensitivity of the voltage at bus k when changing a step of transformer's OLTC at the HV/MV substation.

4.3.2 Distributed implementation

A searching method to obtain the optimal set point of the OLTC is proposed by comparing the amounts of control actions in the cells (outgoing feeders). The control algorithm can be implemented by negotiation among moderators on the agent's platform.

If the voltage violation in cell i is not solved after implementing the autonomous control actions, the *moderator* M_i sends an *Information* message to the superior moderator SM with the residual violated voltage ΔV_k. SM starts adjusting the tap changer of the transformer and sends a CFP message to its participating moderators. The message aims to check if there is any voltage violation in the cells after adjusting the tap changer or not. If any moderator M_j detects a consecutive voltage violation, it implements the autonomous voltage regulation as mentioned in the previous section and sends the total amount of control actions to the SM. After collecting all response from the moderators, the SM can judge and create a better position for the OLTC. The algorithm is presented as pseudo-codes for the moderators and the superior moderator in Algorithm 4.3 and 4.4.

Algorithm 4.3 Pseudo-Code for each moderator M_j in coordination for voltage regulation i

---

$Received(Mode) \leftarrow Message(objective)$
if $Mode = 1$ **then**
   $Information(\Delta V_k) \leftarrow A_k$
   $minimize : f_{cell-i} \leftarrow Autonomous\_Control$
   if $\Delta V_k \neq 0$ **then**
      $Information(\Delta V_k) \rightarrow SM$
   end if
end if
if $Mode = 2$ **then**
   $CFP(\Delta T) \leftarrow SM$
   $\Delta V_j \leftarrow (T + \Delta T)$
   if $(\Delta Delta V_j \neq 0)$ **then**
      $minimize : f_{cell-i} \leftarrow Autonomous\_Control$
      $Proposal(f_{cell-i}) \rightarrow SM$
   end if
end if

Algorithm 4.4 Pseudo-Code for the superior moderator SM in coordination for voltage regulation i

---

$Received(Mode) \leftarrow Message(objective)$
if $Mode = 1$ **then**
  $Information(\Delta V_k) \leftarrow M_i$
  if $V_k > 0$ **then**
    $\Delta T = 1$
  else
    $\Delta T = -1$
  end if
  $CFP(\Delta T) \rightarrow M_j; \forall j = 1, \ldots, n$
end if
if $Mode = 2$ **then**
  $Proposal(f_{cell-i}) \leftarrow M_i$
  if (receive all responses) **then**
    $f_{\Sigma} = \sum\limits_{i=1}^{n} f_{cell-i} + \omega_T \Delta T$
    if $f_{\Sigma} < f_{\Sigma}^0$ **then**
      $Accept\_Proposal(\Delta T) \rightarrow M_i; \forall i = 1, \ldots, n$
    end if
  end if
end if
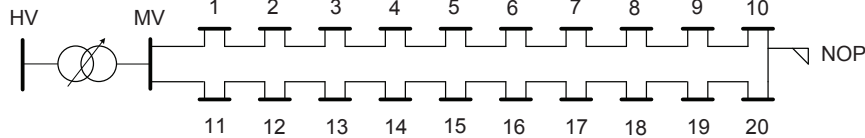
Figure 4.4: Single-line diagram of the MV radial test network.

4.4 Simulation and results

4.4.1 Steady-state simulation

A Matlab script modified from the Power System Analysis Toolbox (PSAT) [123] is used to investigate the proposed voltage regulation algorithms. The simulation investigates a typical Dutch MV network as shown in Figure 4.4. The network includes two feeders which can be connected through a Normally Open Point (NOP). Data of generation and load is presented in Table 4.1.

Other network parameters are given as follows:

- HV/MV transformer: regulation range of the OLTC is $\pm 5\%$ in steps of 2.5% of the 10kV nominal voltage.

- Line section: π-equivalent circuit, section lenght $l = 2$km, $r = 0.125\Omega$/km,

Table 4.1: Generation and load data of the test network

Units: MW, MVAr

Location	Feeder 1				Feeder 2			
	P_G	Q_G	P_L	Q_L	P_G	Q_G	P_L	Q_L
1/11	3	0	1	0.48	-	-	1	0.48
2/12	3	0	1	0.48	-	-	1	0.48
3/13	3	0	1	0.48	3	0	1	0.48
4/14	3	0	1	0.48	-	-	1	0.48
5/15	3	0	1	0.48	3	0	1	0.48
6/16	3	0	1	0.48	-	-	1	0.48
7/17	3	0	1	0.48	3	0	1	0.48
8/18	-	-	1	0.48	-	-	1	0.48
9/19	-	-	1	0.48	3	0	1	0.48
10/20	-	-	1	0.48	-	-	1	0.48
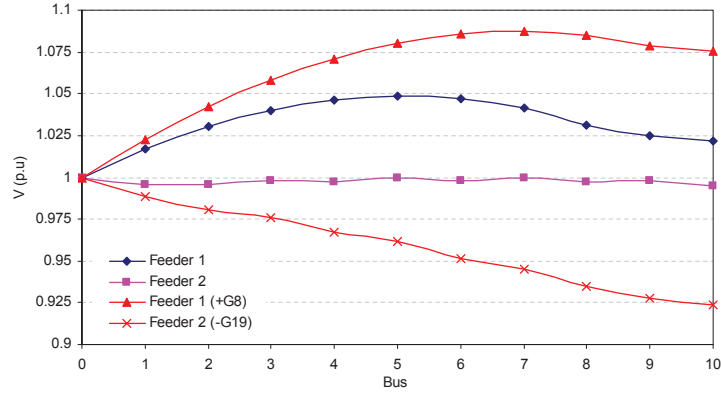
Figure 4.5: Voltage profiles of two feeders without control actions.

$l = 0.2833$mH/km, $c = 0.53\mu F$/km.

- Generator: $P_{max} = 3$MW; $P_{min} = 30\%P_{max}$; $\cos\varphi_{inductive-max} = 0.95$; $\cos\varphi_{capacitive-max} = 0.9$.

- Ratio of weighting factors $\omega_P/\omega_Q = 2$.

In this simulation, the acceptable voltage range is supposed equal to 5% arround the rated value (that means $V_{min} = 0.950p.u.$, $V_{max} = 1.050p.u.$). The simulation investigates two scenarios: (1) voltage rise when more generators (i.e., G_8) are connected to feeder 1; (2) voltage drop when one generator (i.e., G_{19}) is out of service in feeder 2. Figure 4.5 shows the voltage profiles of the two feeders and their violations when the two secnarios are considered which need voltage regulation actions to be applied.
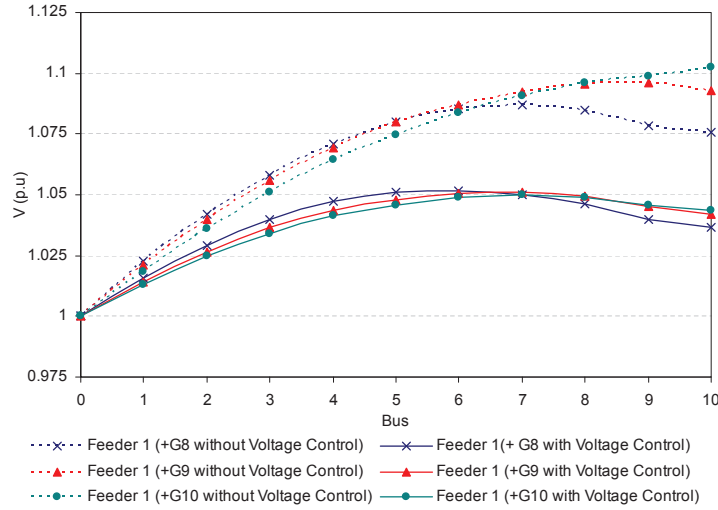
Figure 4.6: Effect of autonomous voltage control in case of voltage rise .

Case of voltage rise

In this case, integration of more DGs (G_8, G_9, and G_{10}) causes a voltage rise
to the end of the feeder 1. The dash lines in Figure 4.6 are the voltage profiles
of feeder 1 in case of connecting extra DG units respectively. In the worst case
when all generators are connected, the voltage magnitude at bus 10 is above
$1.1p.u.$ When the autonomous voltage regulation is applied, the voltage profiles
are adjusted to be within normal voltage range, see continuous lines in Figure
4.6.

   Table 4.2 shows the power generation dispatch of the DGs to cope with the
voltage rise issue. When an extra generator at bus 8 (G_8) is connected, only the
reactive power re-dispatched is applied on G_5, G_6, G_7, and G_8. However, when
also G_9 is connected, there is a comparison to be made between of ω_Q/β_4 and
ω_P/α_9. With better performance, the active power curtailing of G_9 is selected.
Similarly, installing G_{10} leads to curtail the active power of G_{10} and G_9. The
algorithm is converged after two steps, as can be seen from Figure 4.7. This
important result opens the possibility to implement this technique in on-line
(real-time) applications.

   The simulation results show that a combination of active and reactive power
support can cope with voltage rise to the end of the feeder effectively. A suitable
amount of active power is curtailed instead of much greater amount of reactive
power absorbed. This depends however on the comparison of the sensitivity
factors at the generation buses and the ratio of the weighting factors. The
locations of curtailed generators are quite near to the violated voltage bus,
what makes the control actions quite sensitive.

Table 4.2: DG power generation dispatch

						Units: MW, MVAr
	Cases of DG integration					
	P_{G8}	Q_{G8}	P_{G9}	Q_{G9}	P_{G10}	Q_{G10}
G_1	3	0	3	0	3	0
G_2	3	0	3	0	3	0
G_3	3	0	3	0	3	0
G_4	3	0	3	0	3	0
G_5	3	-0.0840	3	-0.9367	3	-0.9367
G_6	3	-0.9367	3	-0.9367	3	-0.9367
G_7	3	-0.9367	3	-0.9367	3	-0.9367
G_8	3	-0.9367	3	-0.9367	3	-0.9367
G_9	-	-	1.6365	-0.9367	1.4271	-0.9367
G_{10}	-	-	-	-	1.2	-0.9367
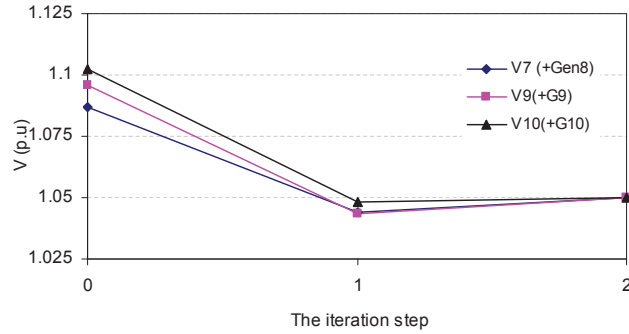
Figure 4.7: Convergence in case of voltage rise.

Case of voltage drop

It is assumed that G_{19} in feeder 2 is out of service due to a contingency or some other operational reason. The voltage magnitude towards the end of feeder 2 decreases significantly below $0.95p.u.$ The remaining DGs connected to the feeder will coordinate to keep the voltage profile within the normal range. Due to the fact that the DG units operate at their maximum active power generation, the reactive power regulation must be used in this case to support the voltage drop.

The proposed method takes two iteration steps to solve the voltage drop problem. G_{15} generates 0.7041MVAr while G_{17} has to produce the maximum amount of reactive power generation (1.3MVAr). The voltage profile of feeder 2 for each control step is shown in Figure 4.8.
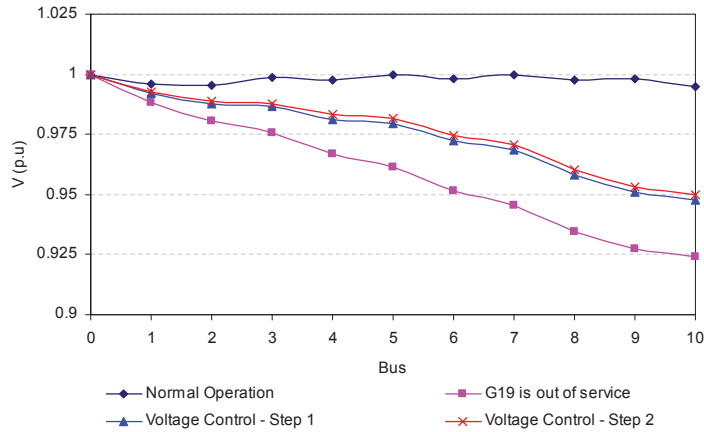
Figure 4.8: Effect of autonomous voltage control in case of a voltage drop.

Case of voltage control coordination

The voltage rise issue due to connecting more DG units in feeder 1 will be investigated again with the voltage control coordination solution. Voltage profiles of both feeders in the different cases are shown in Figure 4.9. Table 4.3 summarizes the results of total DGs active and reactive power changes in the two feeders as well as the tap position when installing G_8, G_9, and G_{10}.
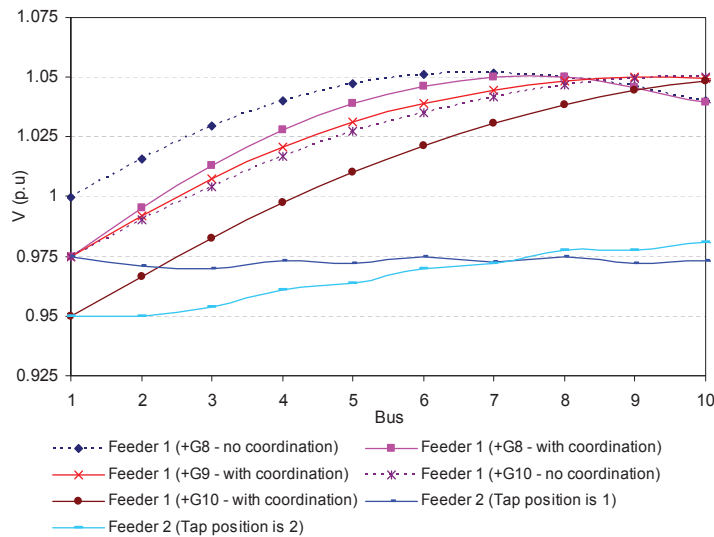
Figure 4.9: Effect of voltage control coordination.

Table 4.3: Coordination of DG dispatch and transformer OLTC

Units: MW, MVAr

	Feeder 1		Feeder 2		OLTC
	$\Sigma\Delta P$	$\Sigma\Delta Q$	$\Sigma\Delta P$	$\Sigma\Delta Q$	position
Connect G_8 without coordination	-	2.8940	-	-	0
Connect G_8 with coordination	-	1.0123	-	-	1
Connect G_9 without coordination	-	4.3719	-	-	1
Connect G_9 with coordination	-	4.3719	-	-	1
Connect G_{10} without coordination	1.7298	5.6202	-	-	1
Connect G_{10} with coordination	0.3550	5.6202	-	2.0201	2

As can be seen from Table 4.3, the voltage control coordination can reduce dramatically the amount of control actions (ΔQ_Σ). In case of connecting G_8, the tap setting is moved to the position 1 without any voltage violation on feeder 2. When G_9 is connected, the voltage control coordination compares the total amount of control actions in case of autonomous dispatch in feeder 1 and keeping the tap position to 1, with case of autonomous control in both feeders, and moving the tap position to 2. Having less total control actions, the first option is selected for coordination. When connecting G_{10}, the voltage control coordination moves the tap position to 2 and the autonomous control is required in both feeders.

As an alternative to centralized voltage control, such coordination might approach the optimal solution.

4.4.2 Dynamic simulation

As mentioned in the previous section, the proposed control algorithm is converged in a few iterations which makes it possible to be implemented in an on-line environment. In this section, a MAS platform is created to support the application of the proposed method in a dynamic simulation under Simulink.

The dynamic simulation is performed on a MV radial test network which comprises four DFIG-based wind turbines, as shown in Figure 4.10. Detailed parameters of the test network are as follows:

- A 100 MVA voltage source (infinite bus).

- A 150/10 kV, 66 MVA transformer.

- Four line sections: π-equivalent circuits, section length $l = 5$km, $r = 0.125\Omega$/km, $l = 0.2833$mH/km, $c = 0.53\mu F$/km.
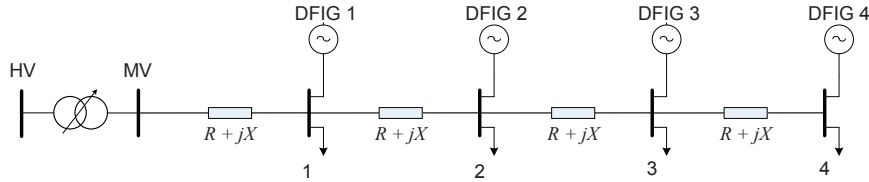
Figure 4.10: Single-diagram of the MV radial test network for dynamic simulation.
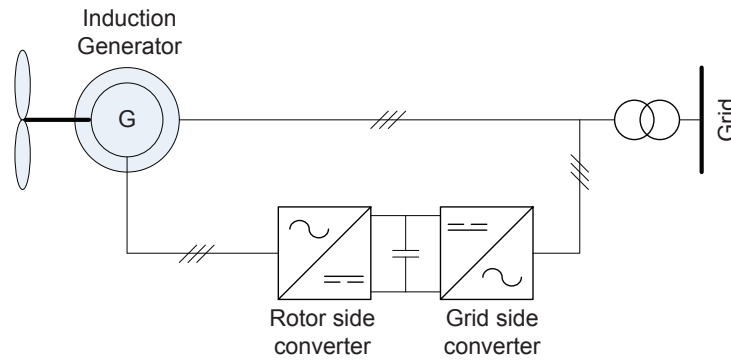
Figure 4.11: Doubly Fed Induction Generator.

- Four constant three-phase loads. At buses 1 and 2: $3\text{MW} + j1.45\text{MVAr}$; At bus 3 and 4: $1\text{MW} + j0.48\text{MVAr}$.

- Four DFIG generators: $S_{nom} = 10\text{MVA}$, $Q_{min} = -1\text{MVAr}$, $Q_{max} = 1.5\text{MVAr}$.

- Ratio of weighting factors $\omega_P/\omega_Q = 2$.

The Doubly Fed Induction Generator (DFIG) based wind turbine was chosen for the simulation as it allows the control of both active and reactive power. The DFIG-based wind turbines use a wound rotor induction generator, for which the active and reactive powers are controlled via the AC/DC/AC converter connecting the rotor windings to the grid, see Figure 4.11.

In the simulation, each DFIG-based wind turbine is managed by an agent who is created by an embedded function block in a Matlab/Simulink environment [124]. Those DG agents are connected to a main moderator agent who implements the voltage regulation algorithms and give reference values to the DFIG generators. The set-up of the agent platform for this dynamic simulation is shown in Figure 4.12.
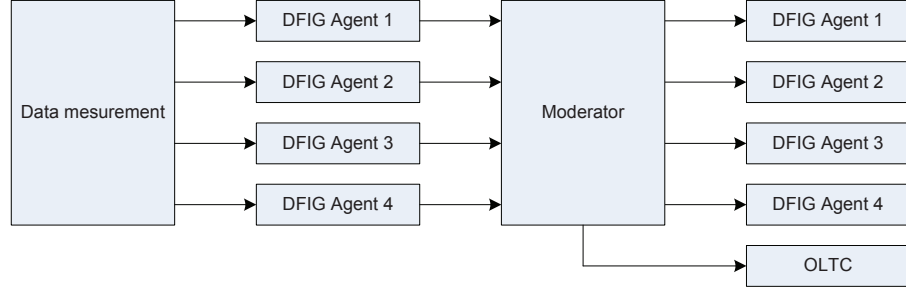
Figure 4.12: Agent platform in Matlab/Simulink.

Table 4.4: List of sensitivity factors

Bus location	α p.u.	β p.u.
1	0.0427	0.3830
2	0.1367	1.0154
3	0.2337	1.6573
4	0.3257	2.2746

Voltage rise - Reactive power control for one generator

Suppose that due to a change of wind speed, at simulation time $t = 50sec.$, from 8km/h to 10km/h, more active power is produced by G_4 from 1.87MW to 3.68MW which causes a voltage rise up to $1.0545p.u.$ at bus 4, as shown in Figure 4.13(a). Other wind generators do not change which is in practice in a small area not so realistic, but it is chosen for purposes here.

Agent at bus 4 detects the voltage rise problem and sends a message to the moderator that requires to keep the voltage of bus 4 at $1.05p.u.$ ($\Delta V_4 = -0.0045p.u$). Based on the ranking of the sensitivity factors from the agents within the feeder, the moderator will decide on a re-dispatch order for the DGs.

In the first iteration, the moderator receives a list of sensitivity factors from the agents which are presented in Table 4.4. Depending on the weighting factors ω_P and ω_Q, a ranking of sensitivity factors will be determined by comparing ω_P/α_i and ω_Q/β_i. The dispatch order is $(\beta_4; \beta_3; \beta_2; \alpha_4; \beta_1; \alpha_3; \alpha_2; \alpha_1)$.

As G_4 has the largest value for the reactive power sensitivity factor, it will be selected to re-dispatch first with an amount of reactive power as follows:

$$\Delta Q_4 = \Delta V_4 \times V_4/\beta_4 = -0.209\text{MVAr} \qquad (4.14)$$

This reactive power change is within the capability of G_4, hence only G_4 is re-dispatched in this case, at $t = 65sec$.

After regulating G_4, the voltage at bus 4 is $1.0501p.u.$, which is slightly above $1.05p.u.$ The regulation procedure can be repeated again to reach more accurate results.
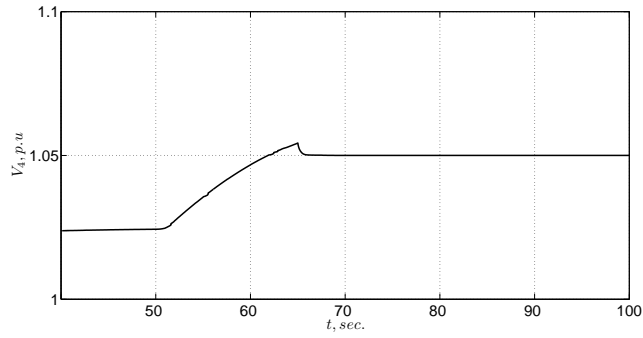
(a) Controlled voltage at bus 4.
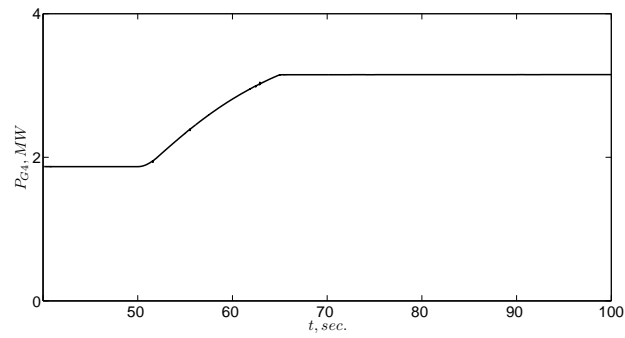
(b) Active power change of DG connected to bus 4.
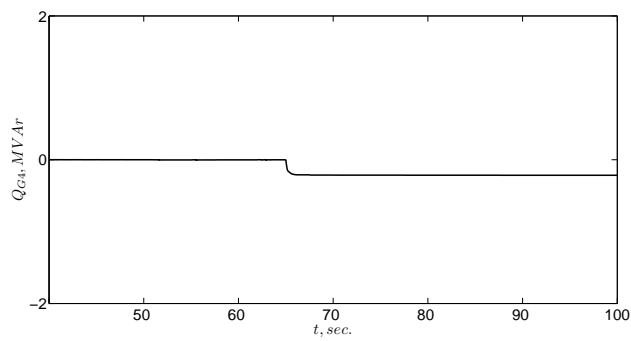
(c) Reactive power change of DG connected to bus 4.

Figure 4.13: Case of voltage rise - reactive power control for more generator.

In this case, the simulation is converged after two iterations with a tolerance less than 10^{-6}. The voltage at bus 4 reaches $1.05p.u.$ when G_4 absorbs -0.217MVAr, see Figure 4.13.

Table 4.5: DG reactive power dispatch in case of voltage rise

Iteration	ΔV_4	Q_4	Q_3
	$p.u.$	MVAr	MVAr
1	-0.0130	-0.614	0
2	-0.0053	-0.859	0
3	-0.0042	-1.000	-0.083
4	-0.0033	-1.000	-0.294

Voltage rise - Reactive power control for more generators

It is assumed that half of loads at bus 3 and bus 4 have been switched off and the wind speed of G_4 changes again from 8km/h to 12km/h, at simulation time $t = 50sec.$, which causes a voltage rise up to $1.063p.u.$ at bus 4. Other generators do not change.

In the first iteration of voltage control, the amount of voltage needed to be changed is $\Delta V_4 = -0.0130p.u.$ The sensitivity factors are similar with the previous case. Due to the largest value of the sensitivity factors, G_4 will be re-dispatched first, at $t = 55sec.$:

$$\Delta Q_4 = \Delta V_4 \times V_4/\beta_4 = -0.614 \text{MVAr} \qquad (4.15)$$

However, the active power of G4 at this moment has not reached its reference value (6.38MW) due to the wind speed change yet. Thus, more active power is produced at G_4 that increases the bus voltage. At the next iteration, the amount of voltage deviation is $\Delta V_4 = -0.0053p.u.$ The dispatch procedure is then repeated again after each period of $2.5sec.$ until the voltage of bus 4 is back in $1.05p.u$, at simulation time around $t = 80sec.$ Please note that the period of $2.5sec.$ is supposed as a communication period in the MAS platform. Table 4.5 shows the dispatch order after several iterations of voltage regulation. At the final stage, the controlled value is $1.05p.u.$ when G_3 absorbs -0.9566MVAr and G_4 absorbs -1MVAr, see Figure 4.14.

Voltage rise - Active and reactive power control

In this case, the total load at bus 4 has been switched off and the change of wind speed from 8km/h to 12km/h is supposed having effect on the active power output of G_2, G_3, and G_4 which changes from 1.87MW to 6.38MW, at simulation time $t = 50sec.$ It is assumed that G_1 does not change.

Under this condition, the voltage at bus 4 rises up to $1.0924p.u.$ which is much too high. At $t = 55sec.$, G_4, G_3, and G_2 will respectively absorb -1MVAr, -1MVAr, and -0.637MVAr according to the dispatch order to regulate the voltage of bus 4. Similar to the previous case, the voltage of bus 4 after the first control iteration is still above $1.05p.u.$ which leads to a comparison of control actions between limiting active power of G_4 and absorbing reactive power of G_1. Because of having better performance, the active power limit of
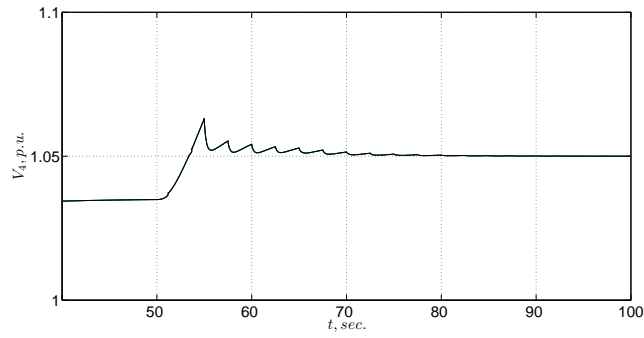
(a) Controlled voltage at bus 4.
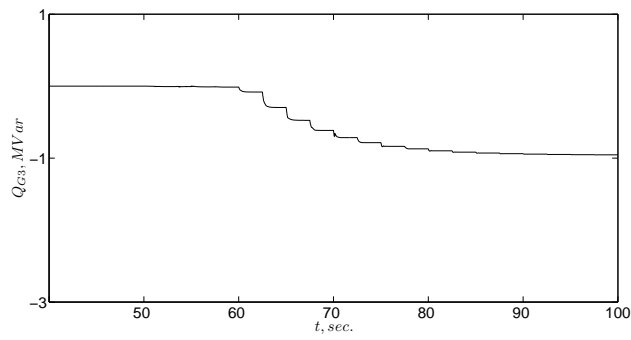
(b) Reactive power change of DG connected to bus 3.
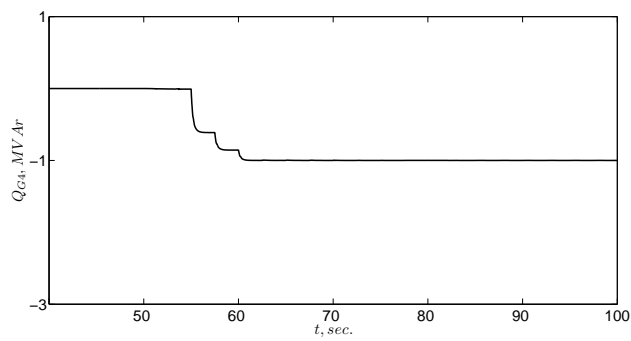
(c) Reactive power change of DG connected to bus 4.

Figure 4.14: Case of voltage rise - reactive power control for multi generators.

G_4 is selected to keep the active power generation at 4.739MW in the second iteration while the reactive power are fully absorbed in G_4, G_3, and G_2, at $t = 57.5sec$.

Table 4.6 shows the dispatch order after several iterations of voltage control.

Further iterations are taken after each period of 2.5*sec.* until the controlled

Table 4.6: DG active and reactive power dispatch in case of voltage rise

Iteration	ΔV_4	Q_4	Q_3	Q_2	P_4
	p.u.	MVAr	MVAr	MVAr	MW
1	-0.0424	-1.000	-1.000	-0.637	-
2	-0.0043	-1.000	-1.000	-1.000	4.739
3	-0.0068	-1.000	-1.000	-1.000	4.717
4	-0.0077	-1.000	-1.000	-1.000	4.505
5	-0.0068	-1.000	-1.000	-1.000	4.055

voltage bus equal 1.05*p.u.*, see Figure 4.16(a). At the final stage, all G_4, G_3, and G_2 absorb -1MVAr, and G_4 generates 3.435MW (curtails -2.945MW). Active and reactive power generations of G_4 are shown in Figure 4.16(b) and 4.16(c).

Voltage drop

With an assumption that the wind speed of G_4 changes from 8km/h to 4km/h at simulation time $t = 50sec$. This is below the average cut-in speed at which the wind turbines can generate power. Hence, active power generation of G_4 changes from 1.87MW to 0MW, see Figure 4.16(b). Other generators do not change. A consequence increasing of the load at bus 4 to be doubled causes voltage drop issue, see Figure 4.16(a).

Similarly with voltage rise cases, in the first iteration of voltage regulation, dispatched values are $\Delta V_4 = 0.0268p.u.$ and $\Delta Q_4 = 1.086MVAr$, at $t = 57.5sec$. The proposed regulation is converged in the third iteration when the voltage at bus 4 is increased up to 0.95*p.u.* by injecting 1.278MVar from G_4, at $t = 62.5sec$., see Figure 4.16.

4.5   Summary

This chapter concerns on voltage deviation/control as one of the barriers limiting DG penetration in the distribution network. Standard methods for this problems were presented which are based on regulation of the OLTC of the transformers and the management of power injection. Drawbacks of the methods are discussed and lead to a proposal for agent-based voltage control method.

Based on the power flow equations and the Jacobean matrix, the relationships between a bus voltage change and the bus power (active and reactive) injection are defined as so called sensitivity factors. The proposed method uses these factors to activate the autonomous characteristic of each controllable component to control a bus voltage. Bus power injections are managed to give an optimal voltage profile for the cell in the ADN. In addition, coordination of voltage regulation between cells is proposed in combination with the regulation of the OLTC. An effective solution can be reached by comparing the amounts of control actions.
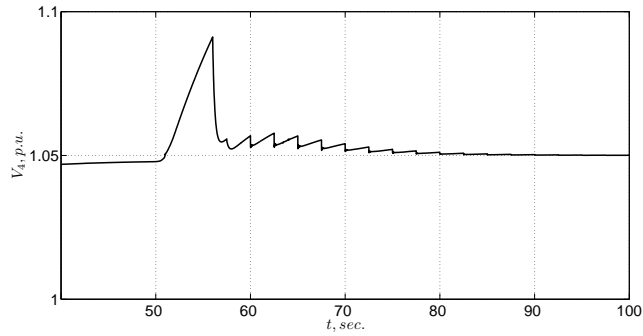
(a) Controlled voltage at bus 4.
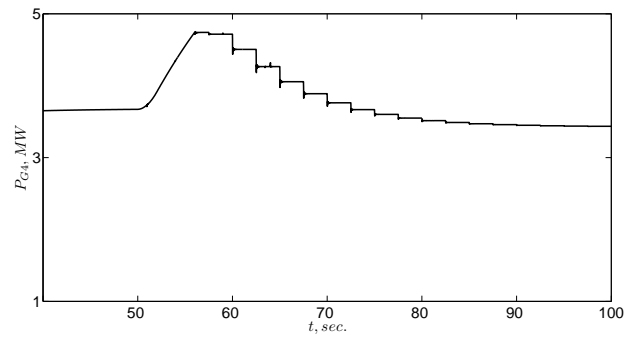
(b) Active power change of DG connected to bus 4.
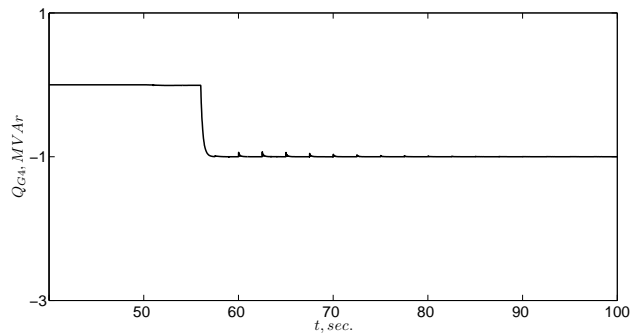
(c) Reactive power change of DG connected to bus 4.

Figure 4.15: Case of voltage rise - active and reactive power control.

A steady-state simulation on a MV test network, with two feeders which are considered as cells, is performed. Autonomous voltage regulation is firstly implemented within each cell by DG's active and reactive power support. The control algorithm can adapt effectively with different scenarios of voltage change,
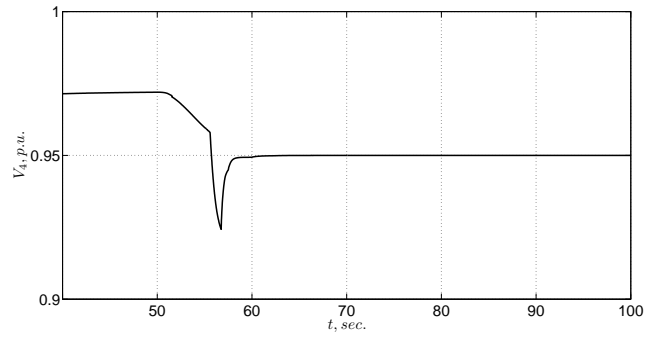
(a) Controlled voltage at bus 4.
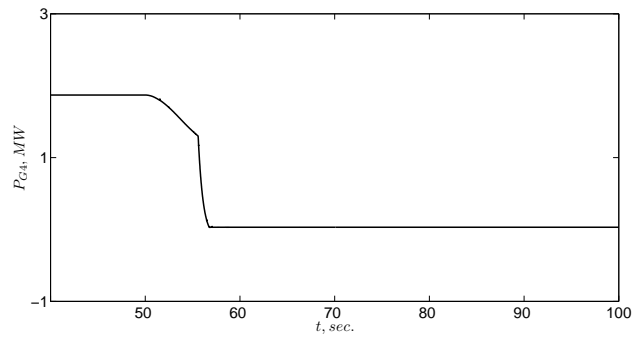
(b) Active power change of DG connected to bus 4.
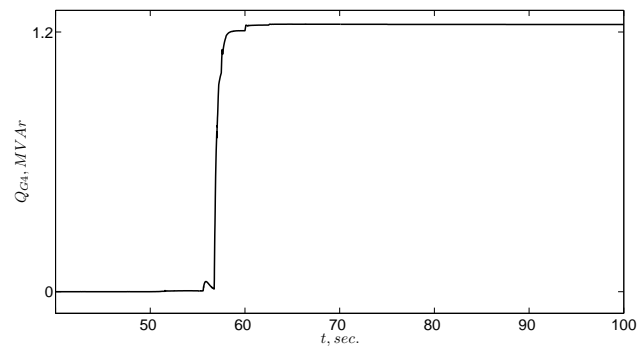
(c) Reactive power change of DG connected to bus 4.

Figure 4.16: Case of voltage drop.

i.e., voltage rise and voltage drop cases, by coordinating DG's active and reactive power.

A dynamic simulation investigated a MV test network with detailed mo-

del units of DFIG. By using the embedded functions in the Matlab/Simulink environment for modeling agents, a MAS platform is created to exchange information among buses in the test network. Each bus agent implements its own voltage control algorithm with interactions from its agent neighbors. Simulation results show that the proposed control method is to be used as an on-line application. Depending on the communication period of the MAS platform, this agent-based techniques can be considered as a secondary voltage control for the ADN.

CHAPTER 5

POWER FLOW MANAGEMENT

The current transition from passive to active distribution networks comes along with problems and challenges related to bi-directional power flow in the network and uncertainty in the forecast of power generation from grid-connected renewable and distributed energy sources. The power flow management has to cope with these challenges. In this chapter, the Optimal Power Flow problem is considered as a minimum cost flow in the graph theory and represented by directed graphs. Two fundamental solutions for the minimum cost flow, i.e., the Successive Shortest Path algorithm and the Cost-Scaling Push-Relabel algorithm, are introduced in a distributed agent environment.

To investigate their performances, the simulation is implemented on both meshed and radial networks. The simulation results shows slightly differences between the Successive Shortest Path (SSP) algorithm and the Cost-Scaling Push-Relabel (CS-PR) algorithm in the meshed networks with respect to number of exchanged messages on the agent platform. However, the CS-PR method has an advantage in the radial network with a significant reduction of the number of computations and thus reduced time for calculation.

5.1   Background

As most DGs are based on RES, their unpredictable generation characteristics are not suitable for current power dispatch schemes which are centralized and rely on highly predictable generation. Without appropriate dispatch mechanisms, voltage deviations caused by the intermittence of RES will restrict the penetration level of DG. In addition, the power flow is governed by Kirchoff's laws and can easily cause over-stressing of lower impedance components. This so called congestion problem limits the available interconnection capacity of any system. Parallel interconnections might cause undesired "loop flows" which

limits power transaction schedules and increases power losses in the network involved.

Using an Optimal Power Flow (OPF) method is the common practice for handling those problems, which is a centralized solution that affects the overall network. It is normally deployed at the economic dispatch stage to find out the optimal operation state of the network with respect to system constraints [125]. The mathematical model of the OPF problem can be presented as follows:

$$
\begin{aligned}
\text{minimize:} \quad & f(x, u) \\
\text{subject to:} \quad & g(x, u) = 0 \\
& h(x, u) \leq 0
\end{aligned}
$$

where $f(x, u)$ is the objective function that can be adjusted to deal with different goals, i.e., power production cost or power loss minimization. The vector of independent variables u presents for the state of the system, the phase angles and voltage magnitudes. The vector of dependent variables x presents the control variables, for example, power generations or tap ratios of OLTC transformers. The equality constraint represents the power balance between supply and demand while the inequality constraint shows the operational limits of the network components.

An OPF requires a large-scale control overview that is impossible to deploy in the distribution networks such as in the ADN concept. To overcome this disadvantage, distributed OPF techniques have been proposed recently [126]. However, they still need complex input information and take relatively long time processing.

Price-based control can also be considered as a distributed OPF solution. By converting the power system parameters into desired market signals, the solution yields nodal prices for generators that cannot only deal with the congestion problem but also contribute to other ancillary services [14]. This can be presented in a mathematical model as follows:

$$
\begin{aligned}
\text{minimize:} \quad & \sum_{i=1}^{n} f(P_i, P_i^{ex}, A_i, A_i^{ex}) \\
\text{subject to:} \quad & P_i - P_i^{ex} - P_i^{load} = 0 \\
& A_i - A_i^{ex} - A_i^{req} \geq 0 \\
& g_i(P_i, A_i) \leq 0
\end{aligned}
$$

where $f(P_i, P_i^{ex}, A_i, A_i^{ex})$ is the aggregated cost function of an autonomous network i; P_i and A_i are the generated power and the provided ancillary service respectively in the network i, and P_i^{ex} and A_i^{ex} present the generation and service coming from outside the network i; the equality constraint represents for power balance; the upper bound condition denotes requirements of ancillary services while the lower bound condition shows the operational limits of network components. The method, however impacts on only the generation side of the system in which owners might be influenced by price signals. Other controllable

devices of the system, i.e., electronic-based power flow controllers, are treated as passive components.

In high voltage networks, using FACTS is one of the effective means to control power flows independently [127]. FACTS elements are categorized into shunt compensation (SVC, STATCOM), series compensation (TCSC, etc.), and hybrid compensation (UPFC). Regarding the distribution network having a high R/X ratio, power electronic series devices such as TCSC or UPFC can work effectively [128]. Also in [128], the concept of an intelligent node is proposed as a series controller that connects feeders based on electronic interfaces such as back-to-back converters. These devices can be used to control the power flow and to limit voltage deviations, leading to increased utilization of network components and higher DG penetration possibilities [48], [49]. However, the influence of FACTS devices is mostly limited to the surrounding areas of the point of connection to the power system. Besides, a requirement of the high cost investment mitigates power companies in implementing FACTS on their grids.

Recently, the concept of an IPR has been proposed as a new control function in power systems [129]. By incorporating generators, power lines, and customers, the IPR not only observes the current network conditions but also cooperates with others to find alternative power flow paths in necessary cases. This approach is quite similar with the ideas of interconnecting cells in the ADN. However, the objective function for making decisions is then just on minimizing load shedding while satisfying the operating constraints. This simple algorithm cannot reach the optimal operation of the complex system. The application of FACTS devices for control purposes makes the performance much better.

Figure 5.1 categorizes the mentioned methods distinguished in centralized and decentralized solutions. It can be seen from the figure, that FACTS can be applied for both operation modes.

5.2 Power flow problems in graph-based model

5.2.1 Problem formulation

In this research, methods are proposed to cope with the optimal power exchange among cells in the ADN concept. However, it can be applied in other types of networks such as the transmission system with available FACTS devices. Basically, the power flow needs to be controlled to avoid congestion in the network, minimize the production cost (overall economic dispatch), maximize the security of the transmission components, and maximize the serving of high-priority loads. Hence, the optimizing problem of power flow management
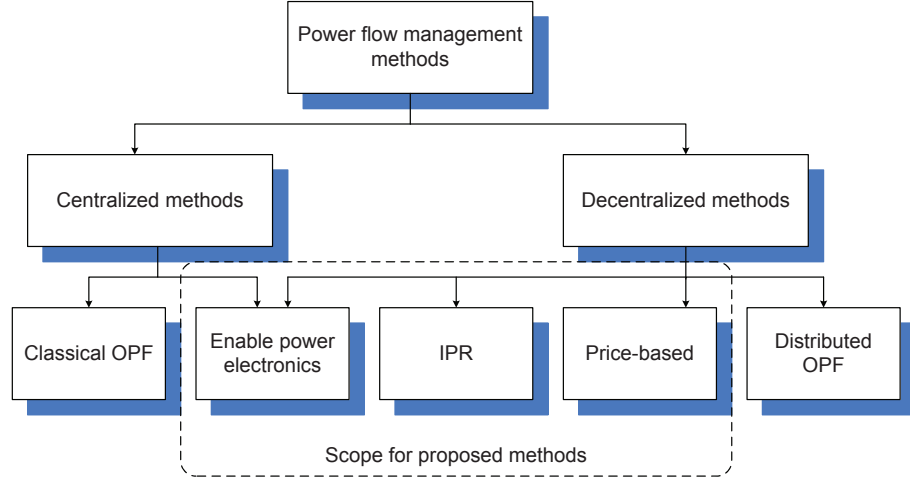
Figure 5.1: Solutions for power flow management.

can be formulated in a mathematical model as follows:

minimize:

$$\mathbf{f} = \sum_{i \in G} \alpha_i P_{G_i} + \sum_{(i,j) \in T} \beta_{ij} P_{T_{ij}} + \sum_{i \in L} \gamma_i P_{L_i} \qquad (5.1a)$$

subject to:

$$\sum_{i \in G} P_{G_i} = \sum_{(i,j) \in T} P_{T_{ij}} + \sum_{i \in L} P_{L_i} \qquad (5.1b)$$

$$P_{G_i} \leqslant P_{G_i}^{\max}, \, \forall i \in G \qquad (5.1c)$$

$$P_{T_{ij}} \leqslant P_{T_{ij}}^{\max}, \, \forall (i,j) \in T \qquad (5.1d)$$

where:

$\mathbf{f}$	total cost function,
$P_{G_i}, P_{T_{ij}}, P_{L_i}$	power generation, power transmission, and load demand,
$P_{G_i}^{\max}, P_{T_{ij}}^{\max}$	power generation capacity, power transmission capacity,
$\alpha_i, \beta_{ij}, \gamma_i$	represent production cost, component availability, and load priority,
G, T, L	generation, transmission, and load component sets.

The objective function of equation 5.1a is the total cost for delivering power from the generation areas to the load parts. Production cost constant α_i is the price for selling electricity that can be defined as the nodal price of each generating cell. Transmission cost constant β_{ij} is defined as the charge for using transmission components that depends on the availability and capacity (rating) of the apparatus. The cost constant γ_i is a price for serving a high-priority

loading cell. The power balance condition is an equality constraint 5.1b, and the transmitted power needs to be within the component's thermal limits in the inequality constraints 5.1c and 5.1d.

Depending on the scale of each cell (sub-network), the reactive power balance will be solved autonomously within cells or globally for a larger area. In the simplified optimization model, the research assumes that all cells are big enough to deal with the reactive power balance autonomously. The voltage constraints can be guaranteed by adjusting the DG's power output and the tap changers of the transformers within cells, as mentioned in chapter 4. Note that the autonomous voltage regulation does not change the power exchange among cells.

Under the ADN concept, a solution to cope with the power flow management problem needs to be flexible, intelligent and must be implementable in distribution systems. A combination of graph theory and intelligent control algorithms is proposed in the following sections.

5.2.2 Graph model

The power system is firstly converted to a directed graph $G(V, E)$, in which $V = \{v_1, \ldots, v_n\}$ presents the set of vertices (cells in the ADN) and $E \in V \times V$ presents edges $e_{ij} = (v_i, v_j)$ (interconnection lines among cells in the ADN). The edge length (edge cost) c_{ij} and residual (available) capacity r_{ij} are associated with each edge e_{ij} which is derived from the transmission cost β_{ij} and the transmission line capacity u_{ij}. Two vertices are added: a virtual source node (s) and a sink node (t). For each cell i with generation, a source edge (s, i) is added with residual capacity r_{si} (cell generation available) and cost c_{si} (cell production cost γ_i). For each cell j with load, a sink edge (j, t) is added with residual capacity r_{jt} (cell load demand) and cost c_{it} (cell load priority cost γ_i).

The graph $G(V, E)$ is initially assumed to be a directed graph for which the direction of each edge (i, j) is defined by the current direction of the flow and is assumed to be remained. However, the power flow might be changed by varying the injecting power or by intentionally using a PFC. Therefore, some edges (i, j) will get another direction, the so called undirected edges $\{i, j\}$. Thus, the algorithm needs to be adaptive with undirected flows. Network transformations can help to convert these undirected edges $\{i, j\}$ to directed edges [107]. Each undirected edge $\{i, j\}$ is firstly replaced by two direct edges (i, j) and (j, i) with the same cost c_{ij} and residual capacity r_{ij}. The flow on undirected edge $\{i, j\}$ is then defined as the association of flows on the direct edges (i, j) and (j, i), i.e., $f_{ij} - f_{ji}$, that is positive when flowing from node i to node j and vice versa.

This procedure is illustrated in detail in Figure 5.2 with an example of a 5-cell (bus) system. The graph model of the system is shown in Figure 5.3. The edges among cells represent interconnection lines with associated transmission cost (β_{ij}) in $p.u.$ and the transmission line capacity (u_{ij}) in MVA. Three directed edges from s to node 1, 2, and 3 represent the generation of cell 1, cell 2, and cell 3, respectively. Associated numbers of these edges are cells power generation cost α_i in $p.u.$ and power generation capacity P_{Gi}^{max} in MW. Five directed edges from 5 nodes to t represent the load demand of each cell, respectively. Associated

numbers of these edges are cells load priority cost γ_i in $p.u.$ and load demand P_{Li} in MW. The SSP and CS-PR algorithms are developed to solve the minimum cost flow problem in this representative graph.

$P_{G1}{}^{max} = 15\text{MW}, \alpha_1 = 7$
$P_{L1} = 5\text{MW}, \gamma_1 = 1$

$P_{G2}{}^{max} = 10\text{MW}, \alpha_2 = 2$
$P_{L2} = 10\text{MW}, \gamma_2 = 1$

$P_{G3}{}^{max} = 18\text{MW}, \alpha_3 = 3$
$P_{L3} = 10\text{MW}, \gamma_3 = 1$

$u_{12} = 7$
$\beta_{12} = 1$

$u_{23} = 5$
$\beta_{23} = 2$

$u_{35} = 8$
$\beta_{35} = 1$

$u_{14} = 5$
$\beta_{14} = 3$

$u_{45} = 5$
$\beta_{45} = 2$

$P_{G4}{}^{max} = 0\text{MW}, \alpha_4 = 0$
$P_{L4} = 5\text{MW}, \gamma_4 = 2$

$P_{G5}{}^{max} = 0\text{MW}, \alpha_5 = 0$
$P_{L5} = 5\text{MW}, \gamma_5 = 2$
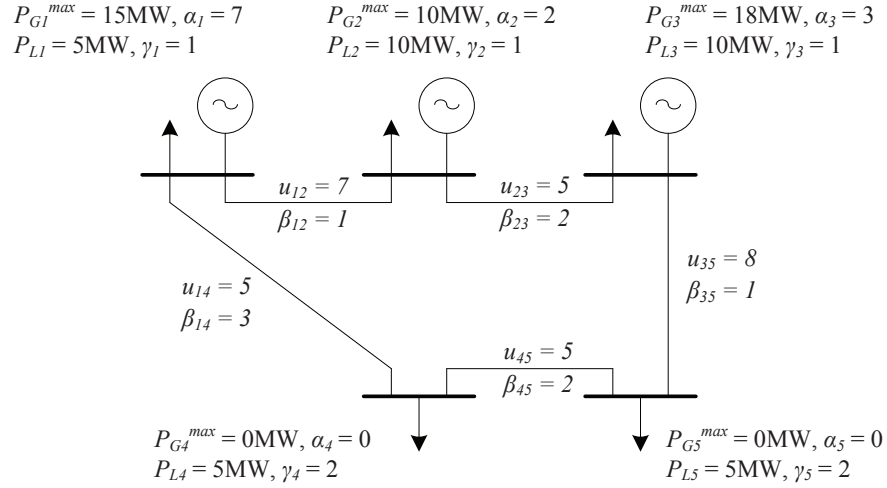
Figure 5.2: Single-line diagram of the 5-cell meshed test network.

5.3   Successive shortest path algorithm

5.3.1   Algorithm description

In the graph theory, the problem formulation in equation 5.1a can be understood as coupling problem of the shortest path (economy) and the maximum flow (capacity). This section describes algorithms and applications in the power system field to cope with each problem separately and dually.

   The shortest path method determines, for every non-source node, a shortest length directed path from node s to node i [107]. In the electrical power system, the shortest path problem can be presented as an optimal cost function for scheduling [130]. It is the problem mentioned in equation 5.1a with equality constraint 5.1b and without capacity constraints, i.e., inequality constraints 5.1c and 5.1d.

   While the power system is represented by a directed graph model with non-negative edge lengths, the Dijkstra algorithm can be used to solve the problem in $O(n^2)$ time. For general and flexible application, the generic label-correcting algorithm has been used in this research. The Bellman Ford algorithm, that solves the shortest path problem in $O(nm)$ time, can be viewed as a special case of the generic label-correcting algorithm. Note that n is the number of vertices
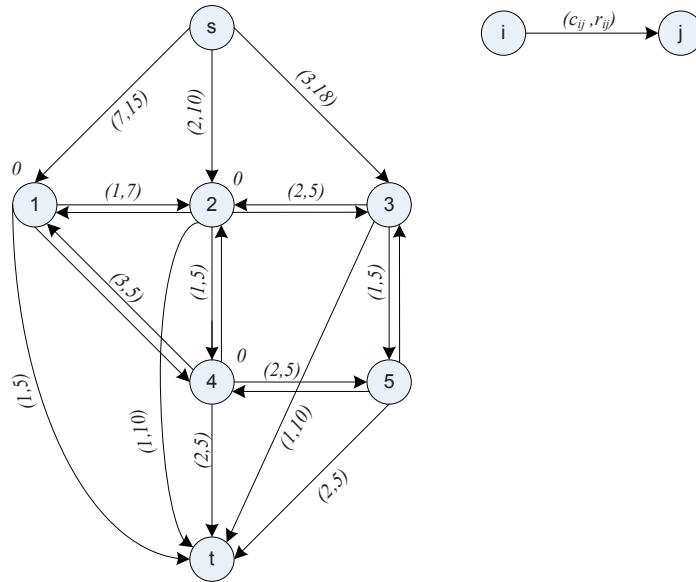
Figure 5.3: Representative directed graph of the 5-cell meshed test network.

and m is the number of edges in the graph $G(V, E)$.

The node potential π_i is defined as the minimum cost needed for a flow from the source node s to node i. It can be associated with each vertex i of the graph $G(V, E)$. The algorithm is a general procedure for successively updating the distance labels until they satisfy the shortest path optimality conditions:

$$\pi_j \leq \pi_i - c_{ij}, \forall (i, j) \in E \tag{5.2}$$

Figure 5.4 illustrates the algorithm used with the above example network. As the problem does not concern the line capacities, the residual capacity r_{ij} of each edge (i, j) is neglected. The node potentials are initiated as 0 for all vertices. The algorithm starts with an updating procedure from the source node s. As the node potential of s is always set to be 0, it sends its information to its neighbors (node 1, 2, and 3). Their node potentials are updated regarding equation 5.2 with received information π_s and cost c_{sj}. The potentials of node 1, 2, and 3 are then updated as -7, -2, and -3, respectively. Node 1 then receives an additional message from node 2 due to incoming line 1-2 with higher value of $\pi_2 - c_{12} = -3$. Hence, the node potential π_1 is updated with a new value of -3. Then after finishing the update step, the algorithm finds out the shortest path of $s - 2 - t$.

The maximum flow problem is another aspect of the network flow that deals with the network capacities while ignoring the costs [107]. Its main target is to send as much power as possible from source node s to sink node t with respect to the edge capacities. The maximum flow problem is applied in power
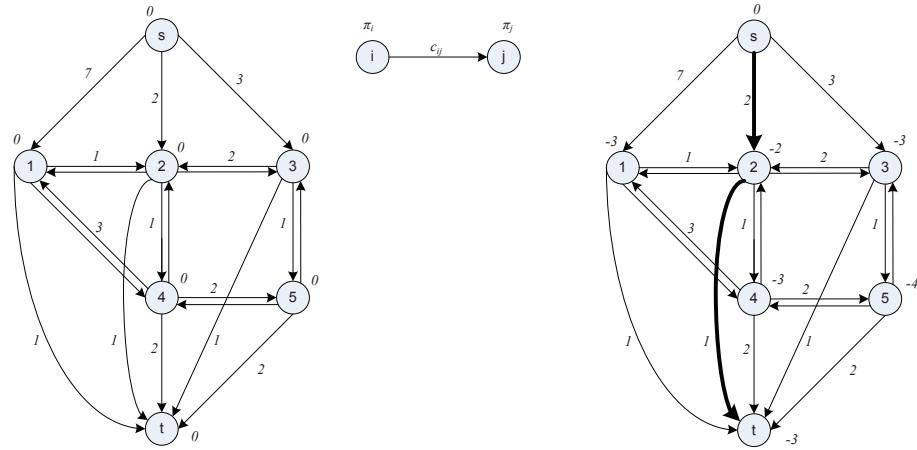
Figure 5.4: Solving the shortest path problem by a generic label-correcting algorithm.

transmission control to determine the set points for FACTS devices and their coordination [130].

Combination of the shortest path and the maximum flow formulates the minimum cost flow problem. It is the central objective of the proposed solution that deals with both network costs and capacities of the electric grid. For the distributed implementation, a simple and effective method to solve the minimum cost flow problem is the SSP algorithm. The algorithm starts by looking for a shortest path by using the generic label-correcting algorithm. Note that a reduced cost defined as follows:

$$c_{ij}^{\pi} = c_{ij} - \pi_i + \pi_j \tag{5.3}$$

is used instead of c_{ij} for each edge. The algorithm then augments the flow along the shortest path from s to t until reaching the capacity of at least one edge. After updating the flow, it finds another shortest path and augments the flow again. The algorithm is terminated when there is no possible path from s to t.

Figure 5.5 illustrates the steps after finding out the shortest path for the example of Figure 5.4. Regarding the limit on capacity, the shortest path can allow flow up to 10MW. After augmenting the flow on $s - 2 - t$, the residual capacities r_{s2} and r_{2t} become 0. The algorithm starts looking for another shortest path. On the right side of Figure 5.5, a new shortest path $s - 3 - t$ is identified and is able to transmit flow up to another 10MW. The residual capacity r_{s3} is decreased to 8 while r_{3t} is 0. The procedure is repeated until all incoming lines to t are at full load. In other words, the load demand of the network is fully met.

As the bus voltages are assumed to be controlled ($1p.u.$) within each cell, the amount of the power loss for each interconnection line can be easily calculated
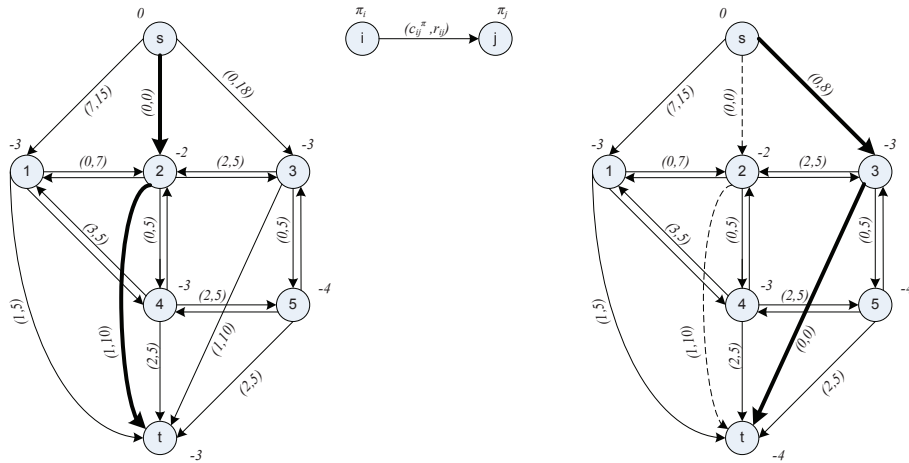
Figure 5.5: Solving the minimum cost flow problem by the successive shortest path algorithm.

and seen as an extra flow. So, the losses are taken into account when the algorithm starts augmenting the flow along each shortest path.

5.3.2 Distributed implementation

Each moderator A_i representing a cell can obtain local area information such as power flow in incoming (outgoing) feeders, power generation reserve, power load demand, and costs of production and load priority. Two additional agents, A_s and A_t, are created to represent a source node s and a sink node t of the graph $G(V, E)$. The distributed implementation of the successive shortest path algorithm is brought under a MAS platform.

The agent A_i firstly updates the local information about cell i. Depending on the characteristic of the cell, A_i will send an *Information* message to A_s or (and) A_t. Then A_i waits for a reply that might be *Getlabel* or *Augment* messages. Behaviors of A_i are summarized in Algorithm 5.1.

After receiving all $Information$ messages from the generating cells (complete update), the source node agent A_s starts updating node potentials by sending *Getlabel* messages to its inferiors. Variable int_s is used to locally monitor algorithm iterations. If there is no possible path from s to t, A_s will receive a notification to terminate the algorithm. Behaviors of A_s are summarized in Algorithm 5.2.

As A_t is the last agent to update the node potential, it will start tracking backwards along the shortest path and augment the flow regarding the residual capacity. Behaviors of A_t are summarized in Algorithm 5.3.

Algorithm 5.1 Pseudo-Code for A_i actions

$\quad Received(Mode) \leftarrow Message(objective)$
$\quad$**if** $Mode = 1$ **then**
$\quad\quad [P_{Li}, \gamma_i, P_{Gi}, \alpha_i, P_{Gi}{}^{max}] \leftarrow Cell i$
$\quad\quad$**if** $P_{Gi} > 0$ **then**
$\quad\quad\quad Information[P_{Gi}, \alpha_i, P_{Gi}{}^{max}] \rightarrow A_s$
$\quad\quad\quad Information[P_{Li}, \gamma_i] \rightarrow A_t$
$\quad\quad$**end if**
$\quad$**end if**
$\quad$**if** $Mode = 2$ **then**
$\quad\quad Getlabel[\pi_j, int_j] \leftarrow A_j$
$\quad\quad$**if** $\pi_i > \pi_j - c_{ij}$ **then**
$\quad\quad\quad \pi_i = \pi_j - c_{ij}$
$\quad\quad\quad r_{ij} \leftarrow \min(r_{ij}, P_{ij}{}^{max} - f_{ij})$
$\quad\quad\quad predecessor_i \leftarrow A_j$
$\quad\quad\quad Getlabel[\pi_i, int_i] \rightarrow neighbor(i)$
$\quad\quad$**end if**
$\quad$**end if**
$\quad$**if** $Mode = 3$ **then**
$\quad\quad Augment[f_{ij} \leftarrow f_{ij} + r_{ij}] \rightarrow predecessor_i$
$\quad$**end if**

5.3.3   Algorithm properties

The successive shortest path algorithm requires $O(nB)$ iterations where B is defined as an upper bound of the largest supply (demand) of any node. By using the generic label-correcting algorithm or Bellman Ford algorithm with $O(nm)$ computation time, the complexity of the SSP algorithm is $O(n^2mB)$.

Since all the potential nodes and reduced costs are updated to eliminate violation of optimal, the successive shortest path algorithm will be terminated. However, augmentations might carry relatively small amounts of flow, resulting in a fairly large number of iterations, $O(nB)$. A modification with a scaling algorithm can reduce the number of iterations to $O(mlogB)$.

5.4   Cost-scaling push-relabel algorithm

5.4.1   Algorithm description

CS-PR belongs to the polynomial-time algorithms to solve the minimum cost flow problem in complex networks. It is different from capacity scaling which is a scaled version of the SSP algorithm investigated in the previous section. The same example of the 5-cell network is used to illustrate the algorithm.

To avoid using a virtual sink node, the algorithm applies associated load demands d_i for every nodes to calculate the *excess* flow into each nodes defined

---

Algorithm 5.2 Pseudo-Code for A_s actions

$Receivede(Mode) \leftarrow Message(objective)$
if $Mode = 1$ **then**
  $[r_{si}, c_{si}] \leftarrow Information[P_{Gi}, \alpha_i, P_{Gi}{}^{max}]$
  if complete update **then**
    $Getlabel[\pi_s, int_s] \rightarrow neighbor(s)$
  end if
end if
if $Mode = 2$ **then**
  $[f_{si}, r_{si}] \leftarrow Augment[f_{ij}]$
  if no shortest path **then**
    STOP
  else
    $Getlabel[\pi_s, int_s \leftarrow int_s + 1] \rightarrow neighbor(s)$
  end if
end if

Algorithm 5.3 Pseudo-Code for A_t actions

$Receivede(Mode) \leftarrow Message(objective)$
if $Mode = 1$ **then**
  $[r_{ti}, c_{ti}] \leftarrow Information[P_{Li}, \gamma_i]$
end if
if $Mode = 2$ **then**
  $Getlabel[\pi_i, int_i] \leftarrow A_i$
  if Get all label **then**
    $Augment[f_{tj}, j \leftarrow predecessor_t] \rightarrow predecessor_t$
  end if
end if

---

as:

$$e_i = \sum_{(i,j) \in E} f(i,j) - d(i) \qquad (5.4)$$

while $f(i,j)$ is *pre-flow* that satisfies the flow bound constraint. A node i with $e_i > 0$ is called *active node*. A branch (i,j) is *admissible* if $-\varepsilon/2 \leq c_{ij}^\pi < 0$.

The algorithm starts with a scaling factor $\varepsilon = max\{\alpha_i, \beta_i\}$, and $\pi_i = 0$. For a given node potential , the reduced cost of an arc is defined as in equation 5.3.

Figure 5.6 shows the representative directed graph of the test network with its parameters. Each active node i can locally detect and perform on an admissible arc (i,j) a push operation:

$$\delta_{ij} = min(e_i, r_{ij}) \qquad (5.5)$$

When the active node i contains no admissible arc, the algorithm applies a relabel operation to update the node potential by

$$\pi_i = \pi_i + \varepsilon/2 \qquad (5.6)$$
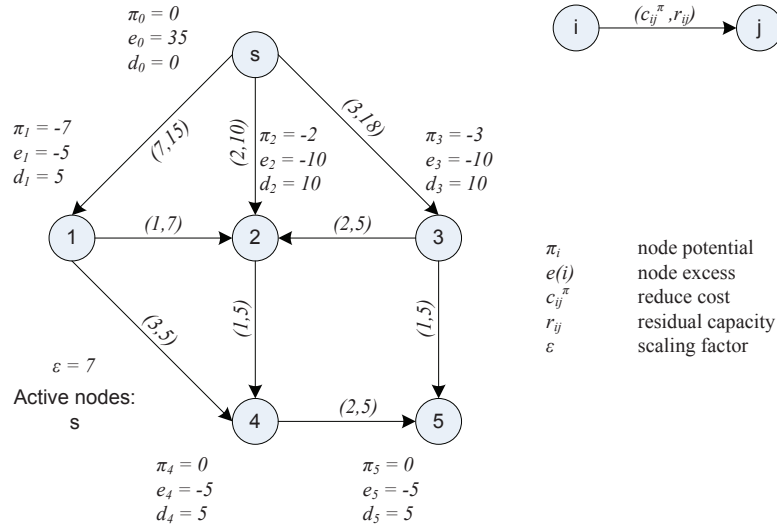
Figure 5.6: Representative directed graph for the CS-PR algorithm.

Note that the relabel operation at node i will increases the units on incoming arcs and decreases units on outgoing arcs of the node due to the reduced cost condition in equation 5.3. Consequently, the algorithm creates new admissible arcs for push operation. When there is no possibility to push flow forward, node i can push flow backward to source node s. Essential steps of the *push-relabel* operation are summarized in Algorithm 5.4.

Algorithm 5.4 $PushRelabel()$

---

if contain admissible $(s, j) \in E$ **then**
  $\delta = min(e_s, r_{sj})$
  $Push(S, \varepsilon) \rightarrow A_j$
else
  $\pi_s = \pi_s + \varepsilon/2$
  $c_{sj}^\pi = c_{sj} - \pi_s + \pi_j; \forall (s, j) \in E$
end if

In the example, as active node s has no admissible branch, it performs relabel operation to update its node potential to $\pi_s = 3.5$, as shown in Figure 5.7. The operation yields two admissible arcs $(s, 2)$ and $(s, 3)$. Consequently, the push operation is applied on these arcs and makes them saturated. As $e_3 = 8$, node 3 is active and added in the list S. The active node list S is built in the first-in-first-out format.

The algorithm repeats until there is no active node in the list. The pre-flow has been converted to ε-optimal flow completely. By decreasing $1/2$ value of
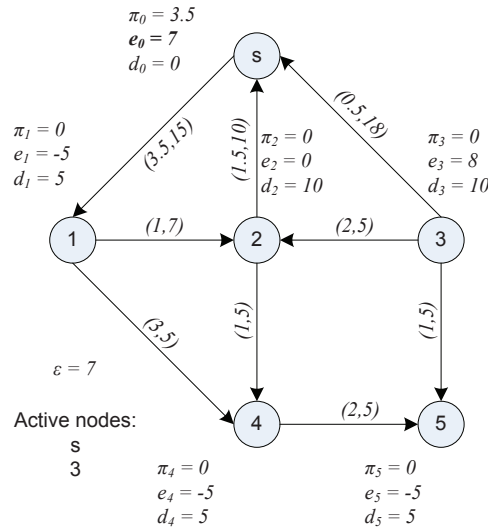
Figure 5.7: Pre-flows after performing relable and push operation.

ε and saturating every arcs with negative reduced costs, the ε-optimal flow is converted to $\varepsilon/2$-optimal pre-flow and a new iteration starts. When $\varepsilon < 1/n$, the algorithm terminates. Algorithm 5.5 shows the pseudo-code for the *cost-scaling* procedure.

Algorithm 5.5 $CostScaling()$

---

   if $S = \emptyset$ **then**
      $\varepsilon = \varepsilon/2$
      if $\varepsilon < 1/n$ **then**
         STOP
      else
         $PushRelabel(S, \varepsilon) \rightarrow A_{S[1]}$
      end if
   else
      $PushRelabel(S, \varepsilon) \rightarrow A_{S[1]}$
   end if

5.4.2 Distributed implementation

In this research, the CS-PR algorithm is implemented in a distributed agent environment. Each normal node i of the graph is represented by a principle agent A_i with its pseudo-code as shown in Algorithm 5.6. The virtual source node is represented by a principle agent A_s with its pseudo-code as shown in Algorithm 5.7. After receiving all *Information* messages from other cells (com-

plete update), A_s deploys *PushRelabel()* function to push flow to the first active node in the list S. Since each node needs only knowledge from its immediate neighborhood to execute the algorithm, it suffices that the nodes exchange the corresponding information with their neighbors each time that there is a change. Thus each node knows when a branch incident to itself is admissible and can take the corresponding action.

Algorithm 5.6 Pseudo-Code for A_i actions of the CS-PR algorithm

---

$Receivede(Mode) \leftarrow Message(objective)$
if $Mode = 1$ **then**
   $[P_{Li}, P_{Gi}, P_{Gi}^{max}, \alpha_i, \beta_{ij}; \forall(i,j) \in E] \leftarrow Gird$
   $e_i = P_{Gi} - P_{Li}$
   if $P_{Gi} > 0$ **then**
      $Inform(P_{Gi}, \alpha_i, P_{Gi}^{max}, e_i, S) \rightarrow A_s$
   end if
end if
if $Mode = 2$ **then**
   while $e_s > 0$ **do**
      $PushRelabel()$
   end while
   $S \leftarrow S - A_s$
   $CostScaling()$
end if
if $Mode = 3$ **then**
   $[\delta_{ji}, S, \varepsilon] \leftarrow Push[\delta_{ij}, S, \varepsilon]$
   $e_i = e_i + \delta_{ij}$
   if $e_i > 0$ **then**
      $S \leftarrow A_s$
      $UpdateS(S) \rightarrow A_i$
   end if
end if

5.4.3 Algorithm properties

The proposed method's convergence properties are analyzed for the min-cost flow algorithm in [131]. Moreover, due to its locality, the algorithm has self-stabilizing and self-healing properties (in response to transient errors or changes in demand/supply, cost or topology), as analyzed in [132]. It is reasonable to assume that the nodes will be able to adapt locally to small changes in the parameters (via push-relabel operations), leading to the fast stabilization and recovery. One may conjecture that more extensive changes, such as a cascade failure effect, will need more time to recover from but this time will be significantly less than other more centralized min-cost flow solutions.

Concerning the convergence time, as there is no global schedule on the order in which the admissible branch operations are activated, the worst case bound

---

Algorithm 5.7 Pseudo-Code for A_s actions of the CS-PR algorithm

---

$Receivede(Mode) \leftarrow Message(objective)$
if $Mode = 1$ then
  $[r_{si}, c_{si}, e_s \leftarrow e_s + e_i] \leftarrow Information[P_{Gi}, \alpha_i, P_{Gi}{}^{max}, e_i, S]$
  if complete update then
    $PushRelabel()$
  end if
end if
if $Mode = 2$ then
  $\varepsilon \leftarrow relabel[\varepsilon]$
  $CostScaling()$
end if
if $Mode = 3$ then
  $[\delta_{si}, S, \varepsilon] \leftarrow Push[\delta_{is}, S, \varepsilon]$
  $e_s = e_s + \delta_{is}$
  if $e_s > 0$ then
    $S \leftarrow A_s$
    $UpdateS(S) \rightarrow A_i$
  end if
end if
if $Mode = 4$ then
  while $e_s > 0$ do
    $PushRelabel()$
  end while
  $S \leftarrow S - A_s$
  $CostScaling()$
end if

---

depends on the size of the network. However, in a normal case the convergence time is expected to be significantly smaller than for other methods.

The set S of the active nodes plays a key role in the push-relabel operation. Along with the amount of flow δ_{ij} on admissible arc (i, j), S is sent from active node i to target node j in $Push$ message called in $PushRelabel()$. After receiving the message, agent A_j will check if it has positive excess e_j taken amount of δ_{ij} into account. The agent A_j will be added at the end of the list S of active nodes if $e_j > 0$. Actually, this global schedule on the order of the active nodes includes a subtle centralized characteristic.
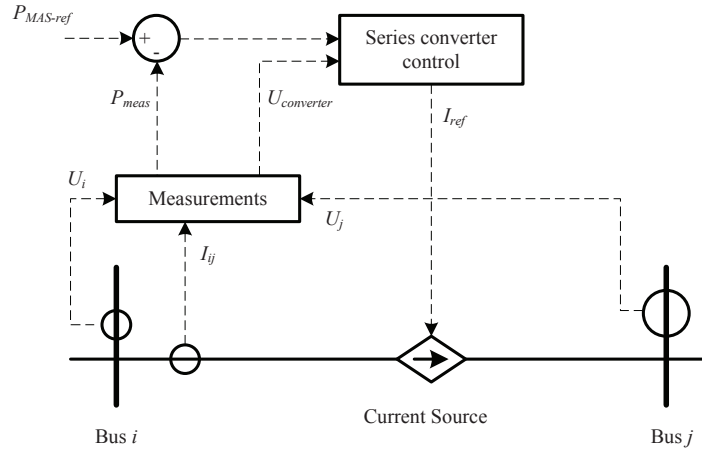
Figure 5.8: A simplified model of PFC.

5.5 Simulation and results

5.5.1 Setting-up the simulation

Electrical Power System Model

The ADN is simulated using Matlab/Simulink. For simplicity, the model of each cell consists of an equivalent generator, an equivalent load, as well as a PFC device. An "Embedded Matlab Function" is created for each cell as part of the power router. Local information about the subsystems is transferred through this block to be processed at the MAS platform. The block then receives control set points for generation and PFC.

In this research, PFC is modified from a series part of the UPFC phasor model, which belongs to SimPowerSystem toolbox [133]. The main objective of this device is to control the active power flow according to reference values given by MAS. Through PI regulators, error values are transferred to the U_d and U_q components of the voltage that are used as control signals of series converters. For simplification, PFC uses a Current Source block instead of a power electronic device to control power flow. The simplified model of PFC is shown in Figure 5.8.

The power flow controller (PFC) is used as a valve to distribute amounts of injected power. Hence, there is no need to have PFC at load cells which only receive power from generating cells. In the simulation, there are only three PFCs installed at generating cells, i.e., cell 1, cell 2, and cell 3.

Multi-Agent System Model

MAS is created under the JADE [92]. JADE has recently been used as a popular platform for application of MAS in power engineering applications. It supports
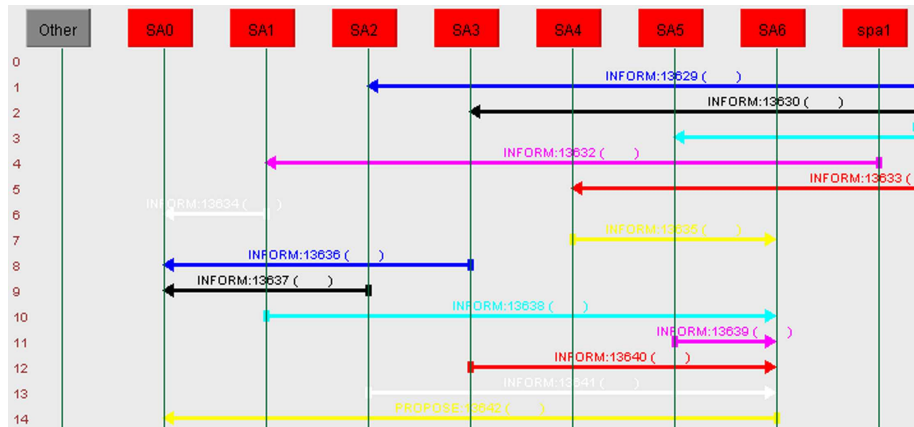
Figure 5.9: Message dialogue of MAS in JADE.

a Graphic User Interface and uses communication languages that follow the FIPA standard.

In this simulation, each subsystem is managed by a pair of the agents, i.e., a socket proxy agent (spa) and server agent Server Agent (SA). While the spa agent is used as the communication agent with Matlab/Simulink, the SA agent is the principal agent that deploys proposed algorithms for power flow management. Two additional server agents, SA0 and SA6, are created to represent the virtual source node s and sink node t of the graph.

The protocol for communication between Matlab/Simulink and JADE is based on client/server socket communication. The socket proxy agent in JADE is used as a server socket. By using the TCP/UDP/IP Toolbox [134], each "Embedded Matlab Function" in Matlab/Simulink can create a client socket to send data to and receive data for the spa agents. The communication time is set at $0.5sec$.

For each communication period, the local information about the subsystems, i.e., label costs, power reserve, and load demand will be sent to the SA agents. Figure 5.9 shows some messages which are exchanged among moderators to update information held by MAS.

At the beginning stage, the five spa agents send local information about the five subsystems to the SA agents, message 1 to message 5, respectively. Each SA itself sends its information to the source agent (SA0) and/or the sink agent (SA6). After updating information about the electrical network, MAS starts by looking for the optimal operation state based on the successive shortest path algorithm or the cost-scaling push-relabel algorithm.

5.5.2　Meshed network experiments

This case uses the input data from the 5-cell meshed test network shown in Figure 5.2 to compare results of the CS-PR algorithm with the SSP algorithm.

The network data is given in Table 5.1.

Values of the minimized objective function **f**, in equation 5.1a, and number of exchanged messages of both SSP and CS-PR are compared and summarized in Table 5.2. In all studied cases, they have more or less the same power generation results but slightly different in power flows. It can be explained by the augmenting characteristic of SSP compared with the push-relabel operation of CS-PR. Number of exchanged messages among agent in JADE in both algorithms is almost the same. A significant difference is in the case of line 2-4 outage, the network becomes a ring configuration in which the CS-PR algorithm performs better in terms of computation speed. This advantage is investigated further in the radial network experiments.

Results of the SSP algorithm in these simulation cases are presented more in detail in following sections.

Table 5.1: 5-cell network data

	Cell 1	Cell 2	Cell 3	Cell 4	Cell 5
Generation rating, MW	15	10	18	-	-
Load demand, MW	5	10	10	5	5
Voltage level, kV			10		
Tie-line impedance, $p.u.$		$R = 0.25; X = 0.178; B = 10e - 5$			

Table 5.2: Comparison between the SSP and CS-PR algorithms in the meshed test network

Cases	SSP		CS-PR	
	$A, p.u.$	No. of messages	$A, p.u.$	No. of messages
Optimal operation	189.74	137	190.60	154
Congestion management	193.62	162	194.23	154
Production cost change	209.06	132	210.57	106
Line 2-4 is out of service	214.36	110	218.48	68
Load demand increases	255.15	119	240.38	117

Optimal operation

At $t = 5sec.$, each agent starts collecting and sharing information across the MAS platform. At $t = 10sec.$, new reference values are set for generation and PFC devices The generators and PFC devices start controlling the power so as to reach new set points. The transient state occurs within around $10sec.$ and the system reaches a new optimal state. The behavior of the system when the proposed method starts working is shown in Figure 5.10.

Figure 5.11 illustrates variations of the power flow and the consequent total cost saving, which is the difference of the objective function **f** before and after applying the control method. The power flows represented by symbols $(-, \triangle, \Diamond)$
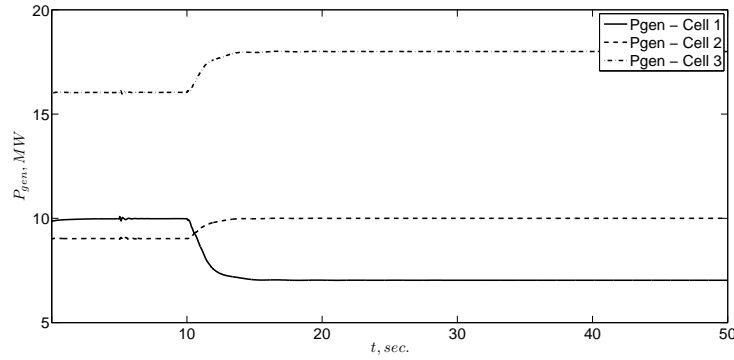
(a) Power generation change.
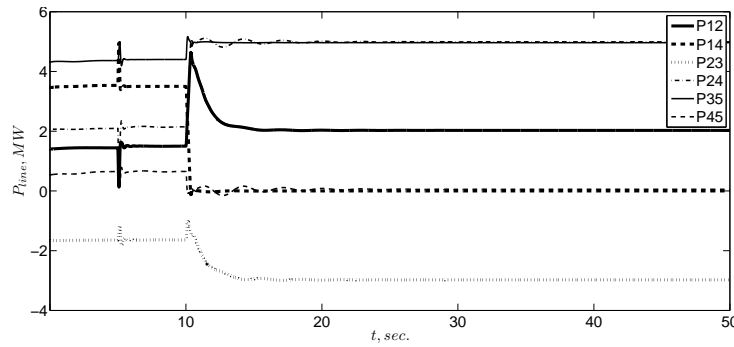
(b) Power flows change.

Figure 5.10: Optimal operation case - The SSP algorithm.

on lines with respect to values without control method, with control method, and the line capacities. The cost differences for each line power flow are represented by bars. A major part of total cost is saved from decreasing the power generation in cell 1. Mitigating the power flows on line 1-4 also reduces significantly the cost. The values of the total cost function A in money-based unit before and after controlling are $208.82p.u.$ and $191.32p.u.$, respectively. In this case, the total cost saving is $17.50p.u.$

To see the ability of the method to cope with congestion, the capacity of line 3-5 is decreased from 8MW to 4MW. Although there is no change in generation dispatch, the power flows are different from the previous case due to the restriction of the lines. Therefore, the total flow cost $194.83p.u.$ is higher than previous case. The power flow variations and transmission cost changes are shown in Figure 5.12. The power flow in line 3-5 reaches its capacity of 4MW. The capacity symbol $\diamond$ and controlled flow $\triangle$ are at the same position.
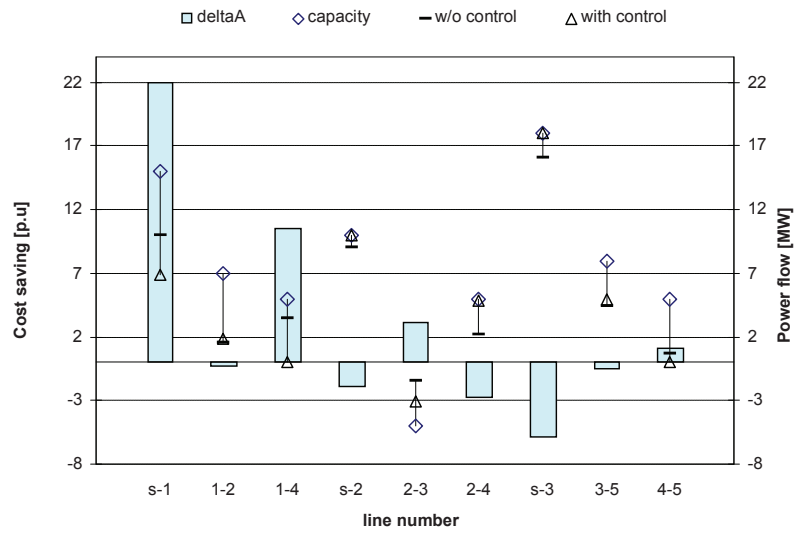
Figure 5.11: Power variation and the cost saving in the optimal operation case - The SSP algorithm.
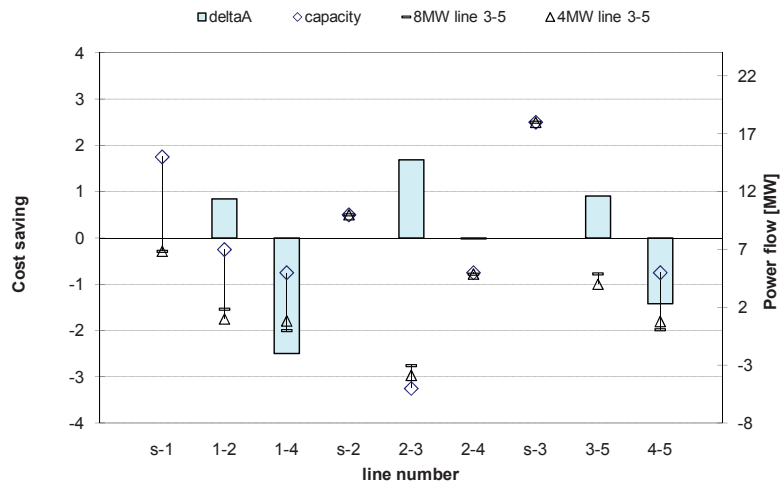
Figure 5.12: Power variation and the cost saving in case of reduced capacity on line 3-5 - The SSP algorithm.

Production cost change

As DGs are coupled often to other processes, the production costs will fluctuate frequently. To see the ability of the method to deal with production cost change, the power generation costs of cell 1, cell 2, and cell 3 are changed from 7, 2, and 3 to 3, 4, and 5, respectively. The difference in production costs establishes a new optimal operation state for the network. These variations are illustrated in Figure 5.13 and 5.14. With new production costs, the total flow costs before and after controlling are $219.03 p.u.$ and $210.07 p.u.$, respectively. Cost saving is accumulated mainly from mitigating the power flow on line 1-4 and decreasing cell 3 power generation.
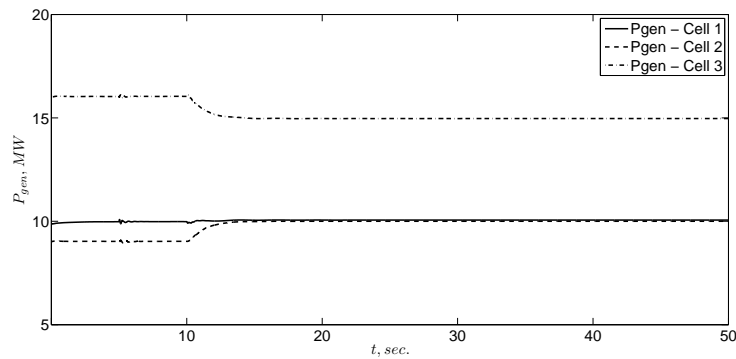
(a) Power generation change.
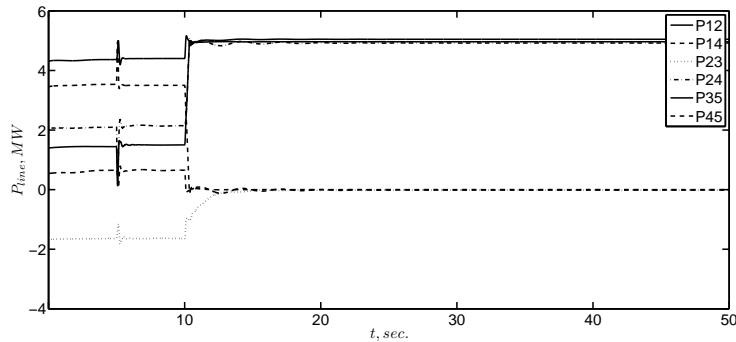
(b) Power flows change.

Figure 5.13: Production cost change - The SSP algorithm.

To see the ability to adapt with variations in the network configuration, the line 2-4 was switched off suddenly. The power flow variations and transmission cost changes are shown in Figure 5.15. The power generation dispatch is almost the same as in previous case, while the power flows show major differences. Despite its high transmission cost, the power flow on line 1-4 still increases until its capacity of 5MW is reached. This flow contributes to a significant increase in the total flow cost ($214.62 p.u.$).
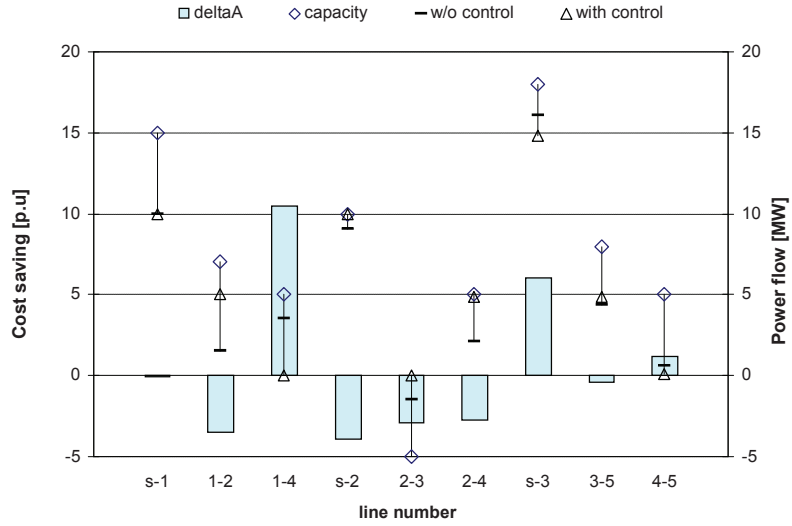
Figure 5.14: Power variation and the cost saving in case of production cost change - The SSP algorithm.
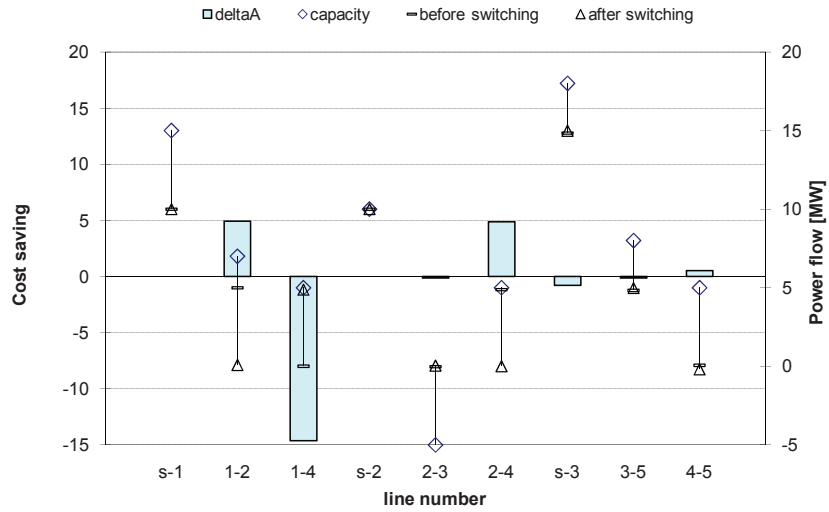
Figure 5.15: Power variation and the cost saving in case of production cost change and line 2-4 is out of service - The SSP algorithm.

Load demand change

The simulation starts running with the new production costs and the optimal state defined in the previous case. At $t = 3sec.$, the load on cell 5 is increased by 4MW additional. At $t = 5sec.$, MAS realizes the increase of the load demand and starts searching a new optimal power generation dispatch and the associated power flows. At $t = 10sec.$, new reference values are given to the cell generation and PFCs. The behavior of the network is shown in Figure 5.16.
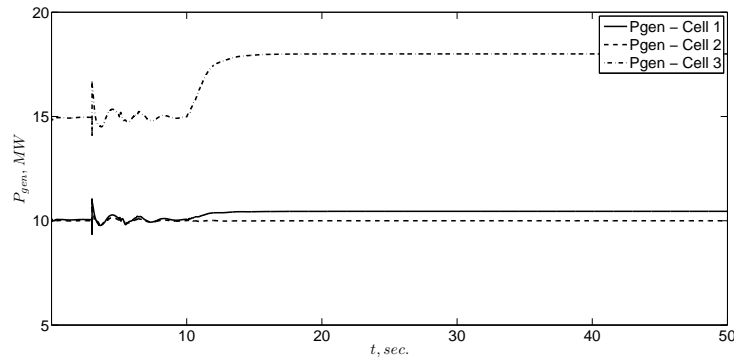
(a) Power generation change.
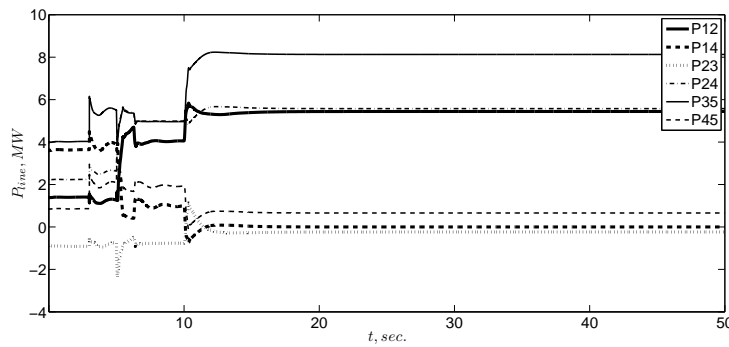
(b) Power flows change.

Figure 5.16: Load demand change - The SSP algorithm.

Figure 5.17 provides information about the system state when the load demand increases. Lines 2-4, 3-5, s-2 (cell 2 generation), and s-3 (cell 3 generation), are full loaded. Congestion on line 2-4 pushes power from cell 1 flowing on line 1-4 with high transmission cost. The total flow cost increases up to $241.88p.u.$ It can be seen that the method is able to deal with variations of the load demand by the optimal power generation dispatch and power flow control.
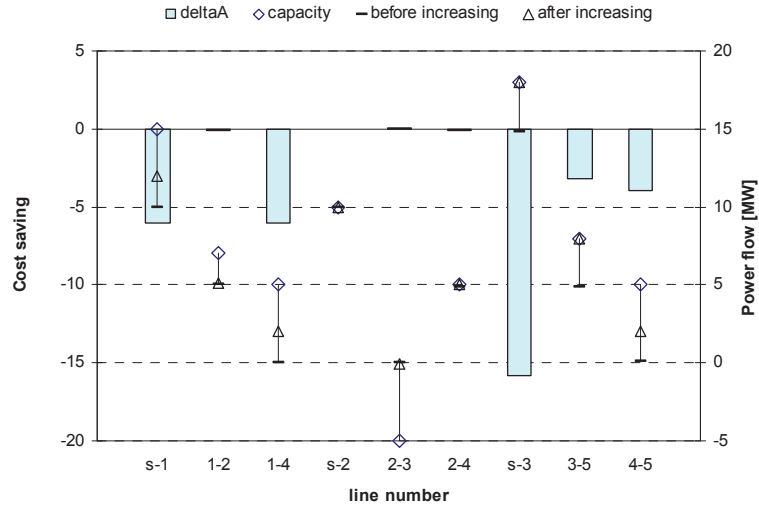
Figure 5.17: Power variation and the cost saving in case of load demand change - The SSP algorithm.

5.5.3   Radial network experiments

Based on the push-relabel principle, the CS-PR algorithm is expected to use much less computation efforts in radial networks. We investigate this advantage of the algorithm on a radial configuration of the 5-cell test network, as shown in Figure 5.18. Two simulation cases, i.e., a base case and an extreme case, are examined.
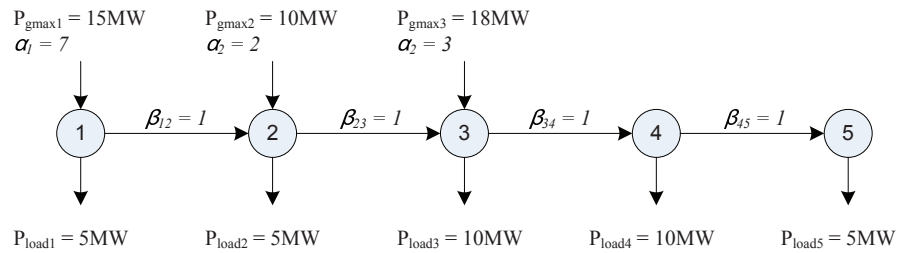
Figure 5.18: Single-line diagram of the 5-bus radial network.

In the base case, the production costs (α_i) of the three buses with generation are remained as in the previous case. The transmission costs (β_{ij}) of all branches are assumed equal $1p.u.$ Figure 5.19 shows power generation during the simulation time. The initial state of the system is generated by SimPower-System toolbox with $P_{G1} = 10.446MW$, $P_{G2} = 9.351MW$, and $P_{G3} = 16.308$.
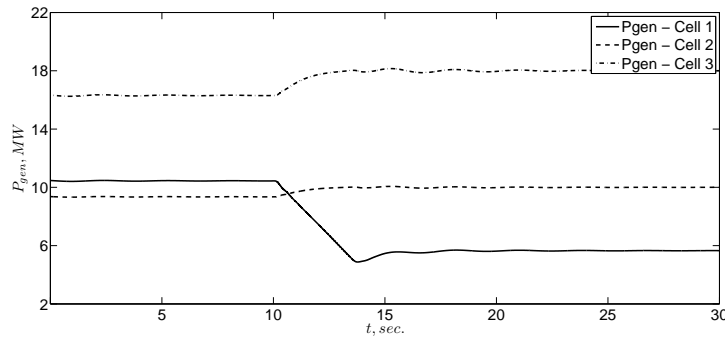
Figure 5.19: Variation of power generation - The CS-PR algorithm.

At $t = 10sec.$, the optimal routing algorithms is started. In this simulation case, the CS-PR algorithm has the same power generation ($P_{G1} = 5.668MW$, $P_{G2} = 10MW$, and $P_{G3} = 18MW$) and flow as SSP with total cost of $126.88p.u.$. However, CS-PR has exchanged significant less messages (76) compared to SSP's (115). As can be seen from the results, the push-relabel operation of CS-PR is very effective in the radial configuration. It omits significant unnecessary loops which the augmenting path algorithm has in the same network.

To see more in detail the CS-PR's advantage, the simulation investigates also an extreme case with power generation injected only in bus 1. It is assumed that there are enough generation and line capacities. Figure 5.20 and 5.21 show the representative directed graphs of the test network for CS-PR and SSP algorithms. The main drawback of the SSP method is shown in the final iteration loop. The algorithm discovers the final shortest path in bold lines which goes through all nodes of the network. The algorithm continues to send flow on the same arcs with previous augmenting path before it fills full the last arc $(5, t)$. On the contrary, CS-PR pushes flows along the individual arcs. An excess of 35 units is pushed from s straightforward through each arc to lower nodes. The final stage of push operation is shown when bus 4 realizes admissible arc $(4, 5)$ and sends 5 units to bus 5. It is quite straightforward and there is no repetitive computation.

Table 5.3 summarizes values of the total cost saving and the number of exchanged messages in both two algorithms. By pushing as much power as possible along the radial feeder, CS-PR takes only 52 messages to converge while SSP needs nearly two times that number in messages (100). In this case, both algorithms have the same power generation and flow result with total cost of $104.13p.u.$.

5.6 Summary

This chapter dealt with bi-directional power flow and intermittent generation of renewable and distributed energy sources. To have a distributed, flexible, and
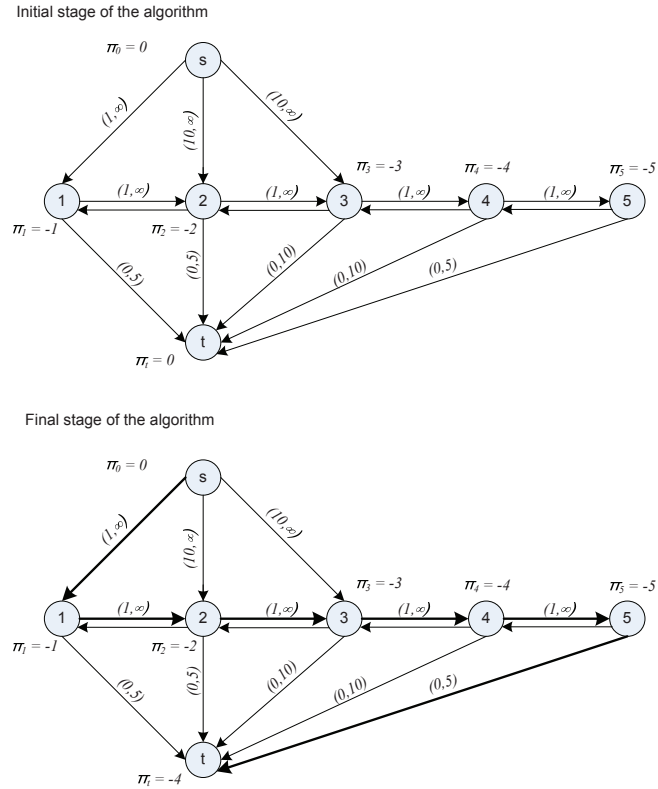
Figure 5.20: Representative directed graphs of the SSP algorithm in an extreme case on the radial test network.

Table 5.3: Comparison between the SSP and CS-PR algorithms in the radial test network

Cases	SSP		CS-PR	
	$A, p.u.$	No. of messages	$A, p.u.$	No. of messages
Base case	126.88	115	126.88	76
Extreme case	104.13	100	104.13	52

intelligent mechanism to manage power in ADN, two graph-based solutions, i.e., the SSP algorithm and the CS-PR algorithm are investigated.

The SSP algorithm solves the problem in the directed graph model that represents the current state of the power system. If there is a sudden change of the power system during processing the algorithm, the later algorithm's solution will not be proper. Any agent can detect this undesirable situation and

Initial stage of the algorithm

$\pi_0 = 0$
$e_0 = 35$

$\varepsilon = 10$

Active nodes:
s

$(1, \infty)$ $(10, \infty)$ $(10, \infty)$

$(1, \infty)$ $(1, \infty)$ $(1, \infty)$ $(1, \infty)$

$\pi_1 = 0$
$e_1 = -5$

$\pi_2 = 0$
$e_2 = -5$

$\pi_3 = 0$
$e_3 = -10$

$\pi_4 = 0$
$e_4 = -10$

$\pi_5 = 0$
$e_5 = -5$

Final stage of the algorithm

$\pi_0 = 5$
$e_0 = 35$

$\varepsilon = 10$

Active nodes:
4

$(-4, \infty)$ $(4, \infty)$ $(6, \infty)$ $(6, \infty)$

$(-4, \infty)$ $(-4, \infty)$ $(-4, \infty)$ $(-4, \infty)$
$(4, \infty)$ $(4, \infty)$ $(4, \infty)$ $(4, \infty)$

$\pi_1 = 5$
$e_1 = 0$

$\pi_2 = 5$
$e_2 = 0$

$\pi_3 = 5$
$e_3 = 15$

$\boldsymbol{\pi_4 = 3.5}$
$\boldsymbol{e_4 = 0}$

$\pi_5 = 0$
$e_5 = 0$
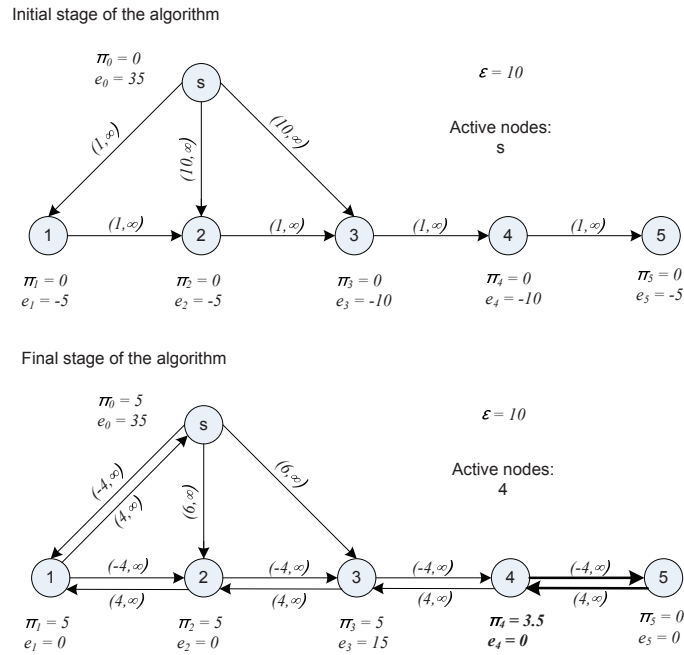
Figure 5.21: Representative directed graphs of the CS-PR algorithm in an extreme case on the radial test network.

can notify this and ask for canceling of the solution on MAS platform. The simulations show that the method can allow both generation and PFC devices to operate optimally. As the complexity of the SSP algorithm is $O(n^2 mB)$, the number of messages following among agents is significant. By selecting a particular shortest path algorithm according to the condition of the power network, this computation burden can be reduced.

Comparing with the SSP algorithm, the distributed implementation of the CS-PR algorithm to manage the power flow in the ADN was investigated. Due to its locality, the algorithm has self-stabilizing and self-healing properties in response to transient errors or changes in the demand/supply, cost or topology. By using a global schedule on the order of the active nodes, the algorithm includes a subtle centralized characteristic. To have a fully distributed algorithm, it is necessary to remove this piece as part of future work.

Performances of the two algorithms are compared in both meshed and radial networks. In the meshed network, there is no significant difference between two methods. The advantage of the cost-scaling push-relabel solution is mainly shown in the radial test network. The number of messages exchanged among agents in this algorithm is significantly smaller than in the successive shortest path method.

The research was intended to investigate a feasible application to manage the power exchange among cells in the ADN concept. In addition, the proposed method needs to be implemented in distributed way by using MAS. Therefore, the simplified model of the cell is sufficient for the scope of the research. Future development can include other control functions, i.e., voltage regulation, reactive power balance, and a more complicated model of each cell (a complete local network).

The two methods proposed in this chapter manage effectively and flexibly the power flow in the ADN. The function of power routing can deal with issues of network variations and constraints.

CHAPTER 6
_____

_____ LABORATORY IMPLEMENTATION

The strong interdisciplinary characteristics of the MAS-based ADN with its integration of power electronics and ICT, increases the complexity of modeling and simulating the power system. Software simulation cannot fully realize the issues related to communication time delay and/or information synchronization. A laboratory-scale set-up is, therefore, established to verify monitoring and control functions of the ADN in more realistic environment.

This chapter describes a 3-phase laboratory platform designed and implemented to demonstrate the performance of a smart power router in a MAS-based ADN as introduced in the previous chapters. The experimental set-up presents the capabilities of the power routing function in managing bidirectional power flows to avoid congestion while keeping voltages within suitable range. Based on MAS, this tool is able to route power in more flexible and intelligent path that is an important function to enable ADN. Inverter control features of the set-up are verified with respect to cases of connecting and disconnecting components of the test network, and changing power reference values. The set-up creates a platform for MAS control on three computers which is to manage three physical network areas. The interaction between the hardware control layer and middleware agent layer under real-time experimental environment is investigated. The set-up aims to provide a realistic test-bed which is a step forward to the practical applications of the concept.

6.1 Experimental set-up

Several laboratory-scale experiments have been implemented recently to verify operational and control functions of new network concepts such as with Micro-Grid [135], [68], [136], Active Distribution Networks [137], or Intelligent Nodes [128]. This chapter has taken experiences from these previous works into account to design a suitable lab configuration for the MAS-based ADN.
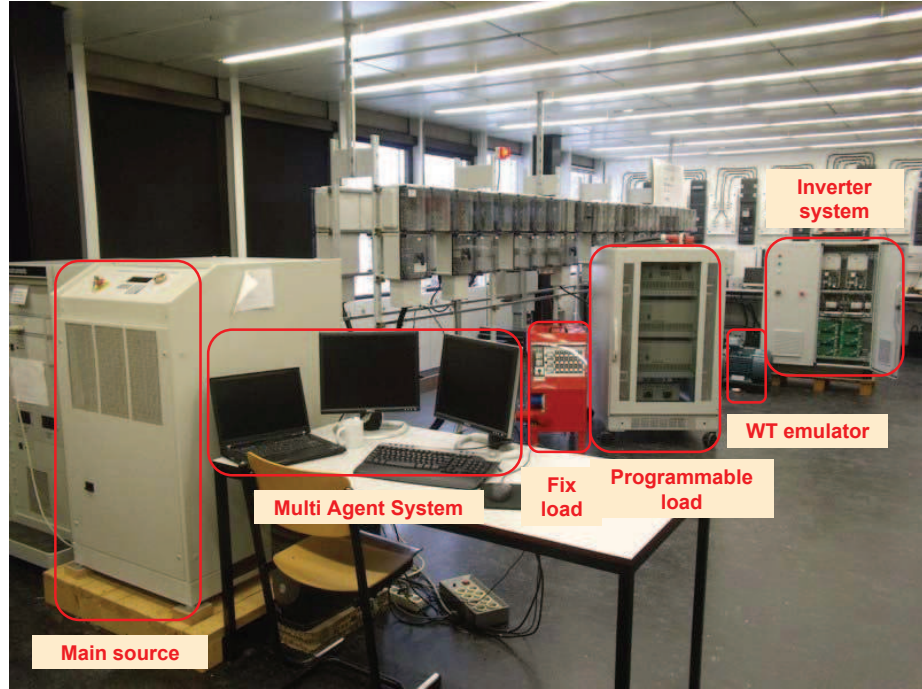
Figure 6.1: Picture of the laboratory set-up.

The realized set-up consists of a physical test network (hardware) which is separated into three areas by inverters. The MAS platform (middleware) is established by an agent-based control layer to support the concept of MAS-based ADN. Matlab/Simulink interfaces (software) are used to exchange real-time data with the agent platform and to steer the inverter controllers. Pictures and a single-line diagram of the set-up are shown in Figure 6.1 and 6.2.

6.1.1 Hardware

The test network includes a 45kVA 3-phase AC power source, an 11kW wind turbine emulator, a threefold 3-phase controllable inverter-rectifier system connected with their DC sides to a common DC bus, and fixed and programmable loads connected to 3-phase feeders. Table 6.1 gives an overview of the electrical components of the set-up and their main parameters.

As can be seen from Figure 6.2, the three inverters are used to decouple the test network into three separate areas which can be considered as cells in the ADN. Each inverter is controlled separately, see Figure 6.3. The switch S_{inv-i} is used to connect the inverter to the grid, feeder or load and is manually controlled; it trips when its current limits are exceeded (10A). The input contactor K_2^{inv-i} is normally closed for power supply to the rectifier to charge
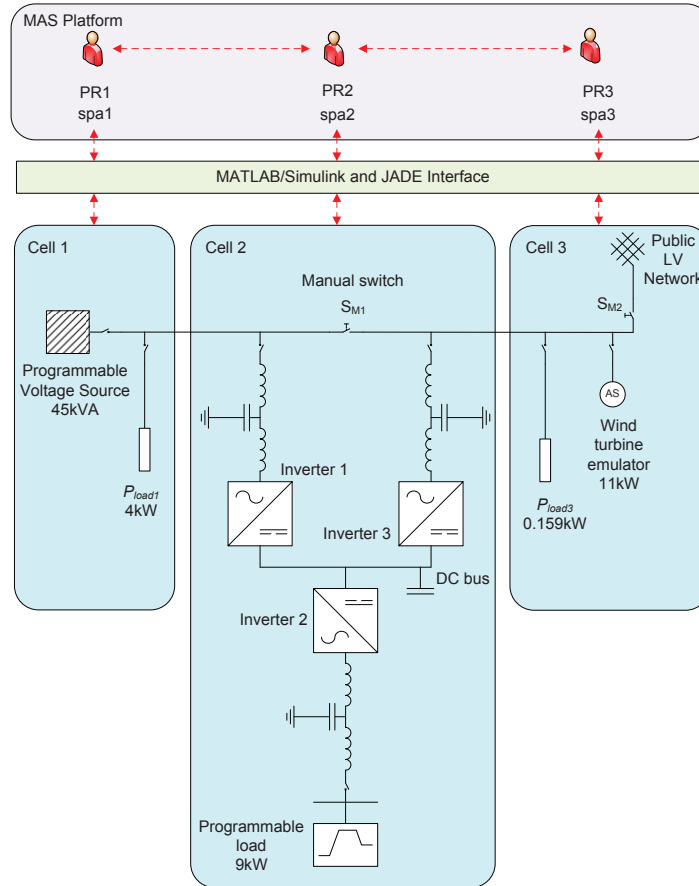
Figure 6.2: Single-line diagram of the laboratory set-up.

the DC bus whilst the output contactor K_1^{inv-i} is for the synchronization of the inverter voltage with the grid or feeder. The LCL filter is for the reduction of higher harmonics of the inverters' output voltages and currents. Via a Real-Time Target interface, measurement data is collected and used for steering inverter controllers via the Matlab/Simulink control blocks.

The wind turbine emulator consists of an 11kW motor-generator set-up. By controlling the motor speed, the variation in wind power can be emulated. It is programmable but with a limit on integrating with user interfaces, i.e., Real-Time Workshop (RTW) environment of Matlab/Simulink. In the set-up, the wind turbine emulator is used as a *non-controllable* generation unit. For starting up and safety during operation, the wind turbine emulator must be connected to the programmable source by closing the manual switches S_{M1}. In cases of opening needs S_{M1}, the wind turbine emulator will be disconnected and the public grid will be used to feed the load in cell 3 by closing S_{M2}.

Table 6.1: Electrical components of the experimental set-up

Components	Parameters	Unit	Value
Programmable source	Nominal power, S_n	VA	45000
	Applied line voltage, V_{line}	V	400
Wind turbine emulator	Nominal power, P_n	W	11000
Inverters	Nominal power, S_{inv}	VA	5000
	Maximum current, I_{max}	A	10
	Resistance at inverter side, R_1	Ω	1-1.5
	Resistance at grid side, R_2	Ω	0.2
	Damping series resistors, R_D	Ω	0
	Inductance at inverter side, L_1	mH	6.4
	Inductance at grid side, L_2	mH	2.1
	Filter capacity, C	μF	2.2
	Switching frequency, f_s	kHz	8
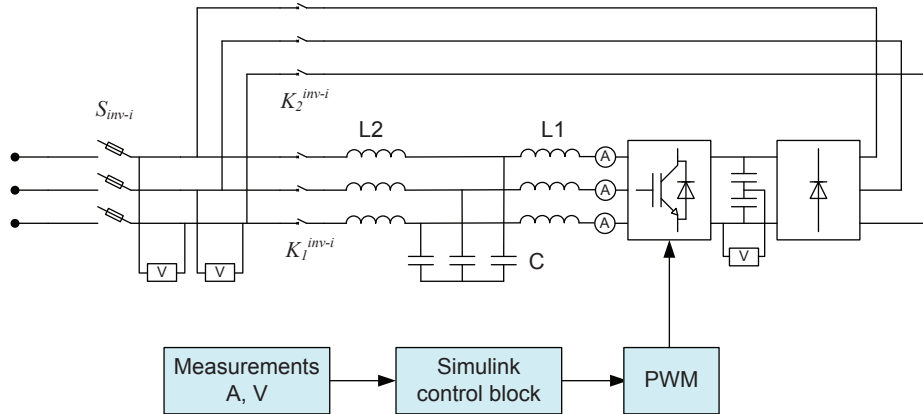
Figure 6.3: Schematic representation of the inverter system with controller.

To create an agent platform to manage the test network, three Personal Computers (PCs) with standard configuration are used. A Linux-based PC is connected to the inverter systems as the Real-Time Target (RTT) to execute all control functions compiled from the engineering PCs.

6.1.2   Middleware

As a popular platform for the application of MAS in power engineering [57], [58], [68], JADE [138] is used in this set-up. The agent communication languages are set by FIPA, an international standard [122]. Figure 6.4 shows the JADE agent platform and the graphical user interface of a power routing agent. Besides the main container of information, the platform includes three additional containers which are created on the three separate computers. Each container consists of a

(a) JADE agent platform.

(b) Graphical user interface of PR agent.
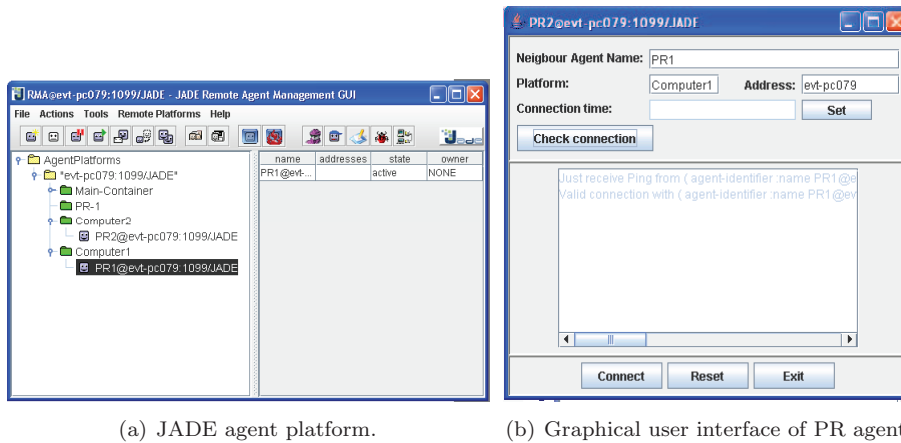
Figure 6.4: The Multi-Agent System platform used in the experiment.

pair of spa and Power Router (PR) agents to manage a cell in the experimental set-up. While spa is used as the communication agent to exchange information between the agent platform and the Matlab/Simulink software, PR is a principal agent to perform the distributed control functions on the relevant devices.

6.1.3   Software

The control algorithms for the inverter systems can be deployed by the Field Programmable Gate Array (FPGA) technology from the engineering PCs in which the inverter controllers are modeled in Simulink under a RTW environment. The Simulink model of the inverter controllers diagrams are compiled in C-code and sent to the RTT on the Linux-based PC. The user can easily monitor the measured data and adjust the parameters of the test network via the client-server interface of Simulink. However, there are some restrictions for which the user can not directly access and obtain data during program execution.

In previous chapters, the TCP/IP/UDP toolbox [139] is used as an interface between the power system modeled in Simulink and the MAS platform created in JADE. However, this function is not supported in combination with the RTW environment [140] which is needed for the laboratory experiment. The S-function [140] is then proposed to create a new interface between the agent and the control layer.

6.1.4   Configuration of smart power router

The principal PR agents of each cell receive from the communication spa agents the state variables which are collected from the physical set-up. Besides mana-
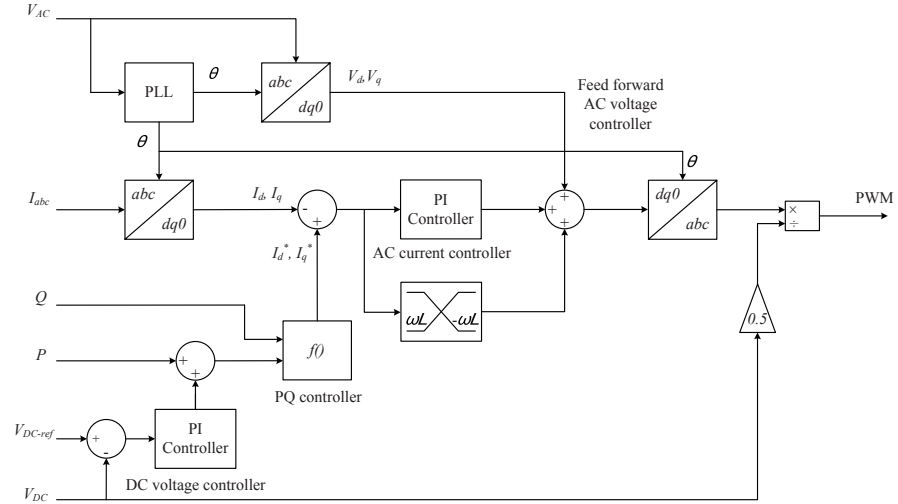
Figure 6.5: Control diagram of the inverter systems.

ging autonomous control actions, these agents can route messages to communicate with the other (same level) agents. Depending on the network situation, the objectives of the coordinated control might be voltage regulation or power flow management. The experimental work described in this chapter focuses on power flow management of the ADN under different conditions of time-varying load demand while taking network constraints into account.

In this set-up, a smart power router is configured by a combination of three inverters, where for instance spa2 and PR2 are agents which are used to manage cell 2. If PR2 detects a load change in cell 2 from measurement data sent by spa2, it will start deploying a routing power strategy in negotiation with PR1 and PR3. The smart power router then decides on the subsequent power flow and gives new set points to the inverter controllers.

6.2   Inverter controller design

6.2.1   Control modes

The inverters themselves are bi-directional and each of them is composed of a 3-phase uncontrolled rectifier followed by a 3-phase VSI with a LCL output filter. Three control modes are possible for the inverters, i.e., DC bus voltage control, AC voltage control and PQ control. A simplified diagram for the control system of the inverters is shown in Figure 6.5.

In the AC voltage control mode, the inverter identifies the voltage amplitude and phase angle measured from another inverter as reference values to adjust its AC voltage output. The inverter, therefore, can be synchronized to the grid by internal communication under the RTW environment. It is also used to

synchronize different network areas while keeping the inrush current lower than $10A$.

To control active and reactive power of the inverters, the current control method with a PI controller applied in the synchronous dq reference frame is used. The controller is based on Phase Lock Loop (PLL) to generate the sine and cosine signals needed for the dq transformations to ensure that the generated voltage is also synchronized to the grid voltage.

The DC bus voltage control is necessary to keep the energy balance when the inverters route the power. The DC bus voltage, V_{DC}, varies around $550V$ when inverter 1 is synchronized. This value is lower than the desired DC bus voltage necessary to generate the needed AC peak phase voltage of $325V$ [141]. Therefore, the DC bus voltage is boosted by drawing more active power. A Proportional Integral (PI) control with an anti-windup loop is used for this operation mode.

6.2.2 Control design

The dq control structure is often associated with PI controllers since they have a satisfactory behavior with a straightforward design [49]. A conventional PI controller drives a process with a transfer function $G(s)$ by a feedback controller with a weighted sum of the error K_P and the integrator time constant T_I. To design a PI controller, it is convenient to use a software simulator such as Matlab/Simulink [142].

Modeling of the experimental set-up considers the LCL filter as a process with the transfer function in the s-domain defined as follows [143]:

$$G(s) = \frac{V(s)}{I(s)} = \frac{L_1 C s^2 + 1}{L_1 L_2 C s^3 + (L_1 + L_2)s} \tag{6.1}$$

where $V(s)$ is the inverter voltage and $I(s)$ is the inverter current.

The transfer function of the PI controller is given as:

$$C(s) = K_P(1 + \frac{1}{T_I s}) \tag{6.2}$$

In the laboratory set-up, a digital controller is implemented using FPGA. Therefore, controlled signals have to be converted from the continuous s-domain to the discrete z-domain [144]. The discretization uses a zero-order hold method at a sampling frequency (T_s) of 8kHz. Equation 6.1 is then rewritten in z-domain with the parameters given in Table 6.1 as follows:

$$G(z) = \frac{0.01665z^2 + 0.01145z + 0.01665}{z^3 + 0.04296z^2 - 0.04296z - 1} \tag{6.3}$$

The transfer function of the PI controller in the z-domain with an additional delay of one switching period is then as follows:

$$C(z) = K_P \left(1 + \frac{1}{T_i} \frac{T_s}{z - 1} \right) \tag{6.4}$$
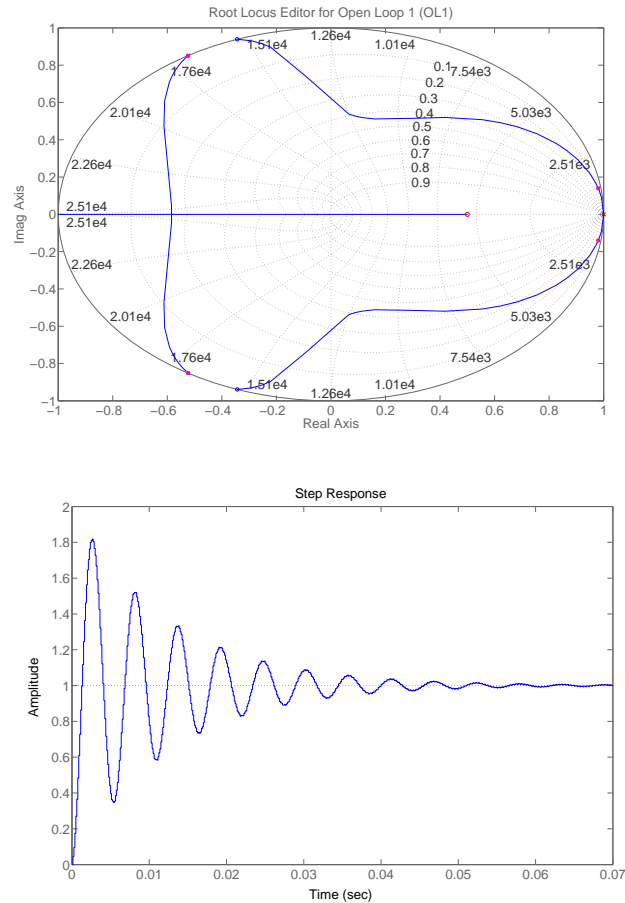
Figure 6.6: Root locus and step response of the experimental model in Matlab/Simulink.

An automated tuning function of the Control System Toolbox in Matlab [124] is used to determine the initial values of gain K_P and integrator time constant T_I of the PI controllers. The root locus and step response respective to these values are shown in Figure 6.6. Due to sensitivity of the protection system, these parameters must be adjusted in the practical experiment taking the dynamic behavior of the inverters into account. New values for the PI controller are turned out as a compromise between decreasing of overshoots to be below the threshold of the protection system and increasing of the step response. In the DC bus control mode, a specific PI controller is used. As the design of this controller aims for system stability, its parameters are tuned with slower time responses to decouple it from the current loop controllers. Table 6.2 presents the control parameters used for the set-up.

Table 6.2: Parameters for inverter control modes

Inverter control parameters	Value
Current control proportional gain, K_P, p.u.	0.08
Current control integrator time constant, T_I, msec.	40
DC control proportional gain, K_{P-DC}, p.u.	0.026
DC control integrator time constant, T_{I-DC}, msec.	12.5

6.3 Inverter controller strategies

6.3.1 Inverters synchronization

In the lab experiment, the inverters with their circuit breakers S_{inv-i} and contactors K_1^{inv-i}, K_2^{inv-i} are used to make synchronization between themselves and the network areas. The process of synchronization entails ensuring that the phase angles and amplitudes of the voltages on the grid side and the controlled voltage of inverter side are equal before the input contactor K_1^{inv-i} are closed.

First inverter 1 is synchronized with the $230V$ rms phase voltage from the grid side. By closing switch S_{inv-1} and contactor K_2^{inv-1}, the common DC bus of three inverters is charged from the grid side via the rectifiers. However, V_{DC} is limited around $550V$ which is not sufficient to perfectly yield back a $230V$ phase-to-ground AC output voltage. To get the same $325V$ peak voltage, inverter 1's output voltage signal will be distorted significantly. A compromise between the distortion and needed voltage amplitude is made to have an inrush current less than $10A$. Figure 6.7(a) presents the voltages on the two sides of inverter 1 and their difference before adjusting voltage amplitude and phase angle.

By closing S_{inv-3} while keeping K_1^{inv-3} open, inverter 3 can provide voltage signal references by measurements from its connected grid side. These references will be converted to Pulse Width Modulation (PWM) signal fed to inverter 1. It is noticed that the angle difference between the reference voltage signal and the actual generated voltage of the inverter is almost a half of one cycle, see Figure 6.7(a). This shift of phase angle is adapted by delaying the references up to the next period. Figure 6.7(b) presents the voltages on both sides of the contactor after inverter 1 is controlled.

6.3.2 Transition of cell operation

As mentioned in Chapter 2, the ADN built up from cells is an efficient and flexible system. The cell which operates often in interconnected mode can switch to islanded operation in necessary cases of maintenances or disturbances. This section investigates the procedure of the three inverter system in the transition from islanded to interconnected operation and vice-versa of cells. By opening the switch S_{M1}, the three cells are completely decoupled and their connections are controlled via the inverters' contactors. The wind turbine emulator is disconnected due to opening of S_{M1} as explained before. Hence, cell 3 of the test
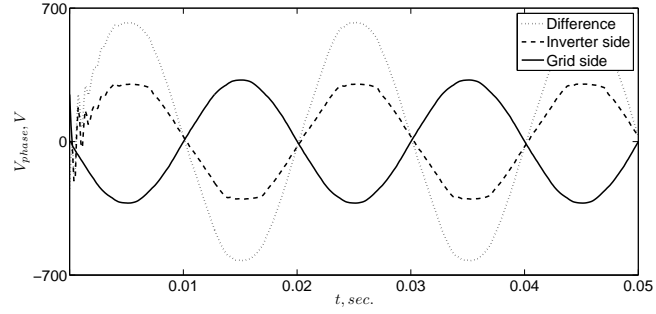
(a) Before adjusting voltage amplitude and phase angle.
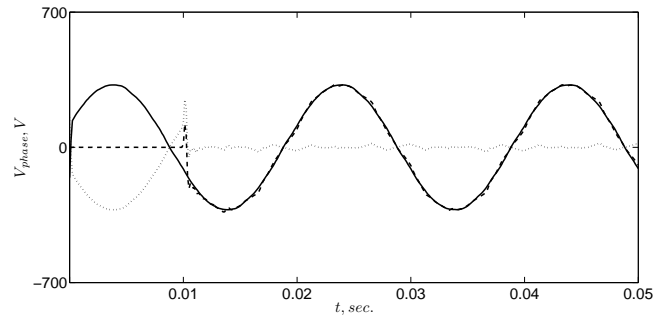
(b) After adjusting voltage amplitude and phase angle.

Figure 6.7: Measured phase-to-phase voltages on the two sides of contactor K_1^{inv-1} and their difference.

network is supplied by the public LV network by closing the manual switch S_{M2}.

Connecting cells

When connecting cells the aim is to connect cell 1 to the public grid via inverter 1 and inverter 3, and cell 3. Figure 6.8 shows a simplified diagram for the experiment of connecting cell 1 to the rest of grid.

Inverter 3 is connected first with the grid and is used to boost the DC bus voltage up to $680V$. Inverter 1 is then connected. To ensure that the voltages between the two sides of K_1^{inv-1} be alike, inverter 1 uses reference from the voltage measurement of inverter 2. By opening S_{inv-2} and closing K_1^{inv-2}, , the measured voltage of inverter 2 can be made equal to the voltage at the inverter side of K_1^{inv-1}. This value will be compared with the voltage measurement of inverter 1 which has the voltage of the programmable source. Using measurements from inverter 2 as a reference aims actually to simplify the lab implementation. In reality, there will be a separated measurement at
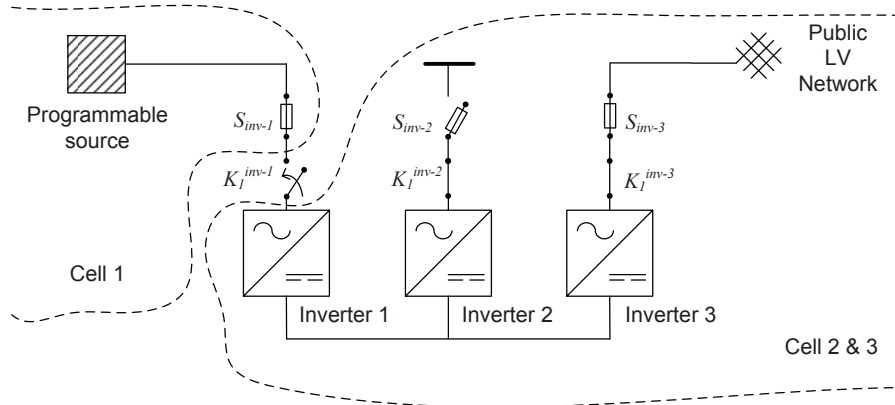
Figure 6.8: Simplified lab diagram of the experiment in case of connecting a cell.

inverter 1 so that cell 2 is not affected.

Disconnecting cells

Since cell 1 is now connected to the grid, inverter 3 takes the responsibility for the DC bus voltage control while inverter 1 operates in the PQ control mode. Inverter 2 uses a feed forward AC voltage controller and supplies the light resistive load of cell 2. When a maintenance or disturbance occurs in a cell, it needs to be isolated from the others. In the set-up, the main power stream is from the programmable source of cell 1 to supply its local load and the variable load of cell 2 via inverters 1 and 2.

To adapt with changing conditions when for instance connection between cell 2 and 3 is interrupted, inverter 1 needs to keep transferring power to the load in cell 2. The DC bus voltage previously controlled by inverter 3 must be maintained to keep the power flow balance. Inverter 1 can take over this function by changing its operation mode from PQ control to DC bus voltage control. Figure 6.9 shows a simplified diagram for the experiment of islanding cells. Note that the removal of one of the inverters, limits the robustness and flexibility of the remaining inverters in the system and must be solved as soon as possible.

6.4   Power routing operation

As a combination between inverter and agent layers, the smart power router managing cell 2 can deploy control functions as follows:

- In the inverter layer, the power router normally appoints inverter 1 to control the DC bus voltage and inverter 3 to operate in the PQ control
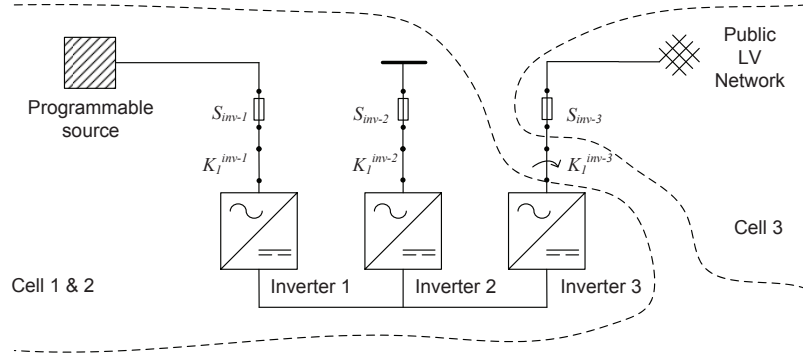
Figure 6.9: Simplified lab diagram of the experiment in case of islanding cells.

mode. By adjusting set points, inverter 3 can control active and reactive power flow from the wind turbine emulator and the main sources feeding to the load demand connected to inverter 2. Note that the initial configuration of the set-up is restored by closing S_{M1} and opening S_{M2}.

• In the agent layer, measurement data of cell 2 is collected from the RTW in Simulink and sent to PR2 via spa2. As the principal agent of the smart power router, PR2 can route a message to other neighboring agents, i.e., PR1 and PR3, to deploy bidding and negotiation strategies if it detects changes of its local load demand in cell 2. This routing process takes network constraints, i.e., nominal power of the inverter, maximum current, etc., into account. After deciding on the amount of power needed, PR2 sends the new values of power reference to inverter 3 through spa2.

The following part describes more in detail the strategy for power routing. The problem of real-time information exchange between two layers and a solution for that are then addressed.

6.4.1   Routing power strategies

As mentioned in chapter 5, two graph-based algorithms, i.e., the successive shortest path and push-relable cost-scaling are proposed for the function of power flow management in the ADN. The lab experiment adopts the successive shortest path algorithm to be suitable for optimizing the flows in the ADN.

The PR agents in three cells can communicate directly with each other for negotiation and coordination. In the experiment, only agent PR2 is really connected to a controlling hardware device which operates the programmable load in cell 2. The other two agents (PR1 and PR3) are preprogrammed with a certain amount of power they can supply and a per unit price of the power they supply. In this case, the switch S_{M1} is closed while the switch S_{M2} is opened and the
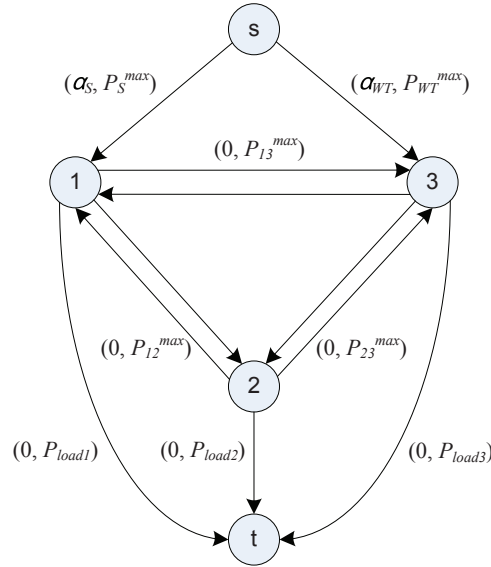
Figure 6.10: Representative directed graph for the laboratory test network.

wind turbine is connected to test network. In cell 1, the programmable source can supply a maximum amount of power, P_S^{max}, at a price, α_S in $p.u.$ In cell 3, the wind turbine emulator can supply a maximum amount of power, P_{WT}^{max}, at a price, α_{WT} in $p.u.$ Figure 6.10 shows a representative directed graph for the experimental set-up to investigate the routing power strategies. The costs for device availability and load priority are neglected. P_{12}^{max} and P_{23}^{max} present the maximum power capacities of inverter 1 and 3 while P_{13}^{max} is the rated power of the manual switch S_{M1}. P_{load1}, P_{load2}, and P_{load3} are the loads of cells 1, 2, and 3 respectively.

When the load of cell 2 increases, it will temporarily be supplied by the main source from cell 1. The power balancing process, because of the DC bus control function activated by inverter 1, can be considered as a primary action. PR2 then communicates with the other agents to request an additional amount of power based on a routing table. The routing table is a ranking of predecessors in the representative graph based on the total label costs for power transmission. This finds any shortest flow paths from cell 1 and cell 3 to cell 2 taking production costs, α_S and α_{WT}, into account. Table 6.3 shows the example of the routing table of PR2 if the production cost of wind turbine emulator is more expensive than the programmable source. PR1 and PR3 will both respond with the amount of power they can supply, P_S^{max} and P_{WT}^{max}. Finally, PR2 must then decide how much power it will consume from each neighboring agent, and sends a response to notify the neighboring agents about the decision made and adjusts the reference values of the smart power router to accommodate the new situation. This procedure is considered as a secondary
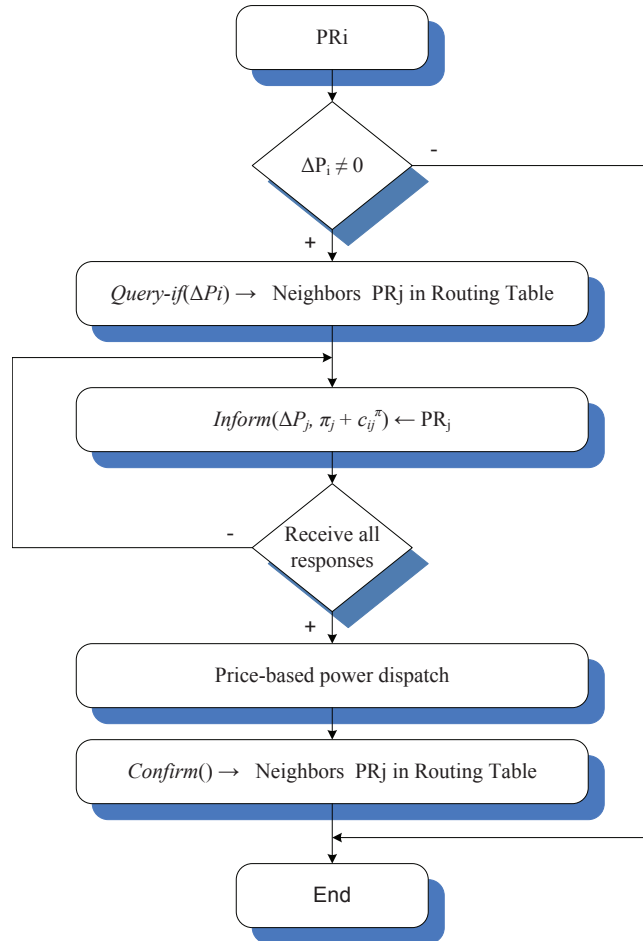
Figure 6.11: Diagram for routing power strategies.

action. Figure 6.11 illustrates the procedure for negotiating power exchange of the smart power router in the general case.

Table 6.3: Routing table of PR2

Order	Predecessor	Total label cost, $p.u.$
1	PR1	α_S
2	PR3	α_{WT}
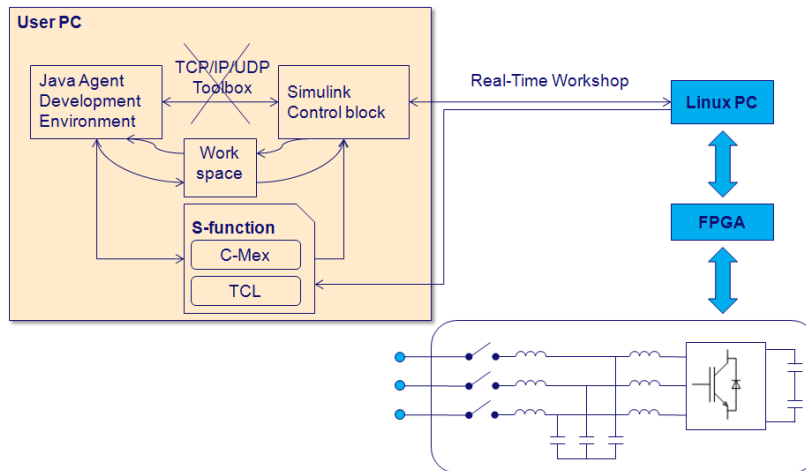
Figure 6.12: Real-time data synchronization.

6.4.2 Real-time data exchange

Figure 6.12 illustrates the real-time data flow of the inverters in the experiment. The three inverters are controlled by a Linux RTT PC through FPGA technology. The FPGA technology allows users implementing any logical function which offers advantages in many applications [145]. The inverter controllers are modeled in Simulink in a combination with RTW, as a client. The models are complied in C code and executed by the Linux RTT PC, as a server. The user can then easily monitors measured data and adjust parameters of the test network via the client-server interface by Simulink. However, there are some restrictions for which the user can not directly access and obtain data during program execution.

To exchange data with MAS, a S-function [140] is programmed to create a TCP/IP connection between the Simulink models on the RTT PC and the spa agents. The S-function includes a C code file which is compiled and used as a component in the Simulink model. A Target Language Compiler (TLC) file is used to generate a C code which is only used on the RTT Linux PC. General Linux Application Programming Interface (API) functions can be applied in TLC code to communicate with external agent applications via the TCP/IP protocol.

6.5 Experimental verifications

The experiments described in chapter first investigate the control functionality of the inverters by connecting them to the grid, disconnecting a part of the network, and changing power reference values. Performance of the power routing function in MAS based ADN is then verified by changing the load demand

connected to cell 2. These experiments have different experimental topologies and are summarized in Table 6.4.

Table 6.4: Experimental topologies

Cases	S_{M1}	S_{M2}	WT emulator	LV public grid
Inverter control test	Closed	Opened	Connected	Disconnected
Switching cells	Opened	Closed	Disconnected	Connected
Power routing test	Closed	Opened	Connected	Disconnected

6.5.1   Inverter control test

As mentioned earlier, the inverters operate in several different control modes depending on the grid situation. Those control functions are verified in following cases:

Connecting inverters

Inverter 1 is enabled at $t = 1sec$. Because of the LCL filter, the measured current is not zero. After adjusting the AC output voltage, contactor K_1^{inv-1} is closed at $t = 2sec$. to connect inverter 1 with the programmable source. Figure 6.13(a) shows the measured current of phase B when synchronizing inverter 1. As the peak value of the inverter current is much less than the threshold of $10A$, the experiment has connected successfully inverter 1 to the grid. At $t = 3sec$., inverter 1 starts operating in DC bus voltage control mode and draws more current to keep V_{DC} at $680V$.

At $t = 20sec$., inverter 3 is connected and operates in the PQ control mode to drive the output power (both active and reactive) of inverter 3 to the initial set points which are set to zero. At $t = 30sec$., inverter 2 is connected too and starts feeding load of cell 2. Figure 6.13(b) and 6.13(c) presents the respective current of inverter 1 at these times of connections.

Figure 6.14(a) shows how V_{DC} responds to the connection of the inverters. After inverter 1 is connected to the grid, it operates in the DC bus voltage control mode and keeps V_{DC} at $680V$. Connections of inverter 2 and inverter 3 cause a change of active power taken from the DC bus. After being connected to the grid, inverter 3 operates in the PQ control mode set points at zero. Therefore, it causes just slightly oscillation for V_{DC}. As inverter 2 is connected to a 0.772kW resistive load, it causes an oscillation of V_{DC} which is well damped after $4sec$. Power changes in the inverters are shown in Figure 6.14(b), 6.14(c), and 6.14(d).

At $t = 65sec$., the active power reference is stepped to 500W, as shown in Figure 6.15(b). Then, at $t = 95sec$., the reactive power reference is stepped to 500VAr, as shown in Figure 6.15(c). Note that positive value indicates the direction of power flow from the grid side to the inverter side. The variation in the active power at $t = 95sec$. is caused by the change in reactive power.
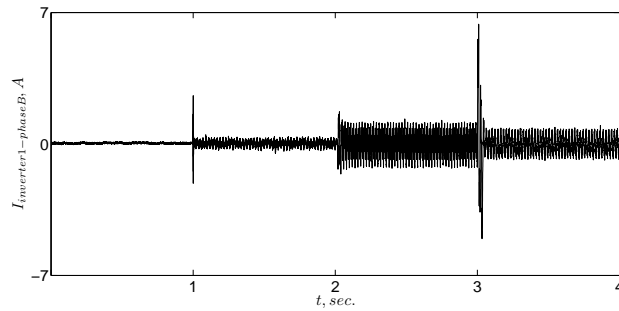
(a) Measured current when connecting inverter 1 to the grid. At $t = 1sec.$, K_2^{inv-1} is closed. At $t = 2sec.$, K_1^{inv-1} is closed. At $t = 3sec.$, the DC bus voltage controller is enabled.
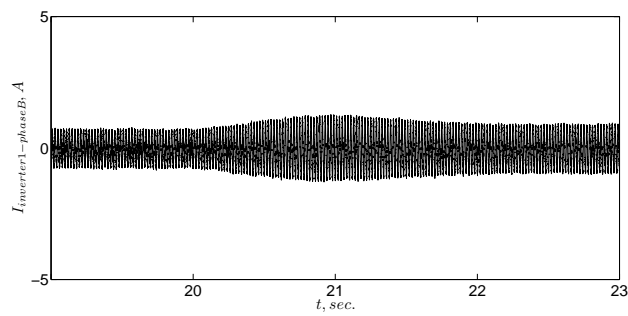
(b) Measured current when connecting inverter 3 to the grid. At $t = 20sec.$, K_1^{inv-2} is closed.
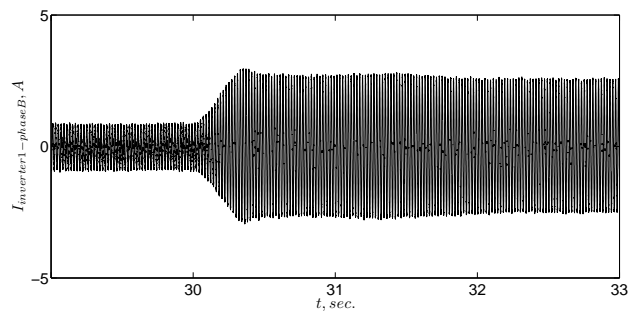
(c) Measured current when connecting inverter 2 to the grid. At $t = 30sec.$, K_1^{inv-3} is closed.

Figure 6.13: Connecting inverters to the grid.
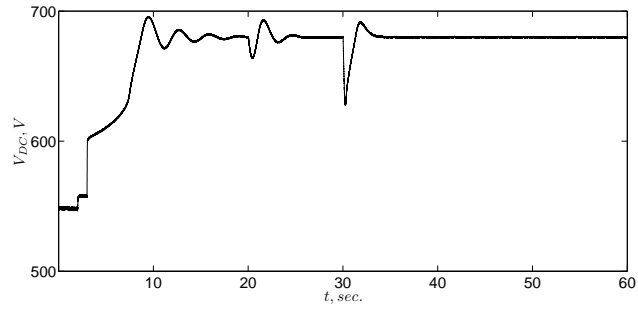
(a) Measured DC bus voltage during connecting inverters.
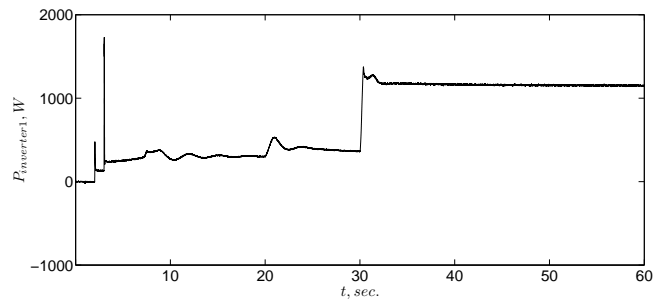
(b) Measured active power of inverter 1.
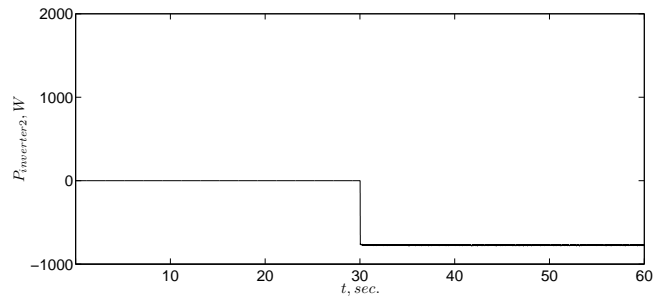
(c) Measured active power of inverter 2.
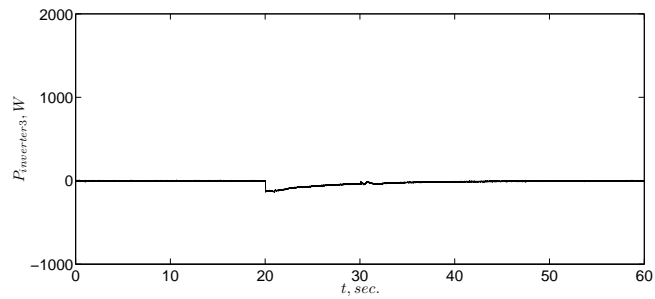
(d) Measured active power of inverter 3.

Figure 6.14: Responses of DC bus voltage and power flows to the inverters (inverter 1 is connected at $t = 2sec.$, inverter 2 is connected at $t = 20sec.$, and inverter 3 is connected at $t = 30sec.$).
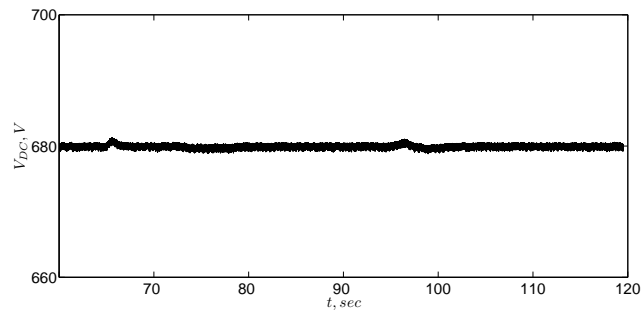
(a) Measured DC bus voltage during changing reference values.
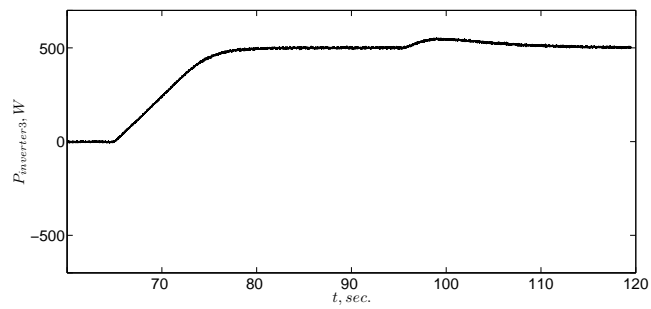
(b) Measured active power flow of inverter 3.
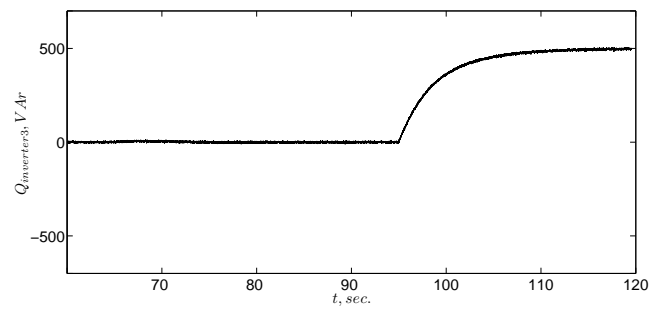
(c) Measured reactive power flow of inverter 3.

Figure 6.15: Case of changing reference values. At $t = 65sec.$, the active power reference is changed to 500W. At $t = 95sec.$, the reactive power reference is changed to 500VAr.
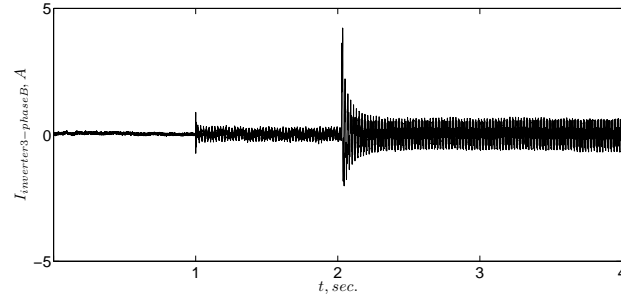
(a) Measured current when connecting inverter 3 to the grid. At $t = 1sec.$, K_2^{inv-3} is closed. At $t = 2sec.$, K_1^{inv-3} is closed. At $t = 3sec.$, the DC bus voltage controller is enabled.
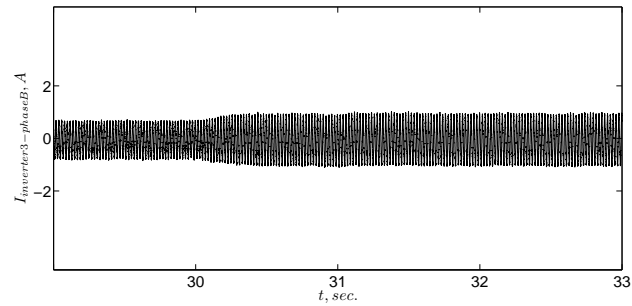
(b) Measured current when cell 1 is synchronized with the rest of the grid, at $t = 30sec.$

Figure 6.16: Case of connecting cells.

Connecting cells

The inverters are used in this situation to synchronize cell 1 supplied by the main source with cell 2 and 3 supplied by the public LV network. At $t = 2sec.$, inverter 3 is connected to the public grid by closing K_1^{inv-3} contactor. The DC bus voltage is then boosted and maintained at $680V$. After controlling the output AC voltage of inverter 1, contactor K_1^{inv-1} of inverter 1 is closed at $t = 30sec.$ to synchronize the main source side and the public grid side. Figure 6.16 presents the current through inverter 3 when cells are connected.

Disconnecting cells

After successful connecting the cells, inverter 3 controls the DC bus voltage while inverter 1 operates in PQ control mode. For maintenance purpose, inverter 3 might need to be disconnected from the grid. Hence, cell 1 and 2 are isolated with cell 3 connected with the public grid. To keep supplying steadily, inverter 1 must take over the DC bus voltage function of inverter 3 at the moment of switching off inverter 3 (at $t = 40sec.$ in this case) until the moment that inverter
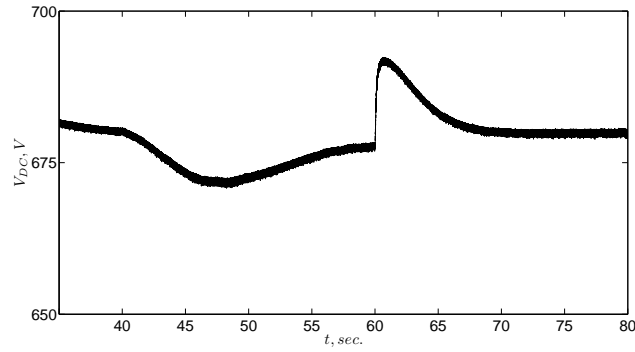
(a) Measured DC bus voltage.
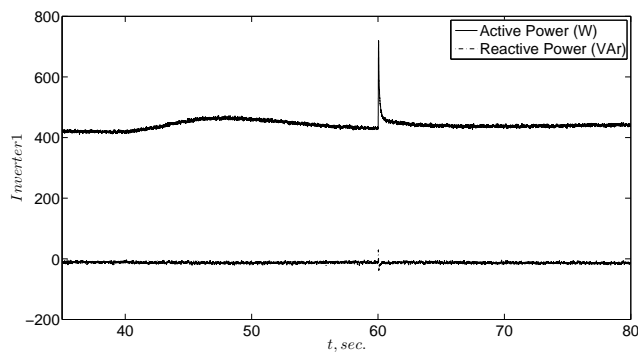
(b) Measured active and reactive power flow through inverter 1.

Figure 6.17: Case of disconnecting cells. At $t = 40sec.$, inverter 3 is disconnected. At $t = 60sec.$, inverter 3 is reconnected.

3 reconnects again (at $t = 60sec.$). Figure 6.17 shows that the test grid is kept stable during the maintenance switching period. There is a small oscillation of V_{DC} which is damped after nearly ten seconds. The active power through inverter 1 is increased slightly because the load of cell 2 was already supplied mainly by the programmable source before disconnection of inverter 3. The reactive power flow of inverter 1 is kept equal to zero. Since the maintenance is finished at $t = 60sec.$, inverter 3 is successfully reconnected to the grid. The inverters are switched back to their previous operation modes.

6.5.2 MAS-based power routing test

To test the power routing function, similar steps of connecting inverters to the grid are carried out. At $t = 50sec.$, the programmable load of cell 2 is increased by $\Delta P_{load2} = 173W$. Because the DC bus voltage control keeps the power flow balance, the extra load demand will be supplied primarily by the main source
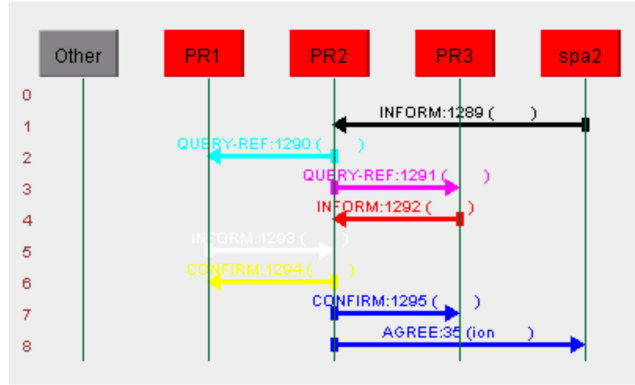
Figure 6.18: Agent messages for routing power.

through the uncontrolled rectifier part of inverter 1. At the same time, the smart power router of cell 2 detects the amount of load change and sends information to spa2 via the Simulink-JADE interface.

Figure 6.18 shows the sequence diagram of MAS to dispatch the power demand. It can be seen that after agent 2 receives an *inform* message about the load change from spa2, it sends *query-ref* messages to agents 1 and 3 to request more power supply. Both agent 1 and 3 send back *inform* messages about how much power they can supply and at what price. Agent 2 will then determine the most economic solution and sends a confirmation message about how much power it will take from each neighboring cell and an *agree* message to spa2 containing information about the new reference values for routing power in the three inverters. These reference values are transferred to the inverter control blocks.

Figure 6.19(a) shows the response of V_{DC} because of the increase of ΔP_{load2}. After about five seconds negotiating time, the smart power router through principal agent PR2 has confirmed a new power dispatch. The active power reference of inverter 3 is set to 73W while the remaining part of ΔP_{load2} (100W) is provided via inverter 1. Actually, only inverter 3 operating in the PQ control mode can adjust directly the power flow to its reference values. The power flow through inverter 1 a subsequent amount yielded by power balancing. At $t = 80sec.$, the power flow through inverter 3 settles to the new operation state. Figure 6.19(b), 6.19(c) and 6.19(d) show the power flows through the three inverters.

6.6   Summary

This chapter investigates the performance of a smart power router in a MAS based ADN with experiments carried out in a laboratory set-up. A brief description of the set-up and integration of hardware components, control structures

of the inverters, and MAS-based control strategies for the smart power router is primarily addressed. The set-up consists of three control functions for the inverters, i.e., DC bus voltage control, AC voltage control, and PQ control are developed in a Simulink diagram.

In case of connecting the first inverter (inverter 1), measurement data is collected from another inverter (inverter 3) and used as a reference signal to adjust the output voltage of the inverter. It is an advantage of the three-inverter system when no more measurement device is needed. The current flow through inverter 1, when the output contactor closes, is much less than the current limit of $10A$. Inverter 1 then operates in DC bus voltage control mode to start boosting V_{DC} up to $680V$. Inverter 3 is connected straightforward afterward. As inverter 2 supplies power to a resistive load, it causes a disturbance for V_{DC} at the connection time. The oscillation is well damped by the DC bus voltage control after one cycle. Step responses of the controllers are also investigated in cases of changing active and reactive power reference values.

The functions of the three-inverters system in the transition from interconnected to islanded operation and vice-versa of cells are investigated. Connecting and disconnecting cells in the set-up is implemented by switching contactors K_1^{inv-i}, K_2^{inv-i}, and switches S_{inv-i}. The set-up experiments on synchronizing cell 1 to the rest of the grid successful. The experiments show also robustness and stability of the controllers in cases of disconnecting network components (inverter 3) because of maintenance or disturbance.

Implementation of a MAS platform has some difficulties on real-time data exchange. An interface based on C-MEX and TLC S-function is developed to cope with challenges on combination with the RTW environment. The set-up works with an obvious power routing strategy for the MAS-based control layer. It shows the possibility to apply the power routing function with more complex algorithm to manage power flow in a MAS based ADN.

The experiments show that the 3-cells configuration of the ADN could operate in an efficient and flexible way based on the power routing interface. The power router included the primary control function of the inverters and the secondary control function of MAS is thoroughly verified.
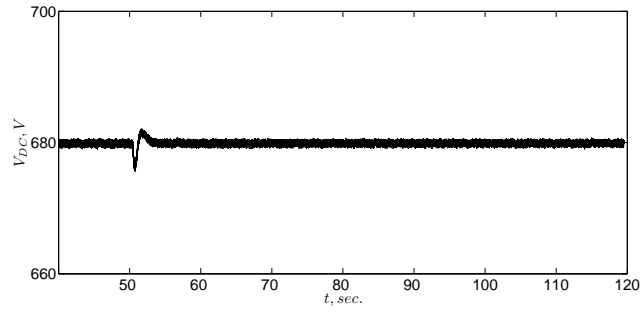
(a) Measured DC bus voltage.
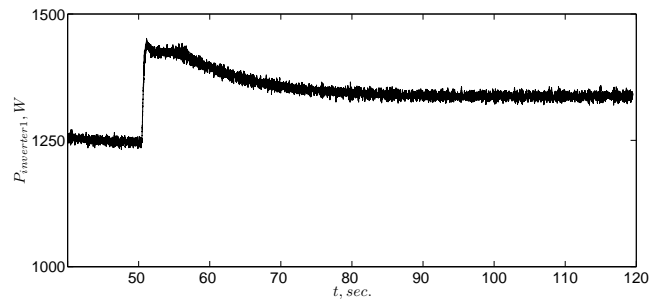
(b) Measured active power flow through inverter 1.
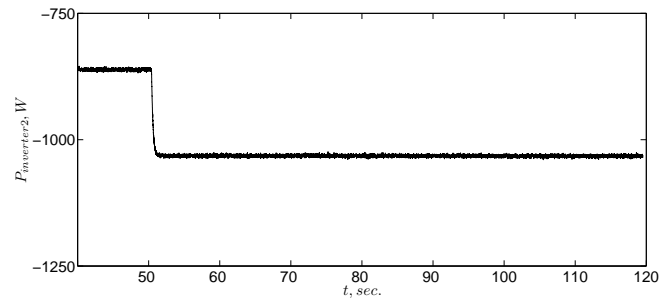
(c) Measured active power flow through inverter 2.
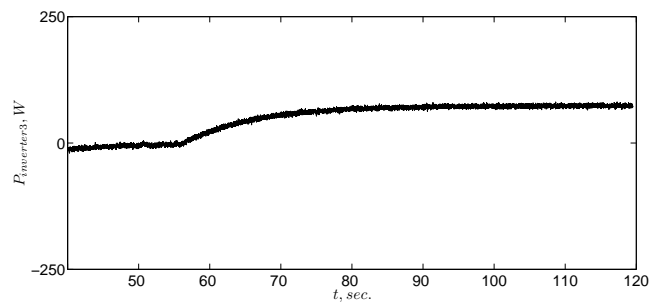
(d) Measured active power flow through inverter 3.

Figure 6.19: Case of power routing. At $t = 50sec.$, the load of cell 2 is increased by $\Delta P_{load2} = 173$W. At $t = 55sec.$, active power reference of inverter 3 is changed to 73W.

CHAPTER 7

CONCLUSIONS, CONTRIBUTIONS AND
RECOMMENDATIONS

7.1   Conclusions

The change from a vertically to a horizontally based electrical power system
structure motivates this thesis research which is aimed at finding an efficient
and flexible distribution system suitable for this new context. The future dis-
tribution network must be active with a robust distributed control framework.
To achieve the main goal of this thesis, the following aspects of design and
operation of distribution networks are investigated:

Active distribution networks

In Chapter 2, the concept of an Active Distribution Network has been elabo-
rated as an essential solution to cope with challenges created by the large-scale
implementation of DERs. The design of the ADN is based on an open control
architecture that can integrate various types of networks and different forms
of operation. These can be called cells and might be MicroGrids, Autonomous
Networks, Power Electronics-coupled substations, or passive area networks. By
focusing on control strategies and communication topologies, the ADN is ex-
pected to have a robust distributed control framework to overcome the current
challenges and be adaptable for future needs.

A Multi-Agent (control) System is regarded as a key technology to enable
distributed monitoring and control functions of the ADN. With characteristics
of reactivity, pro-activeness, and social ability, the MAS technology can offer
numerous benefits in distributed applications. By introducing one more layer
of MAS into each cell of the ADN, controllable loads and DG units can be
interacted with each other and the outside world. In this structure, the cells not

only operate autonomously but also coordinate with others by communicating among the agents.

An operational structure of the MAS-based ADN has been presented with two main elements: Distributed State Estimation (DSE) and Local Control Scheduling (LCS). DSE facilitates distributed monitoring and provides information to the LCS in which the control functions are implemented. This hierarchical architecture can provide support for both autonomous and coordination controls.

Distributed state estimation

In Chapter 3, a state estimation method suitable with the distributed design of the ADN has been developed. The main assumption of the developed Distributed State Estimation (DSE) is that each bus contains an agent to implement distributed algorithms and exchange information with its neighbors. This is applied in the operational structure of the ADN in which each cell is represented by an equivalent bus, including a moderator agent to carry out the DSE function.

The proposed method estimates local state variables by exchanging information iteratively between bus agents on a MAS platform. Exchanged data include local state variables and their covariances for each bus, which are estimated by its respective neighbors. These values are then associated with local measurement data to provide a maximum likelihood estimation. Each bus agent repeats this computation until its state variables are converged.

The accuracy of this new method is compared to the classical WLS estimator in an off-line Matlab simulation for the IEEE 14-bus and IEEE-34 bus test networks. In the cases studied, the convergence of the method, which is a key requirement for distributed approaches, is reached within a few iterations. Also, bad data detection and identification based on the traditional Chi-squares χ^2-test can significantly improve the performance of the DSE.

The interaction between the power system and MAS is investigated by an on-line simulation of a 5-bus test network. Through the MAS platform, local state variables of each bus are iteratively estimated with a period of $40msec.$ of simulation time until they are converged. Simulation results show that the method can respond effectively to dynamic conditions, including noise injection, network topology change, and load increase.

Voltage regulation

In Chapter 4, a voltage regulation method for autonomous and coordinated control has been developed in the operational structure of the ADN. The voltage regulation is considered as a function of LCS, which can receive information regarding network parameters from the DSE function. Therefore, the method can retrieve data within each cell of the ADN to find out a relationship between bus voltage deviations and power injections through power flow calculations and composing the Jacobean matrix. The so called sensitivity factors are allocated

in respective agents of the buses in order to initiate autonomous control actions using moderator agents of the cells. In an upper agent layer, a coordination of the voltage regulation between cells is proposed together with the regulation of the OLTC of the transformers.

The effectiveness of the proposed voltage regulation method has been illustrated through a steady-state simulation of a typical Dutch MV network. Furthermore, the MAS technology creates a possibility to apply the proposed control algorithm on-line in dynamic environments. A dynamic simulation of a 5-bus radial test network with variable wind power units and operating on a MAS platform has been developed in Simulink. The simulation results show that the proposed method can compensate for the drawbacks of the current solutions, dealing with the problem of voltage deviations in the distribution network.

Power flow management

In Chapter 5, a distributed approach to deal with problems of bi-directional flow and congestion in the network has been investigated. An application of the graph theory opens the possibility to solve the optimal power flow using a minimum cost flow algorithm, representing the power system as a directed graph. Two well-known algorithms for the minimum cost flow, i.e., Successive Shortest Path (SSP) and Cost-Scaling Push-Relabel (CS-PR), have been applied. They use two different methods of capacity scaling and cost scaling to fulfill the same objective function. Therefore, their properties in a distributed environment, such as MAS-based, are different and need to be considered.

The performance of each algorithm is investigated in simulations of both meshed and radial test networks. The algorithms are implemented by the interaction of agents on the MAS platform. The properties of the applied algorithms suggest that the CS-PR needs less computation steps than the SSP. Simulation results from the radial network have verified this statement by comparing the number of exchanged messages in the MAS platform. In the meshed network, however, the comparison of each algorithm's performance is inconclusive.

Along with the proposed optimization algorithms implemented on the MAS platform, a power flow controller in the power network is a crucial component which regulates the power flow according to the set points provided by the agents. Their combination leads to a definition of the power router, which can be considered as a flexible interface of the cells in the ADN.

Laboratory implementation

In Chapter 6, operational and control functions of the power router in the MAS-based ADN have been investigated in a laboratory experiment. The setup consists of a physical test network, a MAS platform, and Matlab/Simulink interface to exchange real-time information.

Three inverters are used to decouple the laboratory-scale ADN into three separate cells. As a hardware component of the power router, these inverters

are designed to operate in different modes of DC bus voltage control, AC voltage control, and PQ control. By assigning suitable operation modes for the inverters, strategies for transitions, ranging from interconnected to islanded operation and vice-versa, of the cells have been developed. The experiment verified the robustness of these inverter controllers when the switching approaches are employed.

The power routing strategies are executed in the agent layer of the power router. The graph-based algorithms developed in Chapter 5 have been used in this test network. The optimal results from the routing algorithms are sent to the inverter control layer as set points. In the real-time environment of the laboratory set-up, an interface between the agent and inverter control layers has been established. The experiment has successfully verified the functionality of the power router in situations of load demand change.

7.2   Thesis contributions

The main contributions of the thesis research are as follows:

- **A novel operational structure of the Active Distribution Network based on Multi-Agent System technology.** The thesis proves that the advantages of the MAS technology can be applied to fully enable the efficient and flexible operation of the ADN. The agent's hierarchical structure can be scalable for a wide-range of future conditions.

- **A new method for Distributed State Estimation.** Implementation of MAS in the ADN allows each agent to process information of its cell autonomously. Overlay information between agents, therefore, provides a possibility to monitor a part or the entire ADN.

- **Voltage regulation improvement in the distribution network.** The MAS technology improves the capability of the ADN to coordinate its controllable components. Negotiation among possible control actions of power injections and regarding regulation of the OLTC of the transformer can give a better solution to deal with the voltage deviation issue.

- **Development of power routing algorithms.** The thesis aims to optimally manage power flows, taking network variations and constraints into account. Two graph-based algorithms are adapted in a distributed environment of the MAS platform as effective solutions for the optimal power flow issue.

- **The verification and validation of a power router as a flexible interface between cells in the ADN.** The power router is defined as a combination of an agent and a power flow controller. The agent employs the power routing algorithm and gives set points to the power flow controller. This novel concept was simulated in software models and verified in a laboratory experiment.

7.3   Recommendations for future research

The thesis is completed by opening several interesting research directions and problems. They are highlighted in the following sections:

Integration of agent-based monitoring and control functions

Throughout the thesis, Multi-Agent System technology is used as a key element to enable distributed monitoring and control functions of the ADN. However, an agent-based distributed state estimation must be involved in the current SCADA/DMS system. This raises a need to comply the agent's ontology with existing communication standards applied in the power system, i.e., IEC 61850, or Common Information Model. The interaction of agent-based control functions with current control structure of the DSO and DNO also needed to be considered.

Relationship between power matching, local balancing, and power routing

As mentioned in Chapter 1, the distribution system will be reorganized in order to integrate emerging functions of power matching, power routing, and local balancing. The thesis work mainly focuses on the function of power routing which deals with network loading and constraints during the operation stage. Power matching and local balancing based on the agent technologies are investigated in various research works [30], [68], [146]. Integration of these functions into an unique MAS platform may lead to a new entity of agent service providers.

Application of the Multi-Agent System technology for management of electrical vehicles

A challenge for the DSO and DNO is in managing a large number of mobile electrical vehicles in the future. Optimal charging strategies must be considered under a highly dynamic condition. The MAS technology can be applied to enhance flexibility and intelligence of the solution in a completely distributed and mobile context.

Using Real Time Digital Simulation for scaling laboratory set-up

A verification of operational and control functions of the power router was implemented in the laboratory set-up. The tested cases, however, are limited by the small-scale configuration of the current lab. A larger-scale test-bed combined with Real Time Digital Simulation (RTDS) can create an appropriate environment to completely verify aspects of the agent-based applications.

Role of smart metering in distributed state estimation

Along with increasing the number of smart metering devices in the distribution network, there will be a large amount of information for management and

control purposes. This will significantly enhance the capability of monitoring within the distribution network. An appropriate distributed state estimation must be considered to effectively exploit the available information for improvement of network topology analysis, observability, and bad data detection and identification.

BIBLIOGRAPHY

[1] European Commission Directorate-General for Research (Brussels), "New Era for Electricity in Europe - Distributed Generation: Key Issues, Challenges and Proposed Solutions," Luxembourg, 2003.

[2] Electric Power Research Institute, "Electricity technology roadmap: 2003 Summary and Synthesis - Power delivery and Markets," p. 76, 2003.

[3] N. Jenkins and N. Jenkins, *Embedded generation*. IET, 2000.

[4] F. Provoost, "Intelligent distribution network design," Ph.D. dissertation, Technische Universiteit Eindhoven, 2009.

[5] F. M. González-Longatt, "Impact of Distributed Generation over Power Losses on Distribution System," in *9th International Conference on Electrical Power Quality and Utilisation*, Barcelona, 2007, pp. 1–6.

[6] R. H. Lasseter and P. Paigi, "Microgrid: a conceptual solution," in *IEEE 35th Annual Power Electronics Specialists Conference (PESC)*, vol. 6, 2004, pp. 4285–4290.

[7] N. Hatziargyriou, N. Jenkins, G. Strbac, J. Pecas Lopes, J. Ruela, A. Engler, J. Oyazabal, G. Kariniotakis, and A. Amorim, "Microgrids - Large Scale Integration of Microgeneration to Low Voltage Grids," in *CIGRE General Session*, Paris, 2006.

[8] P. van Den Bosch, A. Jokić, J. Frunt, W. Kling, F. Nobel, P. Boonekamp, W. de Boer, and R. Hermans, "Incentives-based ancillary services for power system integrity," in *6th International Conference on the European Energy Market*, 2009, pp. 1–7.

[9] M. Reza, "Stability analysis of transmission systems with high penetration of distributed generation," Ph.D. dissertation, Delft University of Technology, 2006.

[10] Meeuwsen J.J., "Electricity networks of the future," p. 114, 2007.

[11] P. Kundur, *Power System Stability and Control* . McGraw-Hill Professional, 1994.

[12] European Network of Transmission System Operators for Electricity (ENTSOE), "Operational handbook - Part 1 - Policy 1: Load frequency control and performance," p. 33, 2009. [Online]. Available: https://www.entsoe.eu/fileadmin/user_upload/_library/publications/ce/oh/Policy1_final.pdf [Accessed: 17 October 2010]

[13] L. L. Lai, *Power system restructuring and deregulation: trading, performance and information technology.* John Wiley and Sons, 2001.

[14] A. Jokic, "Price-based optimal control of electrical power systems," Ph.D. dissertation, Technische Universiteit Eindhoven, 2007.

[15] TenneT, "TenneT - Nederlands transportnet." [Online]. Available: http://www.tennet.org/english/index.aspx [Accessed: 17 October 2010]

[16] European Union, "Directive 2003/54/EC of the European parliament and of the council of 26 June 2003 concerning common rules for the internal market in electricity and repealing Directive 96/92/EC," p. 19, 2003.

[17] M. Shahidehpour and W. Yaoyu, *Communication and control in electric power systems: applications of parallel and distributed processing.* Wiley-IEEE, 2003.

[18] S. Chowdhury, S. P. Chowdhury, and P. Crossley, *Microgrids and Active Distribution Networks.* London, United Kingdom: The Institution of Engineering and Technology, 2009.

[19] European Commission, "The European Electricity Grid Initiative (EEGI): a joint TSO-DSO contribution to the European Industrial Initiative (EII) on Electricity Networks," p. 64, 2009.

[20] G. Deconinck, K. Vanthournout, H. Beitollahi, Z. Qui, R. Duan, J. Driesen, R. Belmans, B. Nauwelaers, and E. Van Lil, "A Robust Semantic Overlay Network for Microgrid Control Applications," *Lecture Notes in Computer Science*, pp. 101–123, 2008.

[21] H. La Poutre, W. Kling, and J. Cobben, "Intelligent Systems for Green Developments," *ERCIM News - Special theme: Towards green ICT*, vol. 79, pp. 38–39, 2009.

[22] A. Jokic, "Real-time control of power systems using nodal prices," *International Journal of Electrical Power and Energy Systems*, vol. 31, no. 9, p. 522, 2009.

[23] V. Robu and J. La Poutre, "Designing bidding strategies in sequential auctions for risk averse agents, in: Agent-Mediated Electronic Commerce and Trading Agent Design and Analysis (AMEC VIII)," *Lecture Notes in Business Information Processing*, vol. 13, pp. 76–89, 2009.

[24] KEMA, "Electricity Technology Roadmap - Technology for the Sustainable Society," 2005.

[25] C. Timpe and M. Scheepers, "A look into the future: Scenarios for distributed generation in Europe," p. 25, 2003. [Online]. Available: http://www.ecn.nl/docs/library/report/2004/c04012.pdf [Accessed: 17 October 2010]

[26] C. E. T. Foote, G. M. Burt, I. M. Elders, and G. W. Ault, "Developing distributed generation penetration scenarios," in *International Conference on Future Power Systems*, 2005, pp. 1–6.

[27] G. W. Ault, I. Elders, J. R. McDonald, G. M. Burt, and R. Tumilty, "Electricity Network Scenarios for 2020," 2006. [Online]. Available: http://www.ensg.gov.uk/assets/dwg_pg1-p01_scenarios.pdf [Accessed: 17 October 2010]

[28] Council of The European Union, "Energy and climate change Elements of the final compromise," 2008. [Online]. Available: http://www.consilium.europa.eu/uedocs/cms_data/docs/pressdata/en/ec/104672.pdf [Accessed: 17 October 2010]

[29] B. Kroposki, R. Margolis, G. Kuswa, J. Torres, W. Bower, T. Key, and D. Ton, "Renewable Systems Interconnection: Executive Summary," p. 23, 2008.

[30] More Microgrids, "Advanced Architectures and Control Concepts for More Microgrids," p. 145, 2009. [Online]. Available: http://www.microgrids.eu/documents/668.pdf [Accessed: 17 October 2010]

[31] F. Provoost, J. M. A. Myrzik, and W. L. Kling, "Setting up autonomous controlled networks," in *39th International Universities Power Engineering Conference, (UPEC 04)*, vol. 3, 2004, pp. 1190–1194 vol. 2.

[32] H. Kobayashi and M. Takasaki, "Demonstration Study of Autonomous Demand Area Power System," in *IEEE PES Transmission and Distribution Conference and Exhibition*, 2006, pp. 548–555.

[33] K. Nara and J. Hasegawa, "A new flexible, reliable, and intelligent electrical energy delivery system," *Electrical Engineering in Japan*, vol. 121, no. 1, pp. 26–34, 1997.

[34] F. van Overbeeke, "Active networks: Distribution networks facilitating integration of distributed generation," in *2nd international symposium on distributed generation: power system and market aspects*, Stockholm, 2002, pp. 1–7.

[35] G. W. Ault, C. E. T. Foote, and J. R. McDonald, "UK research activities on advanced distribution automation," in *IEEE Power Engineering Society General Meeting*, 2005, pp. 2616–2619 Vol. 3.

[36] A. Korbik, S. D. J. Mcarthur, G. W. Ault, G. M. Burt, and J. R. Mcdonald, "Enabling active distribution networks through decentralised autonomous network management," in *18th International Conference and Exhibition on Electricity Distribution, CIRED*, 2005, pp. 1–5.

[37] European SmartGrids - Technology Platform, "Vision and Strategy for Europe's Electricity Networks of the Future," 2006. [Online]. Available: http://ec.europa.eu/research/energy/pdf/smartgrids_en.pdf [Accessed: 17 October 2010]

[38] The GridWise Alliance, "GridWise Alliance - Advocating for a Smarter Grid," 2010. [Online]. Available: http://www.gridwise.org/ [Accessed: 17 October 2010]

[39] Electric Power Research Institute, "IntelliGrid," 2010. [Online]. Available: http://intelligrid.epri.com/ [Accessed: 17 October 2010]

[40] The U.S. Department of Energy - Office of Electricity Delivery and Energy Reliability, "The Smart Grid: An Introduction," p. 48, 2008. [Online]. Available: http://www.oe.energy.gov/DocumentsandMedia/ DOE_SG_Book_Single_Pages(1).pdf [Accessed: 17 October 2010]

[41] European Commission, "European Technology Platform for the electricity networks of the future." [Online]. Available: http://www.smartgrids.eu/ [Accessed: 17 October 2010]

[42] D. Pudjianto, C. Ramsay, and G. Strbac, "Virtual power plant and system integration of distributed energy resources," *IET Renewable Power Generation*, vol. 1, no. 1, pp. 10–16, 2007.

[43] D. Coll-Mayor, R. Picos, and E. Garcia-Moreno, "State of the art of the virtual utility: the smart distributed generation network," *International journal of energy research*, vol. 28, no. 1, pp. 65–80, 2004.

[44] On World, "Smart Grid Projects in 90 Percent of U.S. States," 2009.

[45] Zprymer, "Smart Grid: China leads top ten countries in Smart Grid federal stimulus investments," 2010. [Online]. Available: http:// zpryme.com/news-room/smart-grid-china-leads-top-ten-countries/ -in-smart-grid-federal-stimulus-investments-zpryme-reports.html [Accessed: 17 October 2010]

[46] KEMA, "Smart grid development is not limited to the U.S." [Online]. Available: http://www.kema.com/services/consulting/utility-future/ smart-grid/smart-grid-not-limited-to-US.aspx [Accessed: 17 October 2010]

[47] C. Nietsch and D. Povh, "Optimizing power distribution networks," *IEEE Computer Applications in Power*, vol. 14, no. 2, pp. 18–21, 2001.

[48] E. Zabala, E. Perea, and J. E. Rodríguez, "Improvement of the Quality of Supply in Distributed Generation networks through the integrated application of power electronic techniques," in *1st International Conference on the Integration of Renewable Energy Sources and Distributed Energy Resources*, Brussels, 2004.

[49] F. Blaabjerg, R. Teodorescu, M. Liserre, and A. V. Timbus, "Overview of Control and Grid Synchronization for Distributed Power Generation Systems," *IEEE Transactions on Industrial Electronics*, vol. 53, no. 5, pp. 1398–1409, 2006.

[50] M. Emin Meral, A. Teke, and M. Tumay, "Overview of an extended Custom Power Park," in *IEEE 2nd International Power and Energy Conference, PECon*, 2008, pp. 1364–1368.

[51] A. Domijan Jr., A. Montenegro, A. J. F. Keri, and K. E. Mattern, "Simulation study of the world's first distributed premium power quality park," *IEEE Transactions on Power Delivery*, vol. 20, no. 2, pp. 1483–1492, 2005.

[52] T. Ericsen, Y. Khersonsky, P. Schugart, and P. Steimer, "PEBB - Power Electronics Building Blocks, from Concept to Reality," in *3rd IET International Conference on Power Electronics, Machines and Drives*, 2006, pp. 12–16.

[53] ECN, "CRISP - distributed intelligent in CRitical Infrastructure for Sustainable Power," 2006. [Online]. Available: http://www.crisp.ecn.nl/index.html [Accessed: 17 October 2010]

[54] B. M. Buchholz and Z. A. Styczynski, "Communication Requirements and Solutions for Secure Power System Operation," in *IEEE Power Engineering Society General Meeting,*, 2007, pp. 1–5.

[55] SEESGEN-ICT, "SEESGEN-ICT: a Thematic Network to encourage energy efficiency in Smartgrids." [Online]. Available: http://seesgen-ict.erse-web.it/default.asp [Accessed: 17 October 2010]

[56] C. Rehtanz, *Autonomous Systems and Intelligent Agents in Power System Control and Operation.* Springer, 2003.

[57] S. D. J. McArthur, E. M. Davidson, V. M. Catterson, A. L. Dimeas, N. D. Hatziargyriou, F. Ponci, and T. Funabashi, "Multi-Agent Systems for Power Engineering Applications; Part I: Concepts, Approaches, and Technical Challenges," *IEEE Transactions on Power Systems*, vol. 22, no. 4, pp. 1743–1752, 2007.

[58] R. R. Negenborn, "Multi-Agent Model Predictive Control with Applications to Power Networks," Ph.D. dissertation, Technische Universiteit Delft, 2007.

[59] K. Heussen, A. Saleem, and M. Lind, "Control architecture of power systems: Modeling of purpose and function," in *IEEE Power & Energy Society General Meeting*, 2009, pp. 1–8.

[60] K.-C. Chen, P.-C. Yeh, H.-Y. Hsieh, and S.-C. Chang, "Communication Infrastructure of Smart Grid," in *Proceedings of the 4th International Symposium on Communications, Control and Signal Processing, ISCCSP 2010*, Limassol, Cyprus., 2010.

[61] K. El Bakari and W. Kling, "Facilitating sustainability through smart network design in combination with virtual power plant operation," in *The Innovation for Sustainable Production Conference*, Bruges, 2010, p. 19.

[62] S. S. Heragu, R. J. Graves, B.-I. Kim, and A. St Onge, "Intelligent agent based framework for manufacturing systems control," *IEEE Transactions on Systems, Man and Cybernetics, Part A: Systems and Humans*, vol. 32, no. 5, pp. 560–573, 2002.

[63] P. Vytelingum, S. Ramchurn, T. Voice, A. Rogers, and N. Jennings, "Trading Agents for the Smart Electricity Grid," in *Proceedings of the Ninth International Joint Conference on Autonomous Agents and Multi-Agent Systems (AAMAS 2010)*, 2010, pp. 897–904.

[64] M. Hommelberg, C. Warmer, I. Kamphuis, J. Kok, and G. Schaeffer, "Distributed Control Concepts using Multi-Agent technology and Automatic Markets: An indispensable feature of smart power grids," in *IEEE Power Engineering Society General Meeting*, 2007.

[65] M. Braun and P. Strauss, "A review on aggregation approaches of controllable distributed energy units in electrical power systems," *International Journal of Distributed Energy Resources*, vol. 4, no. 4, pp. 297–319, 2008.

[66] Wikipedia, "Smart grid," 2010. [Online]. Available: http://en.wikipedia.org/wiki/Smart_grid [Accessed: 17 October 2010]

[67] FREEDM System Center, "FREEDM System," 2010. [Online]. Available: http://www.freedm.ncsu.edu/index.php?s=1&p=6 [Accessed: 17 October 2010]

[68] A. L. Dimeas and N. D. Hatziargyriou, "Operation of a Multiagent System for Microgrid Control," *IEEE Transactions on Power Systems*, vol. 20, no. 3, pp. 1447–1455, 2005.

[69] EU-DEEP, "The EU-DEEP project home page." [Online]. Available: http://www.eu-deep.com/index.php?id=397 [Accessed: 17 October 2010]

[70] D. Coll-Mayor, M. Paget, and E. Lightner, "Future intelligent power grids: Analysis of the vision in the European Union and the United States," *Energy Policy*, vol. 35, no. 4, pp. 2453–2465, 2007.

[71] C. D'Adamo, S. Jupe, and C. Abbey, "Global survey on planning and operation of active distribution networks - Update of CIGRE C6.11 working group activities," in *20th International Conference and Exhibition on Electricity Distribution*, 2009, pp. 1–4.

[72] M. McGranaghan and F. Goodman, "Technical and system requirements for Advanced Distribution Automation," in *18th International Conference and Exhibition on Electricity Distribution, CIRED 2005*, 2005, pp. 1–5.

[73] G. Simard, D. Chartrand, and P. Christophe, "Distribution automation: Applications to move from today's distribution system to tomorrow's smartgrid," in *IEEE Power & Energy Society General Meeting*, 2009, pp. 1–5.

[74] Electric Power Research Institute, "Technical and System Requirements for Advanced Distribution Automation," 2004. [Online]. Available: http://mydocs.epri.com/docs/public/000000000001010915.pdf [Accessed: 17 October 2010]

[75] IEEE Smart Distirbution Working Group, "Smart Distribution Wiki," 2010. [Online]. Available: http://wiki.powerdistributionresearch.com/index.php?title=Main_Page [Accessed: 17 October 2010]

[76] ——, "IEEE Smart Distirbution Working Group Home Page," 2010. [Online]. Available: http://grouper.ieee.org/groups/td/dist/da/doc/index.html [Accessed: 17 October 2010]

[77] J. A. P. Lopes, N. Hatziargyriou, J. Mutale, P. Djapic, and N. Jenkins, "Integrating distributed generation into electric power systems: A review of drivers, challenges and opportunities," *Electric Power Systems Research*, vol. 77, no. 9, pp. 1189–1203, 2007.

[78] I. J. Laurens, "A decentralized negotiation framework for restoring electrical energy delivery networks with Intelligent Power Routers IPRs," MS thesis, University of Puerto Rico, 2005.

[79] R. A. A. de Graaff, J. M. A. Myrzik, W. L. Kling, and J. H. R. Enslin, "Intelligent Nodes in Distribution Systems - Optimizing Steady State Settings," in *IEEE Power Tech*, Lausanne, 2007, pp. 391–395.

[80] F. L. Bellifemine, G. Caire, and D. Greenwood, *Developing Multi-Agent Systems with JADE*. John Wiley & Sons, Ltd., 2007.

[81] S. D. J. McArthur, E. M. Davidson, V. M. Catterson, A. L. Dimeas, N. D. Hatziargyriou, F. Ponci, and T. Funabashi, "Multi-Agent Systems for Power Engineering Applications; Part II: Technologies, Standards, and

Tools for Building Multi-agent Systems," *IEEE Transactions on Power Systems*, vol. 22, no. 4, pp. 1753–1759, 2007.

[82] M. Wooldridge, *An Introduction to Multiagent Systems*.   West Sussex, England: John Wiley & Sons, Ltd., 2002.

[83] S. D. J. McArthur and E. M. Davidson, "Concepts and approaches in multi-agent systems for power applications," in *Proceedings of the 13th International Conference on Intelligent Systems Application to Power Systems*, 2005, p. 5 pp.

[84] A. M. Uhrmacher and D. Weyns, *Multi-Agent Systems Simulation and Applications*.   Taylor and Francis Group, LLC, 2009.

[85] S. J. Russell and P. Norvig, *Artificial Intelligence: A Modern Approach*, Upper Saddle River : Prentice Hall, Ed., 2004.

[86] IEC, "IEC Communications Networks and Systems in Substations," 2005.

[87] ——, "IEC Energy Management System Application Program Interface (EMS-API) - Part 301: Common Information Model (CIM) Base," 2005.

[88] FIPA, "Agent unified modeling language," 2010. [Online]. Available: http://www.auml.org/ [Accessed: 17 October 2010]

[89] R. G. Smith, "The Contract Net Protocol: High-Level Communication and Control in a Distributed Problem Solver," *IEEE Transactions on Computers*, vol. C-29, no. 12, pp. 1104–1113, 1980.

[90] Cougaar, "An open source agent architecture for large-scale, distributed multi-agent systems." [Online]. Available: http://www.cougaar.org/ [Accessed: 17 October 2010]

[91] Intelligent Automation Inc., "CypelePro." [Online]. Available: http://products.i-a-i.com/ [Accessed: 17 October 2010]

[92] Telecom Italia SpA, "JADE - Java Agent Development Framework," 2010. [Online]. Available: http://jade.tilab.com/ [Accessed: 17 October 2010]

[93] G. James, D. Cohen, R. Dodie, G. Platt, and D. Palmer, "A deployed multi-agent framework for distributed energy applications," in *Proceedings of the fifth international joint conference on Autonomous agents and multiagent systems*, 2006, pp. 676–678.

[94] F. C. Schweppe and J. Wildes, "Power System Static-State Estimation, Part I: Exact Model," *IEEE Transactions on Power Apparatus and Systems*, vol. PAS-89, no. 1, pp. 120–125, 1970.

[95] T. Van Cutsem and M. Ribbens-Pavella, "Critical Survey of Hierarchical Methods for State Estimation of Electric Power Systems," *IEEE Transactions on Power Apparatus and Systems*, vol. PAS-102, no. 10, pp. 3415–3424, 1983.

[96] R. Ebrahimian and R. Baldick, "State estimation distributed processing [for power systems]," *IEEE Transactions on Power Systems*, vol. 15, no. 4, pp. 1240–1246, 2000.

[97] A. J. Conejo, S. de La Torre, and M. Canas, "An Optimization Approach to Multiarea State Estimation," *IEEE Transactions on Power Systems*, vol. 22, no. 1, pp. 213–221, 2007.

[98] H. B. Sun and B. M. Zhang, "Global state estimation for whole transmission and distribution networks," *Electric Power Systems Research*, vol. 74, no. 2, pp. 187–195, May 2005.

[99] J. Zaborszky, K. Whang, and K. Prasad, "Ultra fast state estimation for the large electric power system," *IEEE Transactions on Automatic Control*, vol. 25, no. 4, pp. 839–841, 1980.

[100] I. W. Slutsker, S. Mokhtari, and K. A. Clements, "Real time recursive parameter estimation in energy management systems," *IEEE Transactions on Power Systems*, vol. 11, no. 3, pp. 1393–1399, 1996.

[101] E. A. Blood, B. H. Krogh, and M. D. Ilic, "Electric power system static state estimation through Kalman filtering and load forecasting," in *IEEE Power and Energy Society General Meeting - Conversion and Delivery of Electrical Energy in the 21st Century*, 2008, pp. 1–6.

[102] S. A. Zonouz and W. H. Sanders, "A Kalman-Based Coordination for Hierarchical State Estimation: Agorithm and Analysis," in *Proceedings of the 41st Annual Hawaii International Conference on System Sciences*, 2008, p. 187.

[103] M. M. Nordman and M. Lehtonen, "Distributed agent-based State estimation for electrical distribution networks," *IEEE Transactions on Power Systems*, vol. 20, no. 2, pp. 652–658, 2005.

[104] S. Choi, B. Kim, G. J. Cokkinides, and A. P. S. Meliopoulos, "Autonomous state estimation for the smart grid - laboratory implementation," in *IEEE PES Transmission and Distribution Conference and Exposition*, 2010, pp. 1–8.

[105] A. Abur and A. G. Expósito, *Power system state estimation: theory and implementation*. CRC Press, 2004.

[106] K. Li, "State estimation for power distribution system and measurement impacts," *IEEE Transactions on Power Systems*, vol. 11, no. 2, pp. 911–916, 1996.

[107] R. K. Ahuja, T. L. Magnanti, and J. B. Orlin, *Network flows: theory, algorithms, and applications*. Prentice Hall, 1993.

[108] D. M. Falcao, F. F. Wu, and L. Murphy, "Parallel and distributed state estimation," *IEEE Transactions on Power Systems*, vol. 10, no. 2, pp. 724–730, 1995.

[109] D. P. Bertsekas and J. N. Tsitsiklis, *Parallel and Distributed Computation: Numerical Methods*. Athena Scientific, 1997.

[110] K. Seidu and H. Mukai, "Parallel Multi-Area State Estimation," *IEEE Transactions on Power Apparatus and Systems*, vol. PAS-104, no. 5, pp. 1025–1034, 1985.

[111] University of Washington, "Power Systems Test Case Archive," 2010. [Online]. Available: http://www.ee.washington.edu/research/pstca/ [Accessed: 17 October 2010]

[112] W. H. Kersting, "Radial distribution test feeders," in *IEEE Power Engineering Society Winter Meeting*, vol. 2, 2001, pp. 908–912 vol.2.

[113] Leonardo Power Quality Initiative, "Voltage Disturbances: Standard EN 50160 - Voltage Characteristics in Public Distribution Systems," p. 16, 2004.

[114] S. Cobben, "Power Quality: Implications at the Point of Connection," Ph.D. dissertation, Technische Universiteit Eindhoven, 2007.

[115] S. N. Liew and G. Strbac, "Maximising penetration of wind generation in existing distribution networks," *IEE Proceedings - Generation, Transmission and Distribution*, vol. 149, no. 3, pp. 256–262, 2002.

[116] A. Collinson, F. Dai, A. Beddoes, and J. Crabtree, "Solutions for the connection and operation of distributed generation," p. 79, 2003. [Online]. Available: http://www.ensg.gov.uk/assets/solutions.pdf [Accessed: 17 October 2010]

[117] F. A. Viawan, A. Sannino, and J. Daalder, "Voltage control with on-load tap changers in medium voltage feeders in presence of distributed generation," *Electric Power Systems Research*, vol. 77, no. 10, pp. 1314–1322, Aug. 2007.

[118] M. E. Baran and I. M. El-Markabi, "A Multiagent-Based Dispatching Scheme for Distributed Generators for Voltage Support on Distribution Feeders," *IEEE Transactions on Power Systems*, vol. 22, no. 1, pp. 52–59, 2007.

[119] F. Bignucolo, R. Caldon, and V. Prandoni, "Radial MV networks voltage regulation with distribution management system coordinated controller," *Electric Power Systems Research*, vol. 78, no. 4, pp. 634–645, Apr. 2008.

[120] P. N. Vovos, A. E. Kiprakis, A. R. Wallace, and G. P. Harrison, "Centralized and Distributed Voltage Control: Impact on Distributed Generation Penetration," *IEEE Transactions on Power Systems*, vol. 22, no. 1, pp. 476–483, 2007.

[121] K. De Brabandere, "Voltage and frequency droop control in low voltage grids by distributed generators with inverter front-end," Ph.D. dissertation, Katholieke Universiteit Leuven, 2006.

[122] FIPA, "FIPA Contract Net Interaction Protocol Specification," p. 9, 2002. [Online]. Available: http://www.fipa.org/specs/fipa00029/SC00029H.pdf [Accessed: 17 October 2010]

[123] F. Milano, "The Power System Analysis Toolbox (PSAT)." [Online]. Available: http://www.power.uwaterloo.ca/~fmilano/psat.htm [Accessed: 17 October 2010]

[124] The MathWork, "Using the Embedded MATLAB Function Block." [Online]. Available: http://www.mathworks.com/access/helpdesk/help/toolbox/simulink/25ug/f6-6010.html [Accessed: 17 October 2010]

[125] M. Huneault and F. D. Galiana, "A survey of the optimal power flow literature," *IEEE Transactions on Power Systems*, vol. 6, no. 2, pp. 762–770, 1991.

[126] B. H. Kim and R. Baldick, "A comparison of distributed optimal power flow algorithms," *Power Systems, IEEE Transactions on*, vol. 15, no. 2, pp. 599–604, 2000.

[127] X.-P. Zhang, C. Rehtanz, and B. Pal, *Flexible AC transmission systems: modelling and control.* Springer Berlin Heidelberg, 2006.

[128] R. A. A. de Graaff, "Flexible distribution systems through the application of multi back-to-back converters: Concept, implementation and experimental verification," Ph.D. dissertation, Technische Universiteit Eindhoven, 2010.

[129] I. J. Laurens, "A decentralized negotiation framework for restoring electrical energy delivery networks with Intelligent Power Routers - IPRs," MS thesis, University of Puerto Rico, 2005.

[130] A. Armbruster, M. Gosnell, B. McMillin, and M. L. Crow, "Power transmission control using distributed max-flow," in *29th Annual International Computer Software and Applications Conference, COMPSAC.*, vol. 1, 2005, pp. 256–263 Vol. 2.

[131] A. V. Goldberg, "An Efficient Implementation of a Scaling Minimum-Cost Flow Algorithm," *Journal of Algorithms*, vol. 22, no. 1, pp. 1–29, Jan. 1997.

[132] C. Lenzen, J. Suomela, and R. Wattenhofer, "Local Algorithms: Self-stabilization on Speed," *Stabilization, Safety, and Security of Distributed Systems*, vol. 5873, pp. 17–34, 2009.

[133] The MathWork, "MathWorks - SimPowerSystems - Model and simulate electrical power systems - Simulink," 2010. [Online]. Available: http://www.mathworks.nl/products/simpower/ [Accessed: 17 October 2010]

[134] P. Rydesäter, "MATLAB Central - File detail - TCP/UDP/IP Toolbox 2.0.6," 2010. [Online]. Available: http://www.mathworks.com/matlabcentral/fileexchange/345 [Accessed: 17 October 2010]

[135] M. Barnes, A. Dimeas, A. Engler, C. Fitzer, N. Hatziargyriou, C. Jones, S. Papathanassiou, and M. Vandenbergh, "Microgrid laboratory facilities," in *International Conference on Future Power Systems*, 2005, p. 6.

[136] K. De Brabandere, K. Vanthournout, J. Driesen, G. Deconinck, and R. Belmans, "Control of Microgrids," in *IEEE Power Engineering Society General Meeting*, 2007, pp. 1–7.

[137] J. Svensson, "Active Distributed Power Systems Functional structures for real-time operation of sustainable energy systems," Ph.D. dissertation, Lund University, 2006.

[138] Telecom Italia S.p.A., "Java Agent Development Framework," 2010. [Online]. Available: http://jade.tilab.com/index.html [Accessed: 17 October 2010]

[139] P. Rydesäter, "TCP/UDP/IP Toolbox 2.0.6," 2010. [Online]. Available: http://www.mathworks.nl/matlabcentral/fileexchange/345 [Accessed: 17 October 2010]

[140] The MathWork, "Real-Time Workshop for use with Simulink," 2010. [Online]. Available: http://www.mathworks.com/products/rtw/ [Accessed: 17 October 2010]

[141] N. Mohan, T. M. Undeland, and W. P. Robbins, *Power Electronics: Converters, Applications, and Design*, 3rd ed.   John Wiley & Sons, Ltd., Oct. 2003.

[142] A. Tewari, *Modern Control Design With Matlab and Simulink*.   Wiley, 2002.

[143] R. Teodorescu and F. Blaabjerg, "Flexible control of small wind turbines with grid failure detection operating in stand-alone and grid-connected mode," *IEEE Transactions on Power Electronics*, vol. 19, no. 5, pp. 1323–1332, 2004.

[144] S. Buso and P. Mattavelli, *Digital control in power electronics*.   Morgan & Claypool Publishers, 2006.

[145] Wikipedia, "Field-programmable gate array." [Online]. Available: http://en.wikipedia.org/wiki/Field-programmable_gate_array#cite_note-FPGA-1 [Accessed: 17 October 2010]

[146] ECN, "PowerMatcher: Smartgrid technology." [Online]. Available: http://www.powermatcher.net/ [Accessed: 17 October 2010]

LIST OF ABBREVIATIONS

Notation	Description
ACL	Agent Communication Language
ADA	Advanced Distribution Automation
ADAPS	Autonomous Demand Area Power System
ADN	Active Distribution Network
AGC	Automatic Generation Control
AN	Active Network
ANM	Active Network Management
API	Application Programming Interface
AUML	Agent-based Unified Modeling Language
CDSE	Completely Decentralized State Estimation
CHP	Combined Heat and Power
CNP	Contract Net Protocol
CS-PR	Cost-Scaling Push-Relabel
DER	Distributed Energy Resource
DFIG	Doubly Fed Induction Generator
DG	Distributed Generation
DMS	Distribution Management System
DNO	Distribution Network Operator
DSE	Distributed State Estimation
DSM	Demand Side Management
DSO	Distribution System Operator
DSTATCOM	Distributed Static Compensator
DVR	Dynamic Voltage Restorer
EMS	Energy Management System
EU	European Union
FACDS	Flexible AC Distribution Systems
FACTS	Flexible AC Transmission Systems
FIPA	Foundation for Intelligent Physical Agents

Notation	Description
FPGA	Field Programmable Gate Array
FRIENDS	Flexible, Reliable and Intelligent Electrical eNergy Delivery System
HVDC	High Voltage Direct Current
ICT	Information and Communication Technologies
IED	Intelligent Electronic Device
IPR	Intelligent Power Router
ISO	Independent System Operator
JADE	Java Agent Development Framework
KQML	Knowledge Query and Manipulation Language
LCS	Local Control Scheduling
LLF	Log Likelihood Function
LPC	Loop Power Controller
LV	Low Voltage
MAS	Multi-Agent System
MLE	Maximum Likelihood Estimation
MV	Medium Voltage
NOP	Normally Open Point
OLTC	On-Load Tap Changer
OPF	Optimal Power Flow
PC	Personal Computer
PCC	Point of Common Coupling
PFC	Power Flow Controller
PI	Proportional Integral
PLL	Phase Lock Loop
PQ	Power Quality
PR	Power Router
PWM	Pulse Width Modulation
QCC	Quality Control Center
RES	Renewable Energy Source
RTT	Real-Time Target
RTW	Real-Time Workshop
S&D	Supply and Demand
SA	Server Agent
SCADA	Supervisory Control and Data Acquisition
SDS	Smart Distribution System
SE	State Estimation
spa	socket proxy agent
SSP	Successive Shortest Path
SSTS	Solid-State Transfer Switch
TLC	Target Language Compiler
TNO	Transmission Network Operator
TSO	Transmission System Operator
UK	United Kingdom
US	United States

Notation	Description
VPP	Virtual Power Plant
VSI	Voltage Source Inverter
WG	Working Group
WLS	Weighted Least Square

Notation	Description
A_i	agent i
B	susceptance, siemens or $p.u.$
I	current, A or $p.u.$
M_i	moderator agent i
P	active power, W or $p.u.$
Q	reactive power, VAr or $p.u.$
R	resistance, Ω or $p.u.$
SM	superior moderator agent
V	voltage, V or $p.u.$
V_i^{meas}	measurements of voltage magnitude, V or $p.u.$
V_{AC}	AC voltage, V or $p.u.$
V_{DC}	DC voltage, V or $p.u.$
X	reactance, Ω or $p.u.$
Z	impedance, Ω or $p.u.$
ϵ	scaling factor
$\mathbf{G}$	gain matrix
$\mathbf{R}$	variance vector of the measurement errors
$\mathcal{G}$	directed graph
μ_i	mean or expected value
ω_P	weighting factors for adjusting 1 unit of active power
ω_Q	weighting factors for adjusting 1 unit of reactive power
$\overline{V_i}$	estimation of voltage magnitude, V or $p.u.$
$\overline{\theta_{ij}}$	estimation of voltage angle difference, rad.
π_i	node potential
σ_i	standard deviation
σ_i^{meas}	measurement variances of voltage magnitude
θ_{ij}	voltage angle difference, rad.
c_{ij}	edge cost, $p.u.$

Notation	Description
c_{ij}^{π}	reduce cost, *p.u.*
e_i	node excess
$h_i(x)$	nonlinear function relating the measurement z_i to the state vector
r_i	residual for measurement z_i
r_{ij}	residual capacity, *p.u.*
s	virtual source node
t	virtual sink node
u_{ij}	edge capacity, *p.u.*
x	system state vector
z_i	ith measurement

APPENDIX A

IEEE TEST NETWORKS DATA

The data in this appendix are adopted from [111] and [112].

Table A.1: Bus data of the IEEE 14-bus test network

Bus number	Bus type	V p.u.	Angle p.u.	Load MW	Load MVAr	Generation MW	Generation MVAr
1	3	1.060	0	0	0	232.4	-16.9
2	2	1.045	-4.98	21.7	12.7	40	42.4
3	2	1.010	-12.72	94.2	19	0	23.4
4	1	1.019	-10.33	47.8	-3.9	0	0
5	1	1.020	-8.78	7.6	1.6	0	0
6	2	1.070	-14.22	11.2	7.5	0	12.2
7	1	1.062	-13.37	0	0	0	0
8	2	1.090	-13.36	0	0	0	17.4
9	1	1.056	-14.94	29.5	16.6	0	0
10	1	1.051	-15.10	9	5.8	0	0
11	1	1.057	-14.79	3.5	1.8	0	0
12	1	1.055	-15.07	6.1	1.6	0	0
13	1	1.050	-15.16	13.5	5.8	0	0
14	1	1.036	-16.04	14.9	5	0	0

Table A.2: Line data of the IEEE 14-bus test network

From bus	To bus	R p.u.	X p.u.	B p.u.	Transformer magnitude
1	2	0.0194	0.0592	0.0528	0
1	5	0.0540	0.2230	0.0492	0
2	3	0.0470	0.1980	0.0438	0
2	4	0.0581	0.1763	0.0340	0
2	5	0.0570	0.1739	0.0346	0
3	4	0.0670	0.1710	0.0128	0
4	5	0.0134	0.0421	0.0000	0
4	7	0.0000	0.2091	0.0000	0.978
4	9	0.0000	0.5562	0.0000	0.969
5	6	0.0000	0.2520	0.0000	0.932
6	11	0.0950	0.1989	0.0000	0
6	12	0.1229	0.2558	0.0000	0
6	13	0.0662	0.1303	0.0000	0
7	8	0.0000	0.1762	0.0000	0
7	9	0.0000	0.1100	0.0000	0
9	10	0.0318	0.0845	0.0000	0
9	14	0.1271	0.2704	0.0000	0
10	11	0.0821	0.1921	0.0000	0
12	13	0.2209	0.1999	0.0000	0
13	14	0.1709	0.3480	0.0000	0

Table A.3: Measurement bus data of the IEEE 14-bus test network

Bus	V p.u.	σ_V p.u.
1	1.06	0.001
8	1.09	0.001
9	1.0501	0.001
10	1.0462	0.001

Table A.4: Measurement branch data of the IEEE 14-bus test network

From bus	To bus	P p.u.	σ_P p.u.	Q p.u.	σ_Q p.u.
1	2	1.5591	0.008	-0.20176	0.008
1	5	0.76475	0.008	-0.03723	0.008
2	5	0.41468	0.008	-0.08316	0.008
2	4	0.56017	0.008	-0.09124	0.008
3	2	-0.70203	0.008	0.01329	0.008
3	4	-0.23997	0.008	-0.04038	0.008
4	9	0.16097	0.008	-0.02963	0.008
4	7	0.28424	0.008	-0.11945	0.008
5	4	0.62875	0.008	-0.07053	0.008
5	6	0.43737	0.008	-0.11919	0.008
6	12	0.07794	0.008	0.02692	0.008
6	13	0.17644	0.008	0.07946	0.008
6	11	0.07098	0.008	0.0498	0.008
7	9	0.28424	0.008	0.06375	0.008
8	7	0	0.008	0.20836	0.008
9	10	0.05491	0.008	0.02818	0.008
9	14	0.0953	0.008	0.02707	0.008
11	10	0.03536	0.008	0.03049	0.008
12	13	0.01621	0.008	0.0094	0.008
14	13	-0.05483	0.008	-0.02534	0.008

Table A.5: Bus data of the IEEE 34-bus test network

Bus number	Bus type	V p.u.	Angle p.u.	Load p.u.	Load p.u.	Generation p.u.	Generation p.u.
1	3	1.03	0	0.00000	0.00000	0.43568	0.0239
2	1	1.0291	-0.00032	0.01910	0.00987	0	0
3	1	1.0286	-0.00054	0.00000	0.00000	0	0
4	1	1.0182	-0.00465	0.00529	0.00274	0	0
5	1	1.0182	-0.00465	0.00000	0.00000	0	0
6	1	1.0063	-0.00955	0.00000	0.00000	0	0
7	1	0.99686	-0.01351	0.00000	0.00000	0	0
8	1	0.99654	-0.01365	0.00000	0.00000	0	0
9	1	0.99644	-0.01369	0.00013	0.00007	0	0
10	1	0.99639	-0.01366	0.01130	0.00584	0	0
11	1	0.99351	-0.01522	0.01490	0.00771	0	0
12	1	0.99555	-0.01297	0.01184	0.02336	0	0
13	1	0.99328	-0.01535	0.00206	0.00107	0	0
14	1	0.99351	-0.01522	0.00000	0.00000	0	0
15	1	0.99555	-0.01297	0.00000	0.00000	0	0
16	1	0.98774	-0.01847	0.00000	0.00000	0	0
17	1	0.9876	-0.01855	0.00124	0.00064	0	0
18	1	0.9777	-0.02426	0.00000	0.00000	0	0
19	1	0.9876	-0.01855	0.00000	0.00000	0	0
20	1	0.97743	-0.02442	0.00437	0.00226	0	0
21	1	0.9772	-0.02453	0.00000	0.00000	0	0
22	1	0.97628	-0.02523	0.01000	0.00517	0	0
23	1	0.97689	-0.02445	0.02700	0.02162	0	0
24	1	0.97498	-0.02619	0.05000	0.00000	0	0
25	1	0.97628	-0.02523	0.00000	0.00000	0	0
26	1	0.97481	-0.02617	0.04657	0.02972	0	0
27	1	0.97495	-0.02624	0.00304	0.00157	0	0
28	1	0.97473	-0.02616	0.01310	0.00677	0	0
29	1	0.97481	-0.02646	0.14905	0.01490	0	0
30	1	0.97473	-0.02616	0.00920	0.00476	0	0
31	1	0.97472	-0.02616	0.00886	0.00709	0	0
32	1	0.9749	-0.02688	0.00754	0.00390	0	0
33	1	0.97473	-0.02616	0.00000	0.00000	0	0
34	1	0.97492	-0.02695	0.01945	-0.13443	0	0

Table A.6: Line data of the IEEE 34-bus test network

From bus	To bus	R p.u.	X p.u.	B p.u.	Transformer magnitude
1	2	0.002031	0.000895	0.000001	0
2	3	0.001362	0.000600	0.000001	0
3	4	0.025370	0.011184	0.000011	0
4	5	0.004597	0.002027	0.000002	0
4	6	0.029518	0.013013	0.000013	0
6	7	0.023402	0.010317	0.000010	0
7	8	0.000787	0.000347	0.000000	0
8	9	0.000244	0.000108	0.000000	0
9	10	0.001346	0.000593	0.000001	0
9	11	0.008037	0.003543	0.000003	0
10	12	0.037901	0.016709	0.000016	0
11	13	0.000661	0.000291	0.000000	0
11	14	0.002385	0.001051	0.000000	0
12	15	0.010815	0.004768	0.000047	0
13	16	0.016089	0.007093	0.000071	0
16	17	0.000409	0.000180	0.000000	0
17	18	0.028990	0.012781	0.000012	0
17	19	0.018364	0.008096	0.000081	0
18	20	0.000787	0.000347	0.000000	0
20	21	0.003064	0.006581	0.000006	0
20	22	0.003857	0.001700	0.000001	0
21	23	0.008312	0.003665	0.000003	0
22	24	0.004589	0.002023	0.000002	0
22	25	0.001275	0.000562	0.000001	0
24	26	0.001590	0.000701	0.000000	0
24	27	0.000220	0.000097	0.000000	0
26	28	0.002110	0.000930	0.000001	0
27	29	0.001063	0.000468	0.000000	0
28	30	0.000220	0.000097	0.000000	0
28	31	0.000677	0.000298	0.000000	0
29	32	0.002865	0.001263	0.000001	0
30	33	0.002558	0.001685	0.000001	0
32	34	0.000417	0.000184	0.000000	0

Table A.7: Measurement bus data of the IEEE 34-bus test network

Bus	V p.u.	σ_V p.u.
1	1.03000	0.001
9	0.99644	0.001
24	0.97498	0.001

Table A.8: Measurement branch data of the IEEE 34-bus test network

From bus	To bus	P p.u.	σ_P p.u.	Q p.u.	σ_Q p.u.
1	2	0.43568	0.008	0.02390	0.008
2	3	0.41622	0.008	0.01387	0.008
3	4	0.41599	0.008	0.01377	0.008
4	5	0.00000	0.008	0.00000	0.008
4	6	0.40655	0.008	0.00921	0.008
6	7	0.40184	0.008	0.00715	0.008
7	8	0.39811	0.008	0.00551	0.008
8	9	0.39798	0.008	0.00546	0.008
9	10	0.02317	0.008	0.02915	0.008
9	11	0.37464	0.008	-0.02378	0.008
10	12	0.01187	0.008	0.02331	0.008
11	13	0.35860	0.008	-0.03199	0.008
11	14	0.00000	0.008	0.00000	0.008
12	15	0.00000	0.008	-0.00005	0.008
13	16	0.35646	0.008	-0.03310	0.008
16	17	0.35437	0.008	-0.03395	0.008
17	18	0.35307	0.008	-0.03453	0.008
17	19	0.00000	0.008	-0.00008	0.008
18	20	0.34933	0.008	-0.03617	0.008
20	21	0.02701	0.008	0.02162	0.008
20	22	0.31785	0.008	-0.06010	0.008
21	23	0.02701	0.008	0.02162	0.008
22	24	0.30742	0.008	-0.06545	0.008
22	25	0.00000	0.008	0.00000	0.008
24	26	0.07775	0.008	0.04835	0.008
24	27	0.17920	0.008	-0.11401	0.008
26	28	0.03116	0.008	0.01862	0.008
27	29	0.17615	0.008	-0.11558	0.008
28	30	0.00920	0.008	0.00476	0.008
28	31	0.00886	0.008	0.00709	0.008
29	32	0.02705	0.008	-0.13050	0.008
30	33	0.00000	0.008	0.00000	0.008
32	34	0.01946	0.008	-0.13443	0.008

LIST OF PUBLICATIONS

The results of the research presented in this thesis have been presented in the following conferences and journals:

- **Articles in International Scientific Journals**

  1. Phuong H. Nguyen, Wil L. Kling, Paulo F. Ribeiro, "Smart power router: a flexible agent-based converter interface in Active Distribution Networks", IEEE Transactions on Smart Grid (submitted for review).

  2. Phuong H. Nguyen, Wil L. Kling, Paulo F. Ribeiro, " Multi-agent application for distributed state estimation in Active Distribution Networks", IET Renewable Power Generation (submitted for review).

  3. Phuong H. Nguyen, Wil L. Kling, Johanna M. A. Myrzik, "An application of the successive shortest path algorithm to manage power in Multi-Agent System based Active Networks", European Transaction on Electrical Power, published online: 16 Sep 2009. DOI: 10.1002/etep.390.

- **Articles in International Conferences**

  1. P. H. Nguyen, W.L. Kling, G. Georgiadis, M. Papatriantafilou, L. Anh-Tuan, and L. Bertling "Distributed routing algorithms to manage power flow in agent-based active distribution network", IEEE PES Conference on Innovative Smart Grid Technologies Europe, Gothenburg, Sweden, 2010.

  2. B. Asare-Bediako, P. H. Nguyen, G. M. A. Vanalme, A. Kechroud, and W. L. Kling, "Bi-directional Power Flow Management using MAS-based Active Network Laboratory Setup Design and Implementation", 45th International Universities' Power Engineering Conference, Cardiff, Wales, UK, 2010.

  3. P. H. Nguyen, and W.L. Kling, "Distributed State Estimation for Multi-Agent System based Active Networks", IEEE PES General Meeting, Minnesota, US, July 2010.

4. P. H. Nguyen, G. v. d. Wolk, and W. L. Kling, "Power Router Implementation to enable Active Distribution Networks", Isup-2010, Bruges, Belgium, April 2010.

5. G. v. d. Wolk, P. H. Nguyen, and W. L. Kling, "Lab design and implementation of MAS-based Active Network", IEEE Young Research Symposium, Leuven, Belgium, March 2010.

6. P. H. Nguyen, W. L. Kling, and J. M. A. Myrzik, "Completely decentralized state estimation for active distribution network", Proceedings of the EuroPES conference, Palma de Mallorca, Spain, 2009.

7. P. H. Nguyen, W. L. Kling, and J. M. A. Myrzik, "Power flow management in active networks", Proceedings of the PowerTech Conference, Bucharest, Romania, 2009.

8. P. H. Nguyen, W. L. Kling, and J. M. A. Myrzik, "Coordination of voltage regulation in active networks", IEEE/PES Transmission and Distribution Conference and Exposition, Chicago, US, 2008.

9. P. H. Nguyen, W. L. Kling, and J. M. A. Myrzik, "The interconnection in active distribution networks", International Conference on Energy Security and Climate Change: issues, strategies and options, Bangkok, Thailand, August 6 - 8, 2008.

10. P. H. Nguyen, A. Kechroud, J. M. A. Myrzik, and W. L. Kling, "Voltage control coordination of distributed generators in cell-based active networks", 4th IEEE Benelux Young Researchers Symposium in Electrical Power Engineering, Eindhoven, The Netherlands, February, 2008.

11. P. H. Nguyen, J. M. A. Myrzik, and W. L. Kling, "Promising concepts and technologies for future power delivery systems", 42nd International Universities' Power Engineering Conference, Brighton, UK, 2007.

ACKNOWLEDGMENT

Along with the four years PhD program, I have worked with, and been supported and encouraged by many people both in academic and social environments. I am grateful to all of them and would like to address some in particular.

First of all, I would like to thank my promotor, prof. Wil L. Kling, for his guidance and patience during the last four years. His trust in me during the early stages as well as his great time and effort during the final stage of my PhD project are highly appreciated. I also honor him for giving me the freedom to do this research.

I then would like to thank prof. Johanna M.A. Myrzik who made the first contact with me for the PhD position. My gratitude is for her efforts at the beginning of this research project and her time for being a member of the committee for this thesis.

A special thank would be sent to prof. Paulo F. Ribeiro for his voluntary supervision since he started working with our group at the TU/e. His valuable comments and remarks have raised the quality of this thesis.

I am grateful to the doctoral examination committee for taking the time to go through my work and giving their constructive suggestions to improve the thesis.

Many thanks to my colleagues in the intelligent network group: Sjef, Greet, Anton, Frans, Cai, Choukri, Roald, Edward, Peter, Hamid, Sharmistha, Fei, Chai, Glenn, Totis, Vladimir, Petr, Ioannis, and Ballard. It was always my pleasure to attend EOS and IOP regular meetings with all of you. A special thank goes out to Jasper for his great effort to help me translate the summary of the thesis.

I would like to thank other colleagues in EES for creating a relaxed and friendly atmosphere via the social talks during the coffee breaks.

From a non-academic side of my life, I am endlessly grateful to my family for their continuing encouragements. I treasure the support of my brother, Bi, my sisters, Lien, Van, and my friends whom I could not mention all here but they know who they are.

Finally, I would like to express a million thanks to my wife Trang and my son Shin, for being with me in my life.

Phuong H. Nguyen was born on 09-06-1980 in Hanoi, Vietnam. After finishing Bachelors degree in Electrical Engineering in 2002 at Hanoi University of Technology in 2002 in Vietnam, he studied Master program of Electrical Energy department at Asian Institute of Technology in Bangkok, Thailand. In 2004 he graduated within the Electrical Power System Management group on Transient Stability and Contingency Ranking topic. From 2004 to 2006 he worked as a researcher at the Power Engineering Consulting Company No. 1, Electricity of Vietnam. From 2006 to 2010 he started a PhD project at Eindhoven University of Technology at Eindhoven, the Netherlands about "Electrical Infrastructure of the Future" of which the results are presented in this dissertation. Since the end of 2010 he is employed at the same group as a researcher.

His research interests include distributed state estimation, control and operation of the power system, multi-agent system and their applications in the future power delivery system.